Kham, A.Z. (1996). Frequency estimation of pre-stressed and composite floors. (Unpublished Doctoral thesis, City University London)

CITY UNIVERSITY LONDON

City Research Online

Original citation: Kham, A.Z. (1996). Frequency estimation of pre-stressed and composite floors. (Unpublished Doctoral thesis, City University London)

Permanent City Research Online URL: http://openaccess.city.ac.uk/7929/

Copyright & reuse

City University London has developed City Research Online so that its users may access the research outputs of City University London's staff. Copyright © and Moral Rights for this paper are retained by the individual author(s) and/ or other copyright holders. All material in City Research Online is checked for eligibility for copyright before being made available in the live archive. URLs from City Research Online may be freely distributed and linked to from other web pages.

Versions of research

The version in City Research Online may differ from the final published version. Users are advised to check the Permanent City Research Online URL above for the status of the paper.

Enquiries

If you have any enquiries about any aspect of City Research Online, or if you wish to make contact with the author(s) of this paper, please email the team at publications@city.ac.uk.

FREQUENCY ESTIMATION OF PRE-STRESSED AND COMPOSITE FLOORS

Dissertation

Submitted In Fulfilment Of The Requirement For
The Degree
Of

Doctor Of Philosophy

By

ARSHAD ZAMAN KHAN

September 1996

CITY University

SCHOOL OF ENGINEERING

Department Of Civil Engineering

CONTENTS

LIST OF TABLES

Chapter 1

Chapter 4

Chapter 5

Chapter 6

LIST OF FIGURES

==========

Chapter 2

Chapter 3

Chapter 4

Chapter 5

ACKNOWLEDGEMENTS

I believe that nothing is impossible with the will of ALLAH (SWT). Therefore, I only seek HIS will, nothing more, nothing less, nothing else!

I would like to tender my grateful thanks and appreciations to my supervisor Prof L F Boswell, Head of the Department, for his generous and continuous support, and guidance throughout the duration of this research and, in particular, for his assistance in arranging the experimental kit. It has been a privilege to work with him and I am enormously appreciative of his encouragement, useful suggestions, criticism, help and advice. It was his special interest in my research that made possible the results achieved and presented in this thesis.

The second most important contribution towards my research has been that of my wife, "Gul". She has continually supported me throughout, not only morally but also physically by accompanying me to all the sites and helping me to carry out the experiments. I am extremely indebted to Gul's help during the experiments, without which the programme would not have been possible. My family members in PAKISTAN have also shown great patience and perseverance and their prayers have been of enormous value to me. Special thanks are due to my friend Dr Abdul-Lateef Bello for his advice and prayers.

I would also like to thank the Ministry of Education of the Government of the Islamic Republic of PAKISTAN for its financial support through a merit scholarship, award No. F.6-48/88-Sch.III. Thanks are also due to the following governing bodies and trusts that provided financial assistance in the later stages of the research:

a) The Committee of the Vice Chancellors and Principals, UK
b) Muslim Aid, UK
c) The Charles Wallace (PAKISTAN) Trust, UK
d) The Sir Ernest Cassel Educational Trust, UK
e) The Sir Richard Stapley Educational Trust, UK
f) The Leche Trust, UK
g) Corporation of London, UK

Finally, I would like to thank all those who assisted in various ways during my experimental programme including the owners of all the structures tested. I am particularly thankful to Mr Sami Khan of Bunyan Meyer & Partners for his useful comments from time to time. Last, but not least, I am grateful to all my friends and colleagues for their invaluable support.

DECLARATION

==========

1. I understand that I am the owner of this thesis and that the copyright rests with me unless I specifically transfer it to another person.

2. I understand that the University requires that I deposit one copy of my thesis in the Library where it shall be available for consultation and that photocopies of it may be made available to those who wish to consult it elsewhere. I understand that the Library, before allowing the thesis to be consulted either in the original or in a photocopy, will require each person wishing to consult it to sign a declaration that he or she recognises that the copyright of the thesis belongs to me and that no quotation from it and no information derived from it may be published without my prior written consent. I, therefore, grant powers of discretion to the University Librarian to allow this thesis to be copied in whole or in part without further reference to me. This permission covers only single copies made for study purposes, subject to normal conditions of acknowledgement.

3. I agree that my thesis shall be available for consultation in accordance with paragraph 2 above.

Arshad Zaman Khan

2 September 1996

ABSTRACT

The modern trends towards economy and the use of high strength materials have resulted in long spans and slender floors of low frequencies. These frequencies may be within the range of the first few harmonics of daily life human activities. Though the problem of resonance with walking vibrations, an activity most common on all floors, is unlikely, high amplitude or persistent vibrations due to these low-level excitations may cause alarm to building occupants. There may also be some problems with the most sensitive equipment. These uncomfortable vibrations are a serviceability limit state problem and can only be avoided by ensuring a high floor fundamental natural frequency and damping. There is a need, therefore, for a method to accurately predict the fundamental natural frequency and damping of these floors and to ensure that they are high enough to avoid any resonance or perceptibility problems.

Available analytical formulae for the estimation of fundamental natural frequency are not directly applicable to actual floors due to various assumptions. The only method that may be reliably used for static or dynamic analyses is the finite element method because it can conveniently model the three dimensional nature of structures and account for the various boundary conditions and material properties.

The research reported in this thesis consists of measuring fundamental natural frequencies and corresponding damping of a range of actual floors. The experimental frequencies have then been compared with those results which are based on the analytical formulae and finite element method. The analytical methods suitable for various categories of floors have been identified. A new linear-elastic single panel or beam finite element model, correlated with the experimental results, has been developed for the accurate estimation of the fundamental natural frequency of these floors. The correct boundary conditions for various categories of floors have been identified. The single-degree-of-freedom (SDOF) formula for the estimation of fundamental natural frequency using static deflections has been modified for the floors tested. This modified SDOF formula can be used for convenient hand calculations by the consultants and designers who want a quick estimation of fundamental natural frequency due to time and cost limitations. The formula may also be used to limit static deflections and, therefore, design loads for any choice of a minimum fundamental natural frequency. Also, new limits on span/depth ratios for flat slabs and span limits for double-T beam floors have been suggested. Similarly, minimum fundamental natural frequencies, damping ratios and maximum static deflections have been suggested for the floors tested. The single panel or beam model may also be used for various parametric studies, both for static and dynamic analyses.

PUBLICATIONS

The research reported in this thesis and its applications have been presented and published in the following papers at the time of submission:

1. "*Predicting Fundamental Natural Frequency of Composite Floors*"
   A Zaman; and L F Boswell
   Journal of Singapore Structural Steel Society, Vol. 6, No. 1, 1996, pages 37-43.

2. "*Frequency Estimation of Long Span Floors*"
   A Zaman; and L F Boswell
   2nd International Conference on Structural Dynamics Modelling: Test, Analysis, Correlation and Updating, Cumbria (UK), 3-5 July, 1996, pages 129-139.

3. "*Review of Acceptability Criteria for the Vibration of Composite Floors*"
   A Zaman; and L F Boswell
   International Seminar on Structural Assessment: The Role of Large and Full Scale Testing, London (UK), 1-3 July, 1996, pages 48.1-48.8.

4. "*Predicting Fundamental Natural Frequency of Composite Floors*"
   A Zaman; and L F Boswell
   Proceedings of the 4th Annual Mechanical Engineering Conference of ISME & 2nd International Mechanical Engineering Conference, Shiraz (IRAN), 14-17 May 1996, Vol. IV, pages 715-722.

5. "*Dynamic Response Testing and Finite Element Modelling of the LBTF Steel-Framed Building Floors*"
   A Zaman; and L F Boswell
   Proceedings of the Second Cardington Conference: Fire, Static and Dynamic Tests at the Large Building Test Facility at Cardington (UK), 12-14 March 1996.

6. "*Dynamic Behaviour of a Composite Beam Before and After Failure*"
   A Zaman; and L F Boswell
   One day Seminar on Composites and Finite Elements in Infrastructure Design and Rehabilitation at British Standards Institution in London, 1 November 1995, pages 18-21

7. "*Using FEM To Predict Floor Vibration Response*"
   A Zaman; and L F Boswell
   Proceedings of the NAFEMS 5th International Conference on Reliability of Finite Element Methods for Engineering Applications, Amsterdam (The NETHERLANDS), 10-12 May, 1995, pages 307-318.

8. "*FE Modelling for Dynamic Analysis of Double-T Prestressed Floors*"
Arshad Zaman
Proceedings of StruCoMe 94, Paris (FRANCE), 22-24 November, 1994, pages 499-510.

9. "*Vibration Criteria for Unbonded Prestressed Concrete Floors*"
P Waldron; R G Caverson; M S Williams; and A Zaman
Proceedings of the FIP Symposium: Modern Prestressing Techniques and their Applications, Kyoto (JAPAN), 17-20 October, 1993, Volume 2, pages 877-884.

10. "*Comparison of Finite Element and Field Test Results for the Vibration of Concrete Floors*"
M S Williams; A Zaman; P Waldron; and R G Caverson
Proceedings of the International Conference on Structural Dynamics Modelling: Test, Analysis and Correlation, Cranfield (UK), 7-9 July, 1993, pages 79-88.

Chapter 1 INTRODUCTION

The trend towards achieving longer spans with slender slab thicknesses and the use of high strength steel and concrete to optimise strength and stiffness properties of floor slabs have led to more economical but rather flexible structures. This has also made long span floors susceptible to vibration problems from a serviceability point of view due to everyday human activities. Moreover, it has caused concern that the dynamic criterion may be of equal importance as the static criterion for design because of the low floor frequencies and high amplitude vibrations.

It is widely recognised that the most important parameter in effecting a floor vibration is the natural frequency of the floor. Slender long-span floors have low natural frequencies (typically less than 10 Hz) and only the first or fundamental mode affects the human perception of floor motion and thus serviceability. It is extremely important to estimate this frequency as accurately as possible and to design the floor for a fundamental natural frequency (hereafter called fundamental frequency) higher than the lowest excitation frequency (for example, walking) to avoid any resonance conditions or objectionable vibrations.

This Chapter examines the importance of floor vibrations and summarises the various methods most commonly used for the estimation of the fundamental frequency of floors. The aims and scope of the research are defined towards the end of the Chapter together with an outline of the thesis.

1.1 Floor Vibrations

Long-span floor slabs are being used increasingly for office buildings and car parks for reasons of economy, lower floor heights, and fast construction etc. These floors can be either post-tensioned concrete: solid flat slabs with or without drop panels, 1-way spanning solid slabs with beams, ribbed, or waffle; pre-tensioned concrete: double-T beams; or composite steel-concrete slabs comprising of profiled steel decking (or sheeting) as the permanent formwork to the underside of concrete slabs spanning between support beams.

Post-tensioned concrete floors allow higher span/depth ratios whereas pre-tensioned double-T beams allow longer spans. The major advantage of composite slab floors over precast or in-situ concrete construction is the reduced construction period. Moreover, steel decking is easy to handle, can be cut to length and is less susceptible to tolerance problems. The shear connectors can be welded or fixed through the decking and the attachments/openings for services can be easily made.

The use of slender sections due to improved methods of construction and design has, however, produced floors which may be susceptible to vibrations. Low amplitude vibration problems in long-span and light-weight composite floors have been encountered and studied in recent years, Wyatt (1989). These vibrations are important at the serviceability limit state only. They range from an uncomfortable environment or annoyance for building occupants due to low amplitude excitations caused by a human footfall or to the large amplitude vibrations caused by rhythmic group activities (i.e. high floor accelerations or deflections). The serviceability limit state should, therefore, be an important consideration in floor design.

Since there is a lack of experimental data on the dynamic behaviour of long-span floors, their advantages, therefore, may be overshadowed if inadequate attention is given to their dynamic serviceability and their vibrational behaviour is not properly understood and taken into account at the design stage.

The serviceability limit state problem due to low amplitude vibrations could only be avoided with higher floor frequencies and damping. This would ensure that resonant conditions do not occur and that vibrations die out quickly. The most important parameter, however, in controlling such vibrations is the fundamental frequency of the floor. Analytical procedures exist to calculate this frequency but lack accuracy in estimation and incorporate various assumptions. Accurate estimation of this frequency, however, is essential for the reliable assessment of the vibrational serviceability of these floors at the design stage.

However, floor slabs are currently designed for stress, strength and stiffness under service loads. Most of the current codes of practice do not include specific requirements for vibration acceptability of these floors and limit their static deflections only. The construction industry also, at present, rely on the use of span/depth ratios to control deflections only and do not consider vibration of suspended floors. While this may be adequate for stiffer and heavier floor systems, it is possible that vibrations rather than deflections may control the design of long-span slabs, particularly its thickness. One design guide, however, is available on composite steel joist-concrete slab floors which considers vibration problems, Wyatt (1989). Most of the research in the area, however, has been centred on the human perception of vibrations. Also, knowledge about the dynamic performance and vibration characteristics of such slabs is very limited. Thus, there is a need for a quick and reliable approach to reduce or eliminate vibration problems by accurately estimating and controlling frequency.

1.1.1 Human Perception

Research into the human perception of vibrations has been extensively carried out for a wide variety of applications. Most of this research has evolved in the form of graphs defining safe/unsafe vibrations for human reaction. These criteria for the control of floor vibrations for human perceptibility and acceptability are mainly based on subjective analysis of a limited amount of data and will vary for different environments. Therefore, the recommendations presented in these criteria tend to be more conservative. The following guides, standards and codes mention these criteria :

i)	BS 6472 (1984)	British Standards Institution, UK
ii)	Technical Report 43 (1994)	Concrete Society, UK
iii)	SCI/CIRIA 076, Wyatt (1989)	The Steel Construction Institute, UK
iv)	CAN3-S16.1-M89 (1989) and National Building Code of Canada (1990)	Canadian Standards Association, Canada
v)	ANSI S3.29 (1983)	American National Standards Institute, USA
vi)	DIN 4150 (1975)	German Institute for Standardisation, Germany
vii)	ISO 2631-2 (1989) and ISO 10137 (1992)	International Organisation for Standardisation, Switzerland

From a review of these guides, it is evident that although tests have been carried out previously to determine the dynamic characteristics of some floors, the biggest deficiency in research has been the accurate estimation of the fundamental frequency of long-span floor slabs which are becoming more common and which can be more slender.

The lack of knowledge of the dynamic behaviour of these flexible slabs, therefore, has prompted an in-situ experimental investigation into their dynamic characteristics to study the existing analytical approaches and design methods for the estimation of fundamental frequency of these floors at scales which cannot normally be achieved in a laboratory.

1.1.2 Fundamental Frequency

The best way to avoid perceptible vibrations is to ensure that the fundamental frequency of the floor is outside the range of excitation frequencies due to various human activities or their higher harmonics for an acceptable sensitivity, Bachmann (1992). This also ensures that the static deflection criterion is critical. Table 1.1 shows Bachmann's recommendations for the minimum fundamental frequencies of floors. Similar recommendations have also been given in CSA (1990).

Table 1.1: Design Frequency Limits, Bachmann (1992)

Type of Structure	Minimum Frequency (Hz)
Office Buildings	4.8 (Damping > 5%) 7.2 (Damping < 5%)
Gymnasia and Sports Halls: Reinforced Concrete Prestressed Concrete Composite Steel-Concrete	 7.5 8.0 8.5
Dancing and Concert Halls (Without Fixed Seating): Reinforced Concrete Prestressed Concrete Composite Steel-Concrete	 6.5 7.0 7.5
Concert Halls, Theatres and Spectator Galleries (With Fixed Seating): Classical or Soft Pop Music Hard Pop Music	 3.4 6.5

1.1.3 Floor Damping

Damping can arise from any structural or non-structural component and is, therefore, extremely hard to predict theoretically. The above guides and recommendations are, therefore, based on experience, observations and some measurements. Table 1.2 shows these recommendations. A fair engineering judgement is required at the design stage to allow for reasonable damping to control small vibrations.

Table 1.2: Recommended Damping Values

Source	Floor Description	Damping (% Critical)
Murray (1975)	Composite Floors	1-20 (Depending on partitions, ceilings, finishes)
Allen & Rainer (1976) and CSA (1989)		3-12 (Depending on partitions, ceilings, finishes, applied dead loads)
CSA (1990)		3-6 (Depending on people on floor)
ISO (1992)		0.8-5.0 (Depending on continuity of floor slab, boundary conditions and partitions)
Allen et al (1979)	Concrete Floors	1-4 (Depending on floor type i.e. cast-in-place, precast; partitions, ceilings, finishes, applied dead loads)
CSA (1990)		2-4 (Depending on the presence of people on floor)
ISO (1992)		0.8-3 (Depending on floor type i.e. cast-in-place, precast prestressed)

1.2 Estimating The Fundamental Frequency Of Floors

There are many different methods for frequency estimation. Each has its merits and demerits, assumptions and application. However, only those methods will be discussed here which have been used or recommended by researchers.

1.2.1 Equivalent Beam Method (EBM)

Lenzen (1966) suggested the use of an equivalent beam model to estimate the natural frequency of any floor made of steel beams or joists and concrete slabs. This is because the behaviour of these floors is mainly one-way and thus a beam model with a single steel beam interacting with the concrete deck on top of width equal to the beam spacing is

considered to closely approximate the floor fundamental frequency using the following equation, Blevins (1995):

$$f_1 = \frac{\lambda^2}{2\pi}\sqrt{\frac{EI}{mL^4}} \qquad (1.1)$$

where f_1 = fundamental frequency of the floor;

λ = π for a simply supported beam, Blevins (1995);

λ = 4.73 for a fixed-ended beam, Blevins (1995);

EI = flexural rigidity of the floor;

L = floor span;

m = mass/length of the floor = ρA ;

ρ = density of the floor material;

A = area of cross-section of the floor.

Allen (1974) clarified that the above equation is particularly applicable for rigid support conditions and extended the method to flexible support conditions by suggesting the use of Dunkerly's Principle, Inman (1994), for each floor component as follows:

$$\frac{1}{f_1^2} = \frac{1}{f_{c_1}^2} + \frac{1}{f_{c_2}^2} + \ldots\ldots\ldots \qquad (1.2)$$

where f_1 = fundamental frequency of the total floor system;

f_{c_1} = first floor component frequency;

f_{c_2} = second floor component frequency and so on.

Allen and Rainer (1976), Allen et al (1985), CSA (1989), Murray (1975), Pernica and Allen (1982) have all applied this approach for estimating the fundamental frequency of composite floors. Allen et al (1979) applied this formula to two concrete floors and noted that the application of the formula is straightforward for simply supported precast T-beams. For cast-in-place beam and slab systems, they used the formula based on an

assumed simply supported T-section and found that the assumption of simple supports generally under-estimated the frequency. The British Standards Institution (BS8110:1985) recommends a width of $\frac{0.75L}{5}$ for the flange of this T-section where L is the beam span length. The width of beam , however, is not included in this assumption and, therefore, should be added to this value for calculation purposes. For composite floors, Wyatt (1989) suggested the effective width of slab to be the smaller of either $\frac{L}{4}$ or beam spacing. Allen-Murray (1993), on the other hand, suggest the smaller of $0.4L$ or beam spacing.

Composite floor slabs with steel decking can normally be regarded as continuous and resting over the supporting floor beams for dynamic analysis. The section properties are, therefore, based on a transformed moment of inertia. This assumption is applied even if the slab is not structurally connected to the beam flange, since the magnitude of the impacts are not sufficient to overcome the friction force between the elements. For the case of a girder supporting beams, it has been found that the beam seats are sufficiently stiff to transfer the shear. Thus, a transformed moment of inertia assumption can be used for the girder as well. But this will result in higher frequencies than those obtained using the girder moment of inertia only assuming the beams as point loads. However, there is no agreement on whether the beam supporting slab is to be used for the system frequency or the girder supporting beams. Normally, the smaller frequency will be assumed to be critical.

1.2.2 Plate Method (PM)

The fundamental frequency (f_1) of a rectangular plate having plan dimensions L_x and L_y ($L_x \geq L_y$) and thickness h is given by Blevins (1995) as:

$$f_1 = \frac{\lambda^2}{2\pi L_x^2}\sqrt{\frac{Eh^2}{12\rho(1-\nu^2)}} \qquad (1.3)$$

where $\lambda = \pi\sqrt{1+\frac{L_x^2}{L_y^2}}$ for a plate simply supported at its edges, Blevins (1995);

E = Young's modulus of elasticity;

ρ = density of the material of the plate;

ν = Poisson's ratio.

For the case of a plate simply supported only at its corners, λ can be obtained from Table 1.3 below.

Table 1.3: Variation of λ^2 with $\frac{L_x}{L_y}$, Blevins (1995)

$\frac{L_x}{L_y}$	λ^2
1.0	7.12
1.5	8.92
2.0	9.29
2.5	9.39

From Table 1.3, the variation of λ^2 with $\frac{L_x}{L_y}$ can be approximated by the following third order polynomial equation (using trendline or least-squares curve-fitting):

$$\lambda^2 \cong 1.5467\left(\frac{L_x}{L_y}\right)^3 - 9.82\left(\frac{L_x}{L_y}\right)^2 + 20.803\left(\frac{L_x}{L_y}\right) - 5.41 \quad (1.4)$$

Although most two-way floor systems can not be idealised as simply supported at their edges or corners, it can be reasonably assumed that the displacements along column lines are negligible in the first mode of vibration. This assumption, however, is only valid for continuous floors with similar span dimensions in both directions.

The method is straightforward for flat plate type floors but the method requires ribbed or waffle type floors to be transformed to an equivalent thickness in each direction. Since these floors have not been studied in the present research, further use of equation 1.3 for these floors will not be mentioned.

1.2.3 Static Deflection Method (SDM)

The natural frequency (f) of a simple spring-mass system is given by $f = \frac{1}{2\pi}\sqrt{\frac{K}{M}}$, where K is the stiffness of the spring and M is the lumped mass supported by the spring, Clough and Penzien (1993). The static deflection (Δ_s) of this system is given by $\Delta_s = \frac{Mg}{K}$, where g is the acceleration due to gravity acting on the mass. Thus the frequency (f) can be calculated by $f = \frac{1}{2\pi}\sqrt{\frac{g}{\Delta_s}}$. This concept can be applied to various floor systems.

This method, however, is well-suited to composite steel-concrete floor systems which consists of different components. In this approach, each floor component is considered separately as a single-degree-of-freedom (SDOF) system for the estimation of static deflections. The total deflection is given as the sum of the component deflections. Wyatt (1989) suggested a weighted average value of static deflection due to self weight and superimposed loads (y_w) as 3/4 of the maximum. The beam and girder-panel mode fundamental frequencies are then calculated by the following equation:

$$f_1 = \frac{1}{2\pi}\sqrt{\frac{g}{y_w}} \cong \frac{18}{\sqrt{y_0}} \qquad (1.5)$$

where y_0 = maximum static deflection in mm;

$y_w = \frac{3}{4} y_0$.

The system frequency is then assumed to be the lowest of the two modes calculated. Other details are given in the design guide by The Steel Construction Institute, Wyatt (1989).

Allen-Murray (1993) used the following formula for the fundamental frequency of the beam and girder-panel modes for composite steel-concrete floor systems:

$$f_1 = 0.18\sqrt{\frac{g}{\Delta_s}} \qquad (1.6)$$

where g = 9806.65 mm/sec^2;

Δ_s = static deflection of beam or girder in mm.

They also considered the critical mode to be the one with lowest frequency. However, they suggested to calculate a combined mode if the beam span (L_b) is less than 1/2 the girder span (L_g). For this mode the static deflections of both the beam and girder-panel modes are added together before using equation 1.6. They assumed beams and girders as simply supported for the purposes of estimating their deflections and the modulus of elasticity of concrete as 1.35 times higher than the calculated value to account for the increase in stiffness under dynamic loading.

For the combined mode, an effective beam-panel width (B_b) should be determined from equation 1.7 below and it should be less than $\frac{2}{3} L_{total}$, where L_{total} is the total floor length perpendicular to the beam :

$$B_b = 2\left(\frac{D_s}{D_b}\right)^{\frac{1}{4}} L_b \qquad (1.7)$$

where D_s is the slab rigidity given by $\frac{I_s}{n}$ (I_s is the slab moment of inertia per unit length and n is the modular ratio) and D_b is the beam rigidity given by $\frac{I_b}{spacing}$ (I_b is the beam moment of inertia and *spacing* is the distance between the centres of the beams).

If the total floor length is less than the effective beam-panel width, the combined mode is restricted and the system is effectively stiffened. This can be accounted for by reducing the girder deflections (Δ_g) to Δ_g' as below:

$$\Delta_g' = \frac{L_g}{B_b}\Delta_g \qquad (1.8)$$

where $0.5 \leq \frac{L_g}{B_b} \leq 1.0$.

Since it is very difficult to calculate deflections of two-way slab systems, this method can be best used in conjunction with the Finite Element Method where static deflections of the model can be closely approximated.

1.2.4 Concrete Society Method (CSM)

The Concrete Society (1994) has proposed the following formulae (Equations 1.9 - 1.13) to calculate the natural frequency of a two-way slab in the x-direction; the characteristics of the y-direction mode are determined by interchanging the x and y subscripts in these equations. This approach assumes two independent orthogonal modes in the two span directions and takes into account the effects of perimeter beams, the difference in stiffness in the two orthogonal directions and the type of slab. The method yields two natural frequencies corresponding to the two span directions.

It may be mentioned here that CSM determines the dynamic response of the fundamental mode which is then multiplied by a factor to give the total dynamic response. However, the method is based on EBM and there is no evidence of its validation against any experimental data or other methods.

In the following equations, n_x is the number of bays in the x-direction, each of span L_x, and n_y is the number of bays in the y-direction, each of span L_y. The flexural stiffnesses of the slab spanning in the two directions are EI_x and EI_y respectively and m is the mass per unit area. Equations for solid slabs will be given here; for others see the design handbook on post-tensioned concrete floors, Concrete Society (1994).

Slabs with Perimeter Beams

The effective aspect ratio (λ_x) of a slab panel is defined as:

$$\lambda_x = \frac{n_x L_x}{L_y}\left(\frac{EI_y}{EI_x}\right)^{\frac{1}{4}} \tag{1.9}$$

This, in turn, is used to calculate a modification factor (k_x) given by:

$$k_x = 1 + \frac{1}{\lambda_x^2} \tag{1.10}$$

The natural frequency of the slab with perimeter beams (f_x') is then given by:

$$f_x' = k_x \frac{\pi}{2}\sqrt{\frac{E I_y}{m L_y^4}} \tag{1.11}$$

Slabs without Perimeter Beams

For slabs without perimeter beams the frequency given by equation 1.11 is modified by the calculation of a frequency f_b given by:

$$f_b = \frac{\frac{\pi}{2}\sqrt{\frac{E I_x}{m L_x^4}}}{\sqrt{1 + \frac{E I_x L_y^4}{E I_y L_x^4}}} \qquad (1.12)$$

The natural frequency of the slab without perimeter beams (f_x) is then given by:

$$f_x = f_x' - (f_x' - f_b)\left(\frac{\frac{1}{n_x} + \frac{1}{n_y}}{2}\right) \qquad (1.13)$$

1.2.5 Finite Element Method (FEM)

The finite element (FE) method was first developed in 1956. It is a powerful numerical technique that uses variational and interpolation methods for modelling and solving boundary value problems. The method is extremely useful for structures with unusual geometric shapes.

A structure is made up of different members connected together. The FE method consists of dividing each member of the structure into a finite number of elements of predictable behaviour. Since the actual variation of the field variable (e.g. displacement, stress, temperature, pressure, or velocity etc.) inside the continuum is not known, the variation inside each element is assumed to be approximated by a simple function. These approximating functions are defined in terms of the values of the unknown field variables at the element nodes. The field equations for the whole continuum are then brought together in an assembly procedure, resulting in global mass and stiffness matrices, which describe the motion of the structure as a whole. Full details of the method are beyond the scope of this thesis, see Zienkiewicz (1981).

The FE method is systematic and modular and may be implemented on a computer to solve a wide range of practical vibration problems simply by changing the input to a

computer program. The method is capable of analysing higher modes of vibration and can model complex geometries with varying boundary conditions. Several large established commercial FE codes are available. However, the FE modelling of the floors in this thesis was carried out by I-DEAS and ANSYS structural dynamic analysis packages.

The FE method provides improved accuracy in calculating the natural frequencies of floors if the geometry and boundary conditions are correctly modelled. The degree of refinement in results is, therefore, superior to the methods which have been discussed previously. However, modelling the correct stiffness for all elements (geometry, density and modulii of elasticity) and boundary conditions (joint and support continuity) require experience and extensive modelling. Various models need to be studied if a higher order of accuracy is desired. Due consideration should be given to the small magnitude of dynamic deflections.

The FE method also allows sensitivity studies once the model is correlated with the experimental results. The most common method of comparing frequencies of experimental and analytical models is to plot them against each other. This plot should be a straight line of slope ± 1 for perfectly correlated data. Any deviation suggests errors in material properties, element type or boundary conditions. Therefore, several models need to be studied before arriving at a reasonable correlation. The method also allows estimation of static deflections and, therefore, frequency estimation using the static deflection approach.

The FE method is based on some assumptions (e.g. shape functions etc.) and approximations (e.g. geometry and material properties). The FE modelling and analysis may also be expensive and time consuming. Therefore, the FE results are not expected to correlate exactly with the experimental results and for all practical purposes a reasonable error is widely accepted by engineers.

This method has been previously successfully used for the validation of experimental frequencies of a composite floor, Osborne and Ellis (1990). However, details on modelling were not given because it was undertaken by a consultancy firm. Maguire and Severn (1987) have used this method for frequency estimation of a chimney, two water tanks and

four bridge beams. They found good correlation of their FE results with their experimental results. Gardner-Morse and Huston (1993) used this method for comparing their experimental frequencies of a pedestrian bridge and found good correlation. More recently, Chen and Aswad (1994) used this method to study the vibration of precast double-T floors. However, they did not carry out any field measurements and only used various loading functions in their study.

It has been established, therefore, that FEM can be successfully used for frequency estimation of prototype structures. However, it has not been used for the estimation of frequency of concrete floors. Moreover, the biggest uncertainty in the use of this method for concrete and composite floors is the correct material properties. Therefore, this method has been extensively studied in the present research to explore the possibility of estimating fundamental frequency of floors using a very simple model and to study the effect of various parameters on this frequency.

1.3 Objectives

The research carried out consisted of in-situ dynamic monitoring of 29 long-span floor slabs of different structural configurations with the following objectives:

i) to examine the importance of vibrations in the design of long-span floor slabs;
ii) to determine experimentally the dynamic characteristics of these floors;
iii) to compare and evaluate the existing design guides and the most commonly used analytical approaches for the calculation of fundamental frequency of floor slabs and to identify the most appropriate method for the estimation of the fundamental frequency of these floors;
iv) to study the use of the finite element method for frequency estimation of floors and to develop an "accurate" model correlated against experimental results;
v) to carry out a parametric/sensitivity study of the FE-models in order to limit the static deflections and span/depth ratios of long-span floors.

1.4 The Scope Of This Thesis

The research is limited to the fundamental frequency estimation of the following structural configurations of long-span suspended floor slabs:

i) Post-Tensioned Concrete 1-Way Spanning Solid Floor Slabs With Beams;
ii) Post-Tensioned Concrete Solid Flat Slab Floors;
iii) Pre-Tensioned Concrete Double-T Beam Floors;
iv) Composite Steel-Concrete Slab Floors.

Other types of floors (waffle, ribbed etc.) have not been included because they could not be tested in a reasonable number to obtain reliable conclusions.

The dynamic testing is carried out under serviceability conditions and only the vertical modes of vibrations are considered. The floors are assumed linear and elastic (due to small deflections and low floor frequencies caused by everyday normal activities).

1.5 Outline

Chapter 2 presents a description of the dynamic testing and data analysis procedures. A brief review of Modal Analysis is presented which is relevant to the present research. The testing equipment is described along with various precautions and requirements.

Chapter 3 presents and discusses the results of all the field tests. Typical experimental graphs (inertance transfer function, corresponding phase diagram and coherence function plots) are given.

Chapter 4 discusses the use of Finite Element (FE) modelling and analyses for the vibrations of long-span floor slabs. Results of various models are also compared for each floor tested. Details of a parametric/sensitivity study of the FE models is also given.

Various plots (fundamental frequency versus span/depth ratios, span lengths and static deflections) are presented which have been obtained from the results of the FE models.

Chapter 5 presents the comparison of experimental results with those obtained through the various analytical methods discussed in Chapter 1 and Chapter 4.

Chapter 6 presents the conclusions and recommendations based on the research. Guidance is provided by presenting the use of the various plots previously discussed in Chapter 4. Suggestions for furthering the research are given at the end of the chapter.

A detailed list of references has been provided. Two appendices are added to provide isometric sketches of the floor types tested with typical dimensions and calculations for frequency estimation for one floor in each category.

Chapter 2 DYNAMIC TESTING

This Chapter presents the method of vibration measurement used for obtaining experimental results for the floors tested. A brief review of the relevant parts of modal analysis which have been used in the research is presented along with the data analysis procedure.

2.1 Modal Analysis

This is a technique to determine experimentally the dynamic characteristics of structures. Of major interest in the present research is the fundamental frequency of floors which is extremely important in predicting and understanding their dynamic behaviour. Full details of the method are beyond the scope of this thesis and, therefore, only the important and relevant details will be briefly discussed here. For details, see Ewins (1995).

The main procedure is to excite the structure by means of an impulse hammer to measure the input force and use an accelerometer to measure the resulting vibration response. The force and acceleration signals are then Fourier transformed into frequency domain functions, from which the frequency response functions (also called transfer functions) are established. The modal parameters: which are the natural frequencies and damping ratios, can then be estimated by curve-fitting.

The fundamental idea behind modal testing is that of resonance. If a structure is excited at resonance, its response exhibits two distinct phenomena:

a) As the driving frequency approaches the natural frequency of the structure, the amplitude at resonance rapidly approaches a sharp maximum value;

b) The phase of response shifts by 180° as the frequency sweeps through resonance, with the value of the phase at resonance being 90°.

These physical phenomena are used to determine the natural frequency of the structure from measurements of the magnitude and phase of the structure's forced response.

Understanding modal testing requires knowledge of several areas. These include instrumentation, signal processing, parameter estimation and vibration analysis. It is important to understand some details of the signal processing performed by the spectrum analyser in order to carry out valid experiments. These are presented below.

2.1.1 Digital Signal Processing

A periodic time signal or function $x(t)$ of period T can be represented by an infinite Fourier series of sinusoids of the form given by:

$$x(t) = \frac{a_0}{2} + \sum_{n=1}^{\infty} (a_n \cos n\omega_T t + b_n \sin n\omega_T t) \qquad (2.1)$$

where $\omega_T = \frac{2\pi}{T}$ and the Fourier or spectral coefficients a_0, a_n and b_n are defined by:

$$a_0 = \frac{2}{T}\int_0^T F(t)dt \qquad (2.2)$$

$$a_n = \frac{2}{T}\int_0^T F(t)\cos n\omega_T t dt \qquad (2.3)$$

$$b_n = \frac{2}{T}\int_0^T F(t)\sin n\omega_T t dt \qquad (2.4)$$

The spectral coefficients represent frequency-domain information about a given time signal. These coefficients also represent the connection between Fourier analysis and vibration experiments.

Figure 2.1 shows a 3-D graph illustrating the addition of sine waves to give a composite waveform. Two of the axes are time and amplitude and the third is a frequency axis. These different views along the time domain (time history) and frequency domain (frequency response spectrum) allow for the visual separation of the individual components of the waveform.

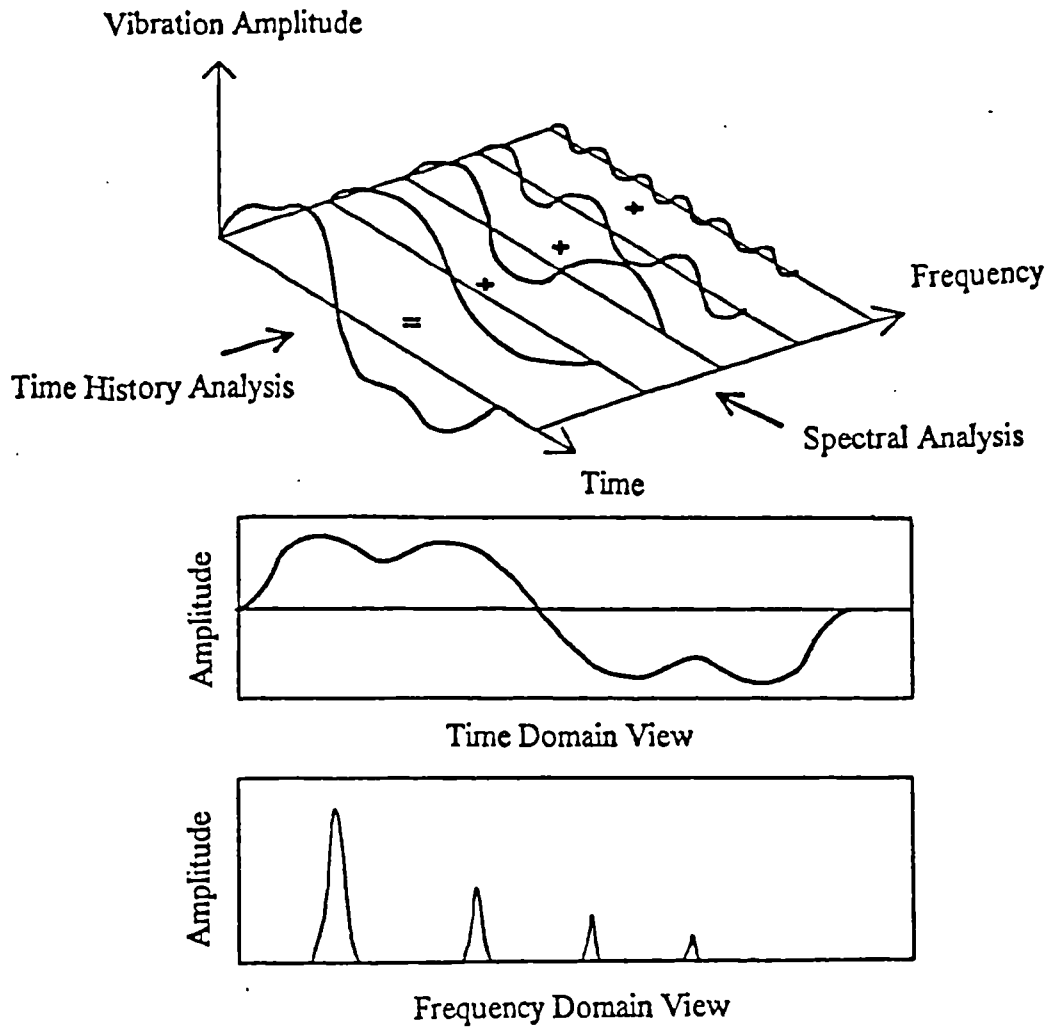

Figure 2.1: 3-D Representation of Vibrations

The analysis done in modal testing is performed in the frequency domain, inside the analyser. The analyser converts the analogue time-domain signal into digital frequency-domain signals and then performs the required computations with these signals. The method used to do this is called fast Fourier transform (FFT) which is essentially the Fourier series analysis explained above.

The analyser receives as its input the analogue output signals from the accelerometer and force transducers. These signals are then digitised and recorded as a set of N discrete values, which are evenly spaced in the period T during which the measurement is made. Assuming the sample as periodic in T, the analyser then calculates the above spectral coefficients of these signals before analysing these signals in the frequency-domain. For analytical details, see Ewins (1995). A typical transient time history and its Fourier transform is shown in Figure 2.2.

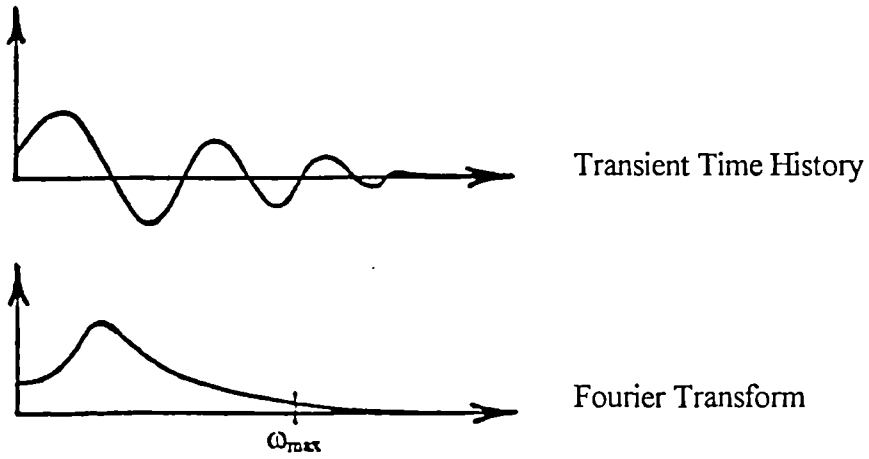

Figure 2.2: Transient Time History and Fourier Transform

The range of the frequency spectrum is 0-ω_{max} (Nyquist frequency) given by $\omega_{max} = \frac{\pi N}{T}$, where N is the number of discrete values and T the sample length. The resolution of lines in the frequency spectrum is given by $\Delta\omega = \frac{\pi}{T}$. As the size of transform (N) is generally fixed for a given analyser (2^n e.g. 256, 512, 1024, etc.), the frequency range covered and the resolution is determined solely by the time length of each sample.

Some of the most important features of digital Fourier analysis, resulting from discretisation approximation of original continuous time history signals, which affect measurements, are discussed briefly below.

2.1.1.1 Sampling And Aliasing

The signals are sampled at different equally spaced time intervals to produce a digital record in the form of N set of numbers. Improper sampling time may cause an error called aliasing when calculating digital Fourier transforms. Aliasing is the misrepresentation of the analogue signal by the digital record. Thus, if the sampling rate is too slow, the digital representation will cause high frequencies to appear as low frequencies (Figure 2.3). This can be avoided by subjecting the analogue signal to an anti-aliasing filter which allows low frequencies through, by maintaining a reasonably small sampling interval. A reasonable sampling rate is two times the highest frequency of interest.

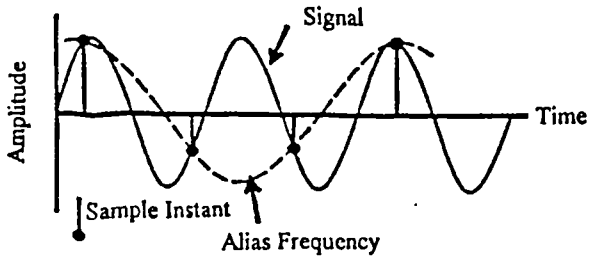

Figure 2.3: Aliasing

2.1.1.2 Leakage

The digital analysis is feasible only if the periodic signal is sampled over a finite time. The digital Fourier transform of finite length signals assumes that the signal is periodic within the sample record length. Thus the actual frequency leaks into a number of fictitious frequencies because a complicated signal containing many different frequencies cannot simply be cut at an integral multiple of its period. Leakage can be corrected by the use of a window function. Figure 2.4 illustrates this phenomenon.

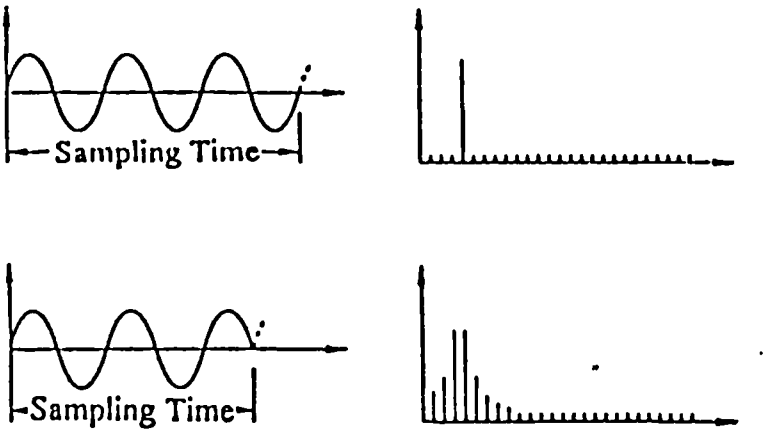

Original Signals (Time Domain)

Fourier Transforms (Frequency Domain)

Figure 2.4: Leakage

2.1.1.3 Windowing

This involves multiplying the original analogue signal by a time function. This forces the signal to be zero outside the sampling period. There are many different types of windows but the most commonly used window for general purposes is the Hanning window. These windows reduce leakage if properly applied to the signals. Figure 2.5 illustrates the use of windowing.

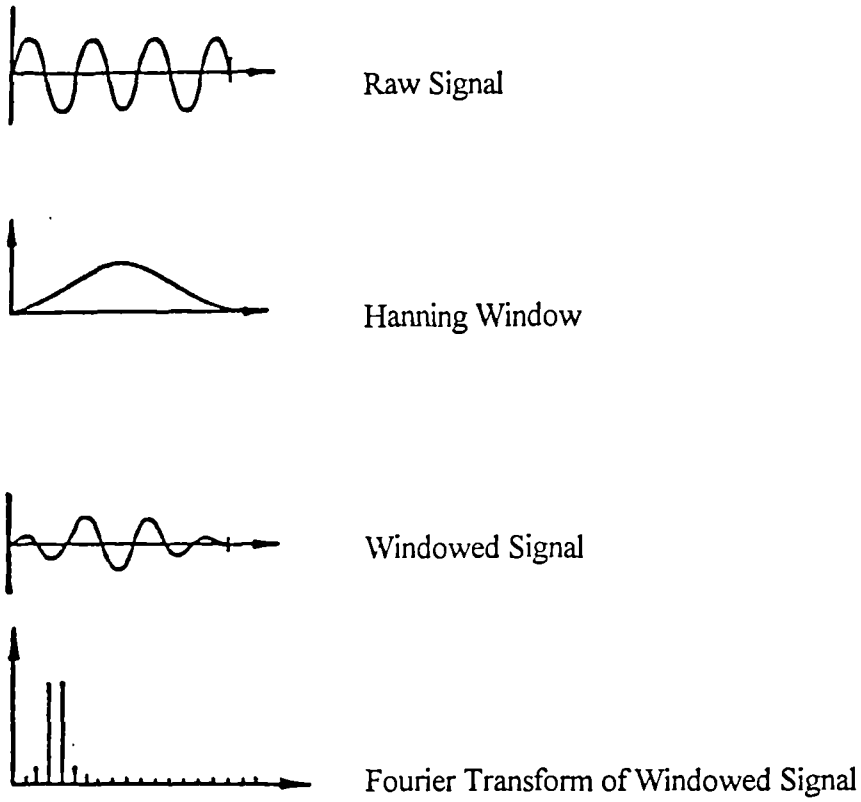

Figure 2.5: Hanning Window and its Effect on a Periodic Signal

2.1.1.4 Averaging

It is necessary to perform an averaging process, involving several individual time records or samples before a result is obtained which can be used with confidence. The two major considerations which determine the number of averages required are the statistical reliability and the removal of spurious random noise from the signals.

2.2 Hammer Testing

In this type of dynamic testing, the floor slabs are excited by an instrumented hammer with a force transducer and the response is measured with an accelerometer. A spectrum analyser is used to extract this information from the hammer signal and compare it to other signals generated by an accelerometer located at various points of interest on the test

object. The analyser instantly displays the inertance transfer function, phase and coherence functions which can be used to study the dynamic behaviour of the test structure.

Hammer testing has not been used previously in the case of suspended concrete slab floors. However, it's use is more common in the case of the structural analysis of piles, and modal analysis of mechanical parts (gear boxes, turbine blades etc.). It has been used previously, though, for a composite floor, Osborne and Ellis (1990); a chimney, two water tanks and four bridge beams, Maguire and Severn (1987); and a pedestrian bridge, Gardner-Morse and Huston (1993). The method was employed for present research because it is the simplest, quickest, easiest, inexpensive and most portable method available. The use of hammer also avoids the mass loading problem. It has the added advantage of being able to measure the force input. This normalised response measurement per unit of force input, therefore, allows subsequent response calculations of the floor slab for a given force. It is assumed, however, that the floors tested are linear and excited only in their linear range. Further, the response of the floors which have been excited by the hammer impulse is identical to the free vibration response to certain initial conditions and contains excitations at a number of the floor's natural frequencies within a selected frequency range.

2.2.1 Equipment

The equipment required to carry out the testing was very compact and straightforward to use after initial familiarity. The following are the main components of the testing equipment:

i) *Instrumented Sledge Impulse hammer*

This is a 5.4 kg (12 lbs) impact hammer (Figure 2.6) designed to excite the suspended floor slabs into motion with a definable force impulse (Figure 2.7). It has an integral piezo-electric force sensor/transducer of the Low Impedance Voltage Mode (LIVM) type to generate the input force signal. This sensor utilises self-generating quartz crystals to generate an output signal (in mV/lb) which is exactly analogous to the impact force of the hammer when it strikes the test

structure. The peak impact force is nearly proportional to the hammerhead mass and the impact velocity. The stress created by the input force impulse results in a strain (motion) in other parts of the test structure and the relationship between this input stress and resulting strain define the transfer characteristics of the structure. This signal thus quantifies the input or forcing function, identifying its phase, amplitude and frequency content, necessary to describe exactly the mathematical form of the impulse, by a spectrum analyser or fast Fourier transformation techniques. The sensor is powered by the constant current type power source of the spectrum analyser. The hammer contains an integral integrated-circuit (IC) amplifier which converts the very high impedance voltage signal from the quartz crystals to a low impedance level output signal which can be read out by spectrum analyser. The hammer sensitivity is 1.17 mV/lb-F and its designed nominal full-scale impact range is 5000 lbs-F with a maximum impulse of 8000 lbs-F.

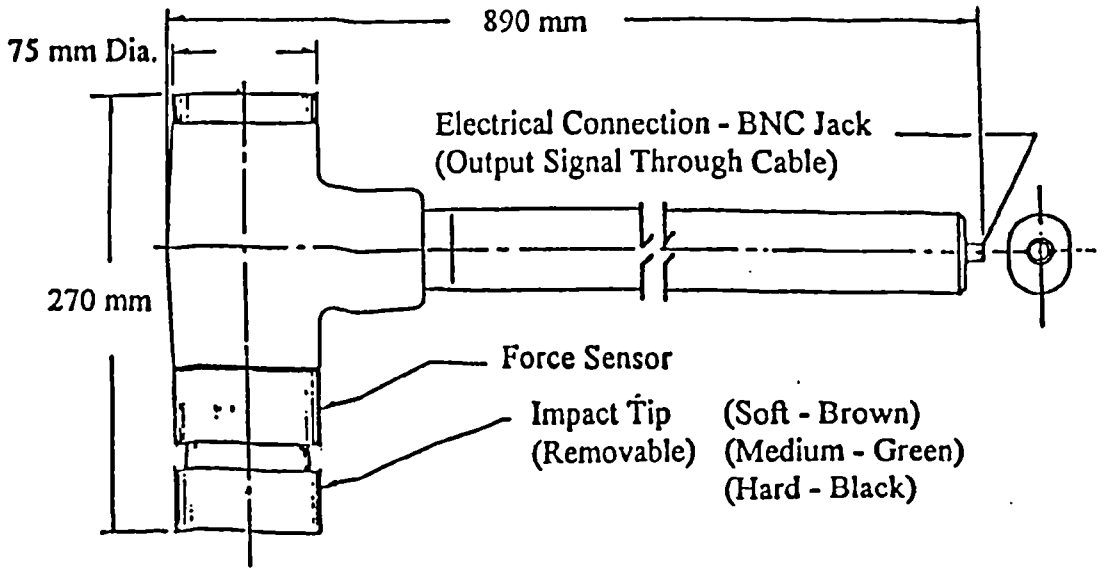

Figure 2.6 Hammer Details

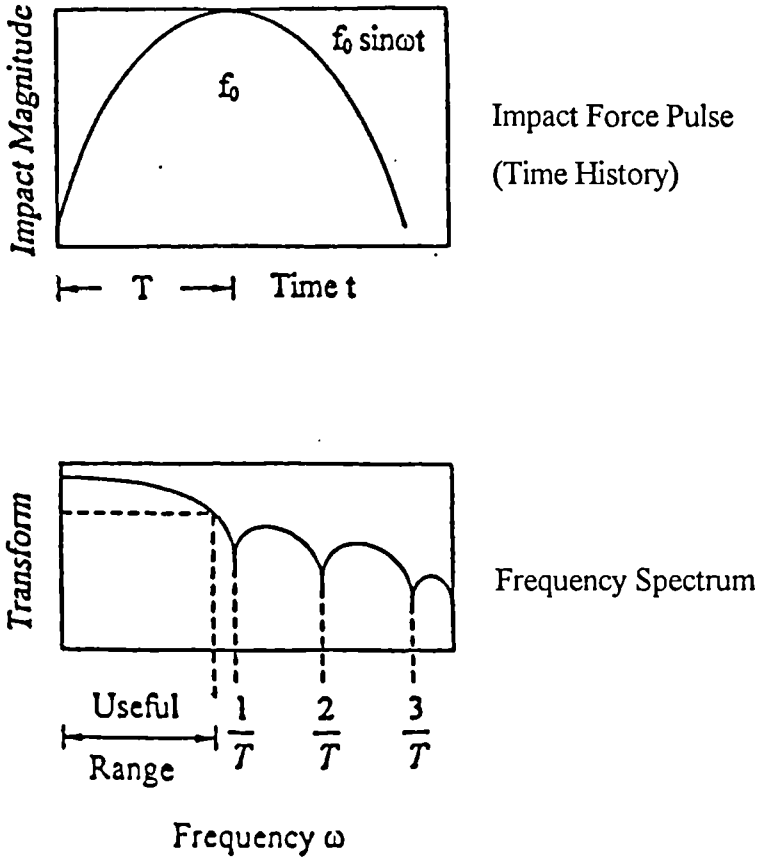

Figure 2.7: Time and Frequency Response of a Hammer Impact

Impact Tips

A hammer hit to the test structure excites a broad range of frequencies depending on the impact tip used. This tip (soft, medium, hard, or tough) is attached to the force sensor and transmits the force of the hammer strike into the sensor. It also protects the sensor face from damage.

The upper frequency limit excited by the hammer is decreased by increasing the hammerhead mass and is increased with increasing stiffness of the tip of the hammer. The soft impact tip provides mostly the low frequency excitation while the tough tip (being very rigid) gives greater high frequency content to the input forcing function. As the hardness of the tip increases, the impact pulse rise time is faster thereby producing a higher frequency energy spectrum. The choice of a tip greatly depends on the response (low/high) in terms of frequency excitation in the

input impulse which in turn depends on the mass and stiffness of both the hammer and the test structure. Since long-span floors are light and flexible with low frequencies, they require less total energy to excite a number of modes into resonance. Therefore, a soft tip is found to be capable of transforming sufficient energy in exciting the floor to obtain adequate response signals in the frequency range of interest. Figure 2.8 below shows the spectra for various tips.

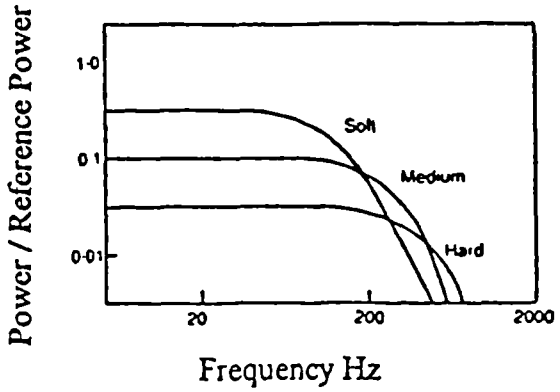

Figure 2.8: Spectra for Various Hammer Tips

Precautions

* When striking the test floor, use direct blows rather than glancing blows;
* Try to strike the test object squarely with the center of the impact tip;
* Keep the hammer head perpendicular to the surface of the test object being excited;
* Do not strike with the edge of the impact tip;
* Use only enough force in the blow to adequately excite the test structure. The magnitude of the signals from the accelerometer located at other locations on the structure will determine the level of excitation;
* Avoid multiple impacts because they cause zeroes in the frequency response spectrum due to the periodic nature of the signal.

ii) *High Sensitivity Accelerometer*

An accelerometer measures the accelerations produced by an impact. Appropriate sensitivity is essential when measuring low frequency floors with low acceleration

levels, because they can be easily excited by ambient conditions such as wind or pedestrian movement etc.

A piezo-electric accelerometer is basically a rigid spring-mass system with essentially zero damping to measure the motion. It contains a seismic mass, made from a very dense tungsten alloy, a quartz element and an amplifier. The seismic mass is tightly pre-loaded against pure synthetic quartz crystals by means of a special pre-load screw under a high compressive force to avoid absolutely no relative motion between the mass, crystals and base. This keeps the non-linearity low and the natural frequency high.

The accelerometer used features a LIVM operation (as in the hammer). Acceleration acting upon the mounting base is transferred to the seismic mass through the crystals creating a force (F = ma). This force stresses the crystals (by compression or release of some pre-load, depending upon the sense of input acceleration) and produces a voltage signal exactly proportional to the input acceleration. This very high impedance signal is fed to the gate of a tiny on-board IC amplifier which drops the output impedance level ten orders of magnitude allowing this instrument to drive long cables without appreciable effect on sensitivity and frequency response. As the accelerometer is powered, the amplifier is turned on at a specific bias voltage. When the accelerometer senses acceleration, the resultant signal is superimposed upon this bias voltage and may be connected directly to the spectrum analyser. The spectrum analyser supplies power to operate the integral IC and separate the signal from the direct-current (DC) bias of the internal amplifier. The accelerometer also features signal ground isolation from the mounting surface to avoid annoying ground loops and hermetic sealing for normal operation in moist and dirty environments. The range of the accelerometer is 50g with a sensitivity of 101 mV/g and frequency range of 0.5-3500 Hz. Figure 2.9 shows the accelerometer used in testing.

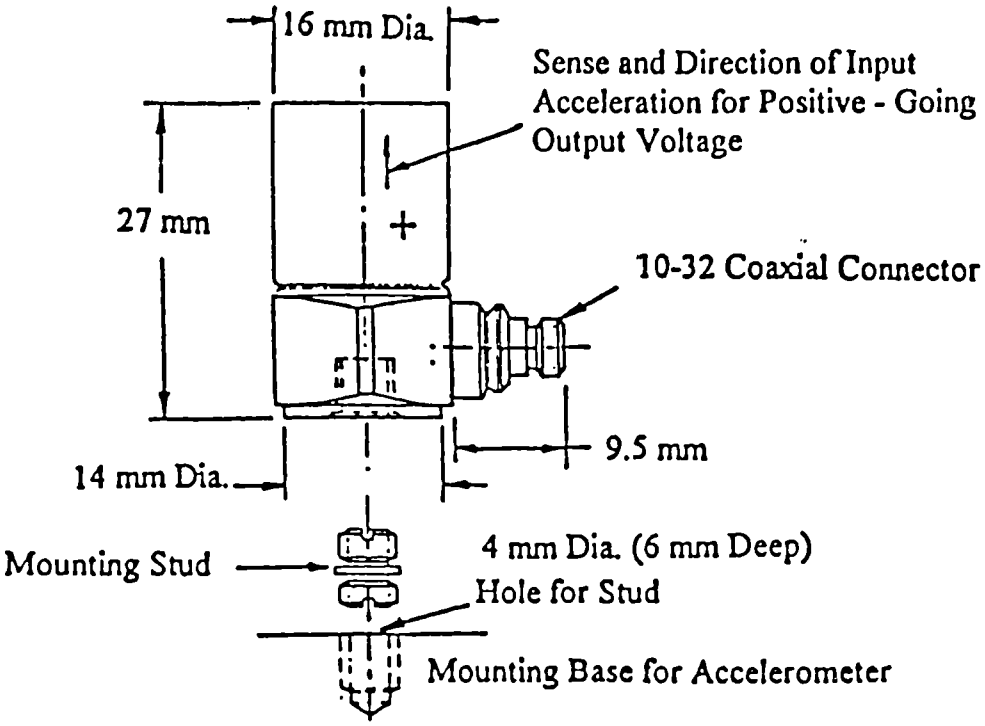

Figure 2.9: Accelerometer Details

Installation

It is necessary to prepare a flat mounting area to install the accelerometer. The flat mounting surface ensures intimate contact between accelerometer base and mounting surface for the best high frequency transmissibility and accuracy. The accelerometer is threaded into the mounting area with a mounting stud after a light coating of silicon grease is spread on either side of the mating surfaces.

Precautions

* Avoid dropping or striking the accelerometer, especially against rigid materials such as concrete and metals. Very high shock induced overloads can damage the built-in amplifier;
* The threaded locking collar of the cable connecting with the accelerometer should be tight enough to avoid loosening under prolonged vibration usage.

iii) *Cables*

The hammer and accelerometer are connected to the spectrum analyser by cables. Bayonet-Neal-Conkenal (BNC) sensor connectors are provided in the spectrum analyser and at the end of the hammer handle to plug in the cable (Figure 2.6). The accelerometer has a 10-32 connector and thus a BNC to 10-32 connector cable is used to connect the accelerometer with the spectrum analyser (Figure 2.9).

Precautions

* Do not allow cables to hang loosely or vibrate unrestrained. Forces generated by such motion may strain the accelerometer base causing spurious output from the crystals;
* Avoid stressing the cables by tying them down to a fixed surface near the accelerometer mounting area.

iv) *Frequency Response Spectrum Analyser*

This is an instrument used for data acquisition and detailed system analysis. The analyser used acts as both a digital storage oscilloscope and as a FFT analyser (converting a signal in the time domain to the frequency domain) with powerful waveform processing capabilities. It manipulates data and calculates complex mathematical processes. It is powered by an internal Nickel-Cadmium (NiCad) battery which can be recharged. It allows the observation of input signals both in the time and frequency domains. Data stored in the time domain can be further reprocessed and stored in the frequency domain.

The analyser receives continuous analogue voltage signals from the output of the transducers where it is proportional to both acceleration and force signals. These signals are filtered, digitised and transformed into the frequency domain for analysis. The analyser has facilities to perform analogue to digital signal conversion, signal filtering for anti-aliasing effects, averaging, windowing, calculating the transfer function, phase and coherence functions and post-processing time-domain data to frequency-domain etc.

2.2.2 Procedure

The test procedure used in the experimental programme is very simple, repetitive and quick. It can be explained in steps as follows:

Selection Of The Test Panel

A typical representative panel of the floor is identified. The selection depends on the plan layout of the floor and dimensions. A panel with the longest spans would give the lowest fundamental frequency and so every effort is made to select such a panel with the least obstructions.

Marking The Test Grid

A grid of reasonable size is marked on the test panel. An aspect ratio of one or as close to one as possible is maintained, depending on the size of the panel. The more grid points, the more accurate are the average values of the experimental results.

Selecting The Accelerometer / Hammer Impact Location

The accelerometer is placed on a grid point that gives good response (i.e. not near a nodal line) at the natural frequencies of interest. The choice can be quickly made by testing a few points. Normally, the midspan point gives the best response and the accelerometer is placed at this point to measure the vibrations. In the case of floors with false flooring, the accelerometer is moved from point to point on the grid and only a few floor panels are removed near the midspan for exciting the floor with the hammer.

Exciting The Floor

The floor is excited with the hammer at the various grid points in turn. A minimum of five impacts may be used at each grid point to obtain an average value of the response at these locations.

Storing The Data

The spectrum analyser performs the analysis and provides plots of the transfer function, phase and coherence functions. A frequency band-width of 25 Hz may be used for the

analyser for good resolution of low frequencies of the floors. Data for each test grid location measured in the above manner is then stored on the spectrum analyser. It is later transferred to a personal computer for further analyses to extract the dynamic properties.

2.3 Data Processing

After obtaining the transfer function and phase for each grid location for each test through the spectrum analyser, the following procedure was used to extract the modal parameters (fundamental natural frequencies and damping ratios) of all the test floors.

Curve-Fitting

A multi-degree-of-freedom (MDOF) curve-fit program, MODENT, was used to extract the fundamental frequency and corresponding damping ratios for all the grid locations of each test. For procedural details see MODENT (1993) manuals.

The MDOF curve-fitting used a least-squares approach and is carried out for each mode of vibration in the region of its natural frequency. It can identify closely spaced modes because the transfer function in the region of a mode is dominated by its resonating frequency. In the frequency range around the resonant peak, it is assumed that the plot is due to the response of a damped MDOF system due to a harmonic input at and near that natural frequency. Thus frequencies are obtained by noting the location of the peaks and examining the value of phase at these frequencies, which ideally should be 90°.

The damping ratio (ξ) associated with each peak is determined by the Half-Power (Band Width) technique by the relation $\xi = \frac{\beta_b - \beta_a}{2}$, Inman (1994), Figure 2.10.

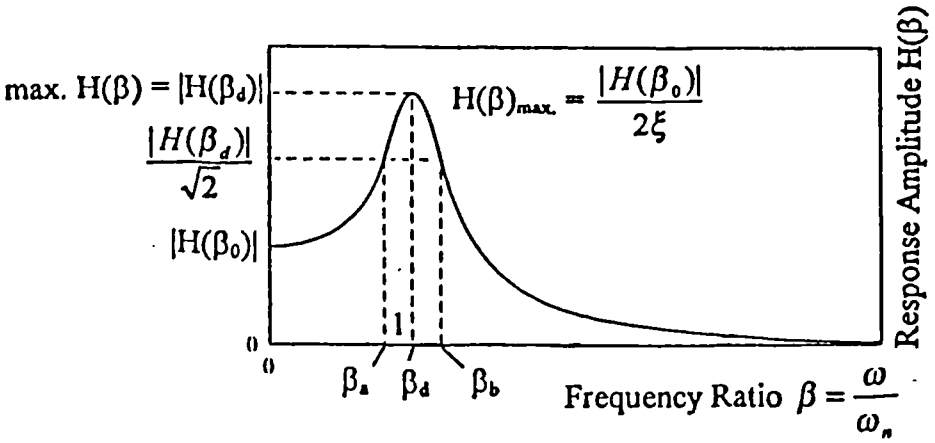

Figure 2.10: Estimating Damping

Maximum amplitudes occur in damped vibrations when the forcing frequency (ω) equals the system's damped natural frequency (ω_n). In Figure 2.10, β_a and β_b are the frequency ratios at which the response amplitude is reduced to $\frac{1}{\sqrt{2}}$ times its peak value, β_d is the frequency ratio at which the maximum amplitude occur. The accuracy with which the damping ratio is determined using this method depends on the frequency resolution in the original frequency response data.

Averaging

The results for frequency and damping for each grid location were averaged to obtain a reliable estimate of these properties.

Caution

Although the MODENT software estimates frequency and damping reliably by comparing all the data files for each test grid location, in many cases, however, it is necessary to study the phase diagrams closely. This is because of interference in the data due to unavoidable ambient vibrations and noise. Therefore, every test was analysed a number of times for a more reliable and average estimate of frequency and damping.

Chapter 3 EXPERIMENTAL RESULTS

This Chapter presents the field test results of the floor slabs tested in the experimental programme. The experimental technique and methods of analysis have been presented in Chapter 2.

Although the choice of floors was governed by availability, every effort was made to test as many floors as possible. The floors tested are divided into four main categories as follows:

i) Post-Tensioned Concrete 1-Way Spanning Solid Floor Slabs With Beams
ii) Post-Tensioned Concrete Solid Flat Slab Floors
iii) Pre-Tensioned Concrete Double-T Beam Floors
iv) Composite Steel-Concrete Slab Floors

Many owners of office buildings were reluctant to grant access for fear of causing alarm to occupants. Therefore, most of the floors tested were either unoccupied offices at the time or car parks. In many cases the designers and owners were reluctant to provide all information including layout drawings and material properties. Most of those who did provide drawings did not want them to be included in the thesis or published in the research papers. Therefore, only a general plan layout drawing with a typical cross-section is given for each category. Structural details for each floor are given individually along with the experimental fundamental natural frequency. Although the main theme of the research was the estimation of fundamental natural frequency, experimental damping estimates are also given. Typical experimental graphs (transfer function, phase and coherence function plots) are given for each individual floor. General comments on individual floor testing and results are also given.

3.1 Post-Tensioned Concrete 1-Way Spanning Solid Floor Slabs With Beams

Only four (4) floors of this type could be tested. All of them had beams along the long-span direction. Figure 3.1 shows a general layout for this floor type with a typical cross-section (see also Appendix A). Specific dimensions are given for each floor individually.

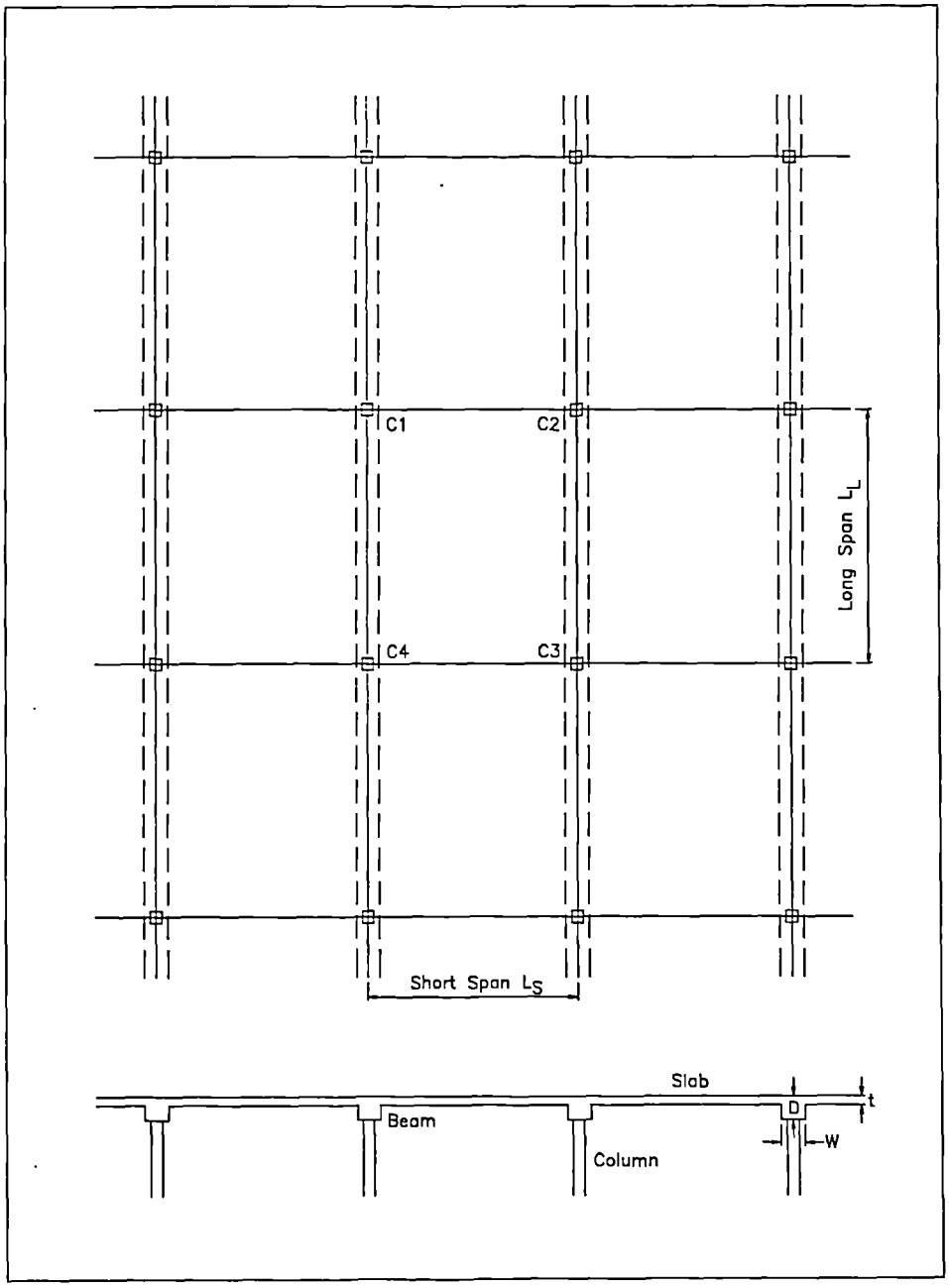

Figure 3.1: Typical Plan Layout and Cross-Section

3.1.1 Wycombe Entertainment Centre Multi-Storey Car Park, Level 1+

Structure Description (see Figure 3.1)

Location	:	High Wycombe
Typical panel	:	L_S = 7.305 m, L_L = 12.05 m
Beams	:	D = 650 mm, W = 665 mm
Columns	:	C1 = C2 = 300 mm x 800 mm
		C3 = C4 = 1600 mm x 450 mm
Slab	:	t = 210 mm
Finishing	:	None
Test date	:	Tuesday 21 April 1992

Test Results

Fundamental natural frequency	:	10.2 Hz
Floor damping	:	2.5 % critical

Comments

At the time of the test, there was some noise due to the construction work in progress at the site and also due to the generator used for power supply to the testing equipment. The accelerometer sensitivity was, therefore, increased to measure floor vibrations due to the hammer impact. The effect of noise is visible in the coherence function.

Measurements were taken when no vehicle was parked on the floor. The presence of vehicles could reduce the frequencies due to the added mass. The floor damping was low but may be increased with the presence of vehicles. Low damping was also due to the fact that the floor was newly constructed uncracked solid concrete with no finishes or suspended ceilings etc.

Graphs

Figure 3.2 shows the typical experimental inertance transfer function, corresponding phase diagram and coherence function plots.

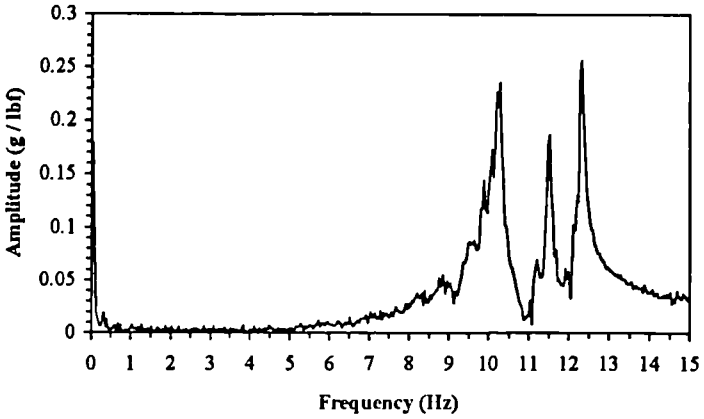

Transfer Function

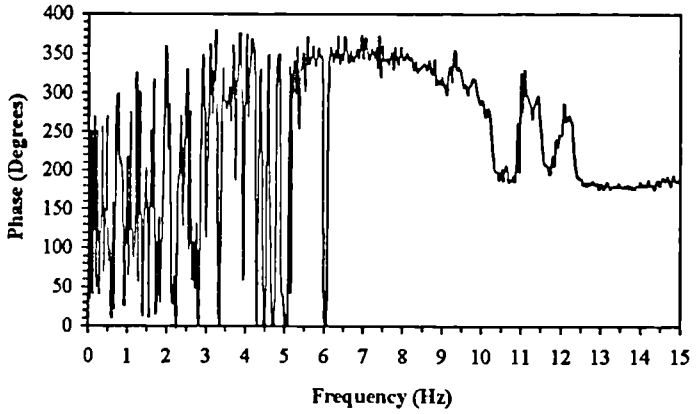

Phase

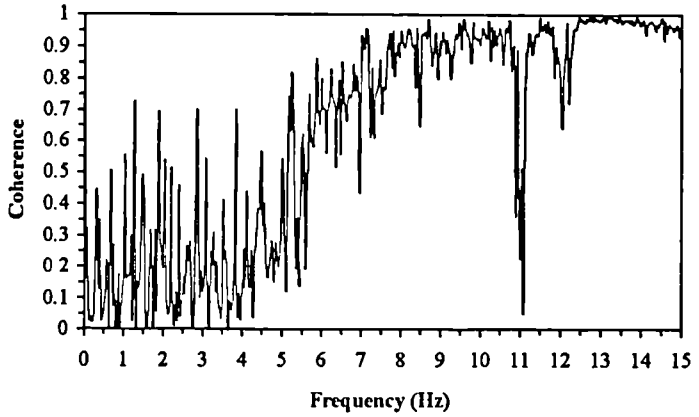

Coherence Function

Figure 3.2: Typical Transfer Function, Phase and Coherence Function

3.1.2 Wimbledon Town Hall Development Car Park, Basement-1

Structure Description (see Figure 3.1)

Location	:	Wimbledon
Typical Panel	:	L_S = 7.5 m, L_L = 14.0 m
Beams	:	D = 500 mm, W = 1200 mm
Columns	:	C1 = C2 = C3 = C4 = 500 mm x 500 mm
Slab	:	t = 200 mm
Finishing	:	None
Test Date	:	Thursday 3 December 1992

Test Results

Fundamental natural frequency	:	5.8 Hz
Floor damping	:	2.1 % critical

Comments

The car park is close to the London Underground railway line and so the vibrations due to the moving trains have affected the results. Again, the accelerometer sensitivity was increased to measure hammer impacted floor vibrations. The effect of noise is visible in the coherence function.

Measurements were taken when no vehicle was parked on the floor panel tested. However, there were a few vehicles parked on other floor panels nearby. Their effect on frequency and damping could not be ascertained because testing could not be repeated for the case of no vehicle on the floor. However, the floor frequency and damping were quite low and, therefore, resulted in perceptible vibrations. Low damping was also due to the absence of any finishing and suspended ceilings etc.

Graphs

Figure 3.3 shows the typical experimental inertance transfer function, corresponding phase diagram and coherence function plots.

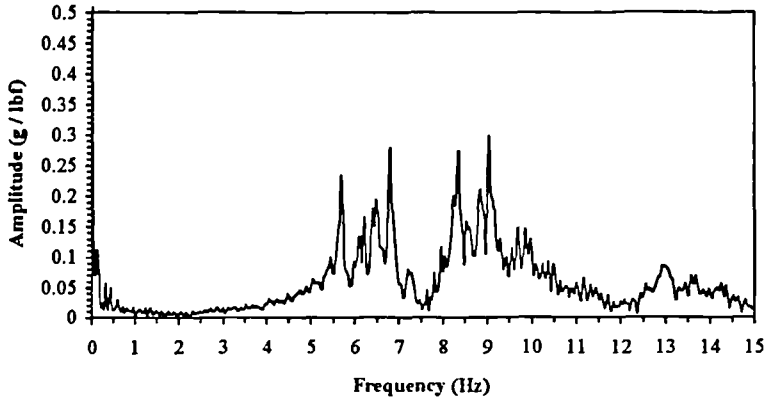

Transfer Function

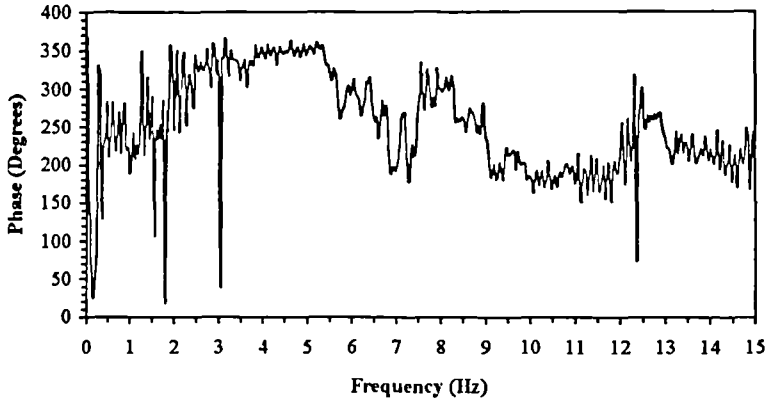

Phase

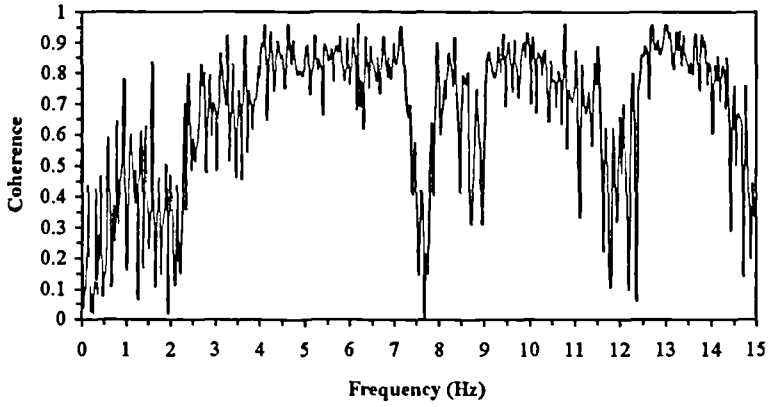

Coherence Function

Figure 3.3: Typical Transfer Function, Phase and Coherence Function

3.1.3 The Hart Shopping Centre Car Park, Level-1

Structure Description (see Figure 3.1)

Location	:	Fleet
Typical panel	:	L_S = 7.2 m, L_L = 8.0 m
Beams	:	D = 375 mm, W = 1200 mm
Columns	:	C1 = C2 = C3 = C4 = 300 mm x 600 mm
Slab	:	t = 200 mm
Finishing	:	Asphalt Layer
Test Date	:	Sunday 6 December 1992

Test Results

Fundamental natural frequency	:	11.2 Hz
Floor damping	:	1.9 % critical

Comments

At the time of the test, there was a strong wind and light drizzle coming in through the floor wall openings. This caused some ambient vibrations and, therefore, the accelerometer sensitivity had to be increased. Also, some floor area was wet during testing and thus any hammer impact on the wet area also produced noise due to splashing of water. Data for a few grid points was, therefore, affected. It may, however, be noted that the coherence function plot shows a better response of floor when compared with previous floors.

Measurements were taken when a few vehicles were parked near the test panel. Moreover, other vehicles continued to move around the floor for parking and exiting purposes. The floor damping, however, did not show any improvement due to the presence of an asphalt layer, when compared with the previous car parks.

Graphs

Figure 3.4 shows the typical experimental inertance transfer function, corresponding phase diagram and coherence function plots.

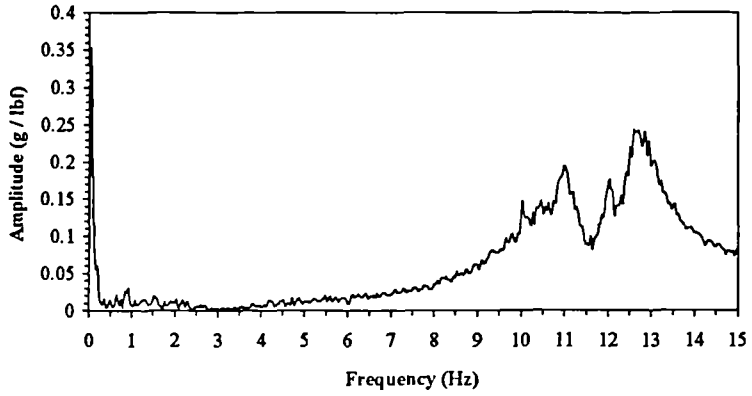

Transfer Function

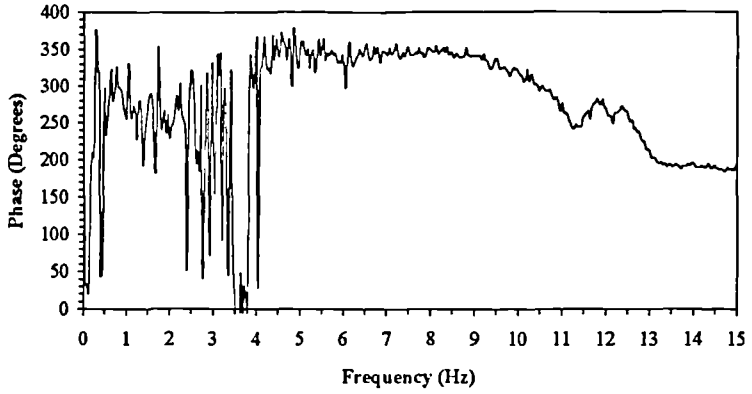

Phase

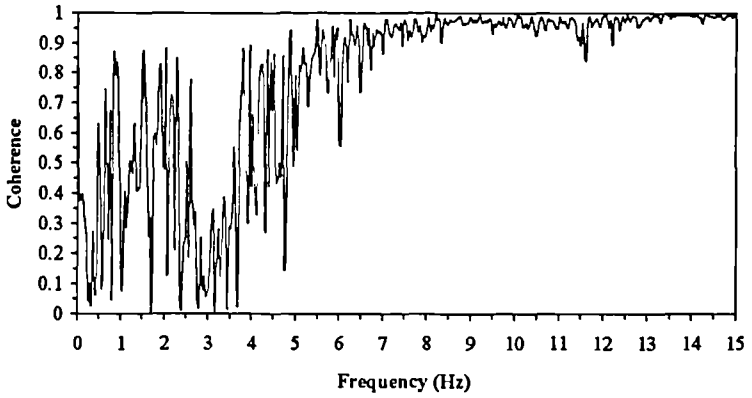

Coherence Function

Figure 3.4: Typical Transfer Function, Phase and Coherence Function

3.1.4 The Exchange Shopping Centre Multi-Storey Car Park, Level-1

Structure Description (see Figure 3.1)

Location	:	Ilford
Typical panel	:	L_S = 7.2 m, L_L = 15.6 m
Beams	:	D = 700 mm, W = 600 mm
Columns	:	C1 = C2 = 600 mm x 400 mm
		C3 = C4 = 400 mm x 800 mm
Slab	:	t = 160 mm
Finishing	:	None
Test Date	:	Thursday 10 December 1992

Test Results

Fundamental natural frequency	:	7.3 Hz
Floor damping	:	3.7 % critical

Comments

At the time of the test, there was a strong breeze coming in through the floor wall openings. This caused some ambient vibrations and, therefore, the accelerometer sensitivity had to be increased. The coherence function indicates the effect of this disturbance.

Measurements were taken when no vehicle was parked on the floor. The floor damping was more than that of previous floors, mainly due to the presence of a storage room near the floor panel tested and the side ramp for vehicles. The presence of the storage room and the ramp resulted in a breakage of the continuous nature of the floor and acted as dampers.

Graphs

Figure 3.5 shows the typical experimental inertance transfer function, corresponding phase diagram and coherence function plots.

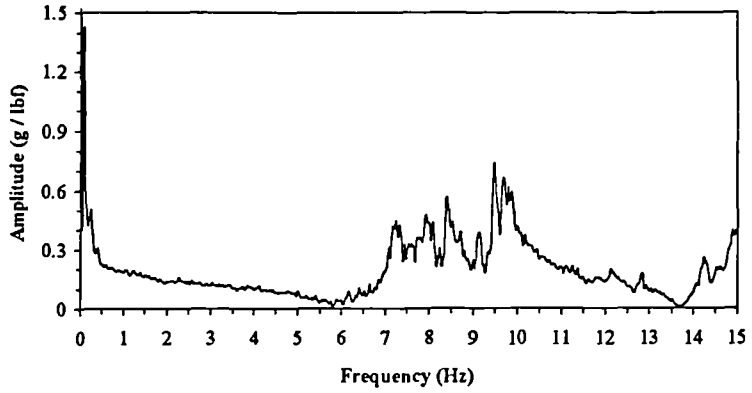

Transfer Function

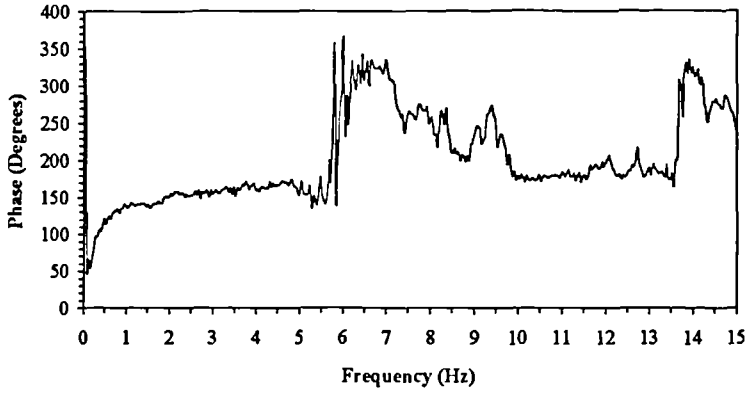

Phase

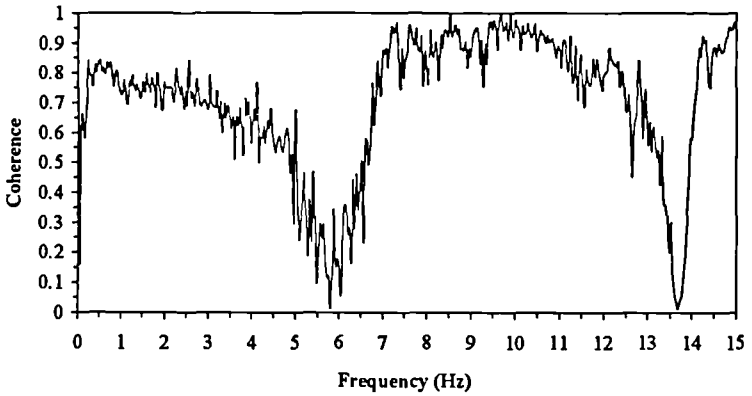

Coherence Function

Figure 3.5: Typical Transfer Function, Phase and Coherence Function

3.2 Post-Tensioned Concrete Solid Flat Slab Floors

Only twelve (12) floors of this type could be tested. Figure 3.6 shows a general layout for this floor type with a typical cross-section (see also Appendix A). Specific dimensions are given for each floor individually.

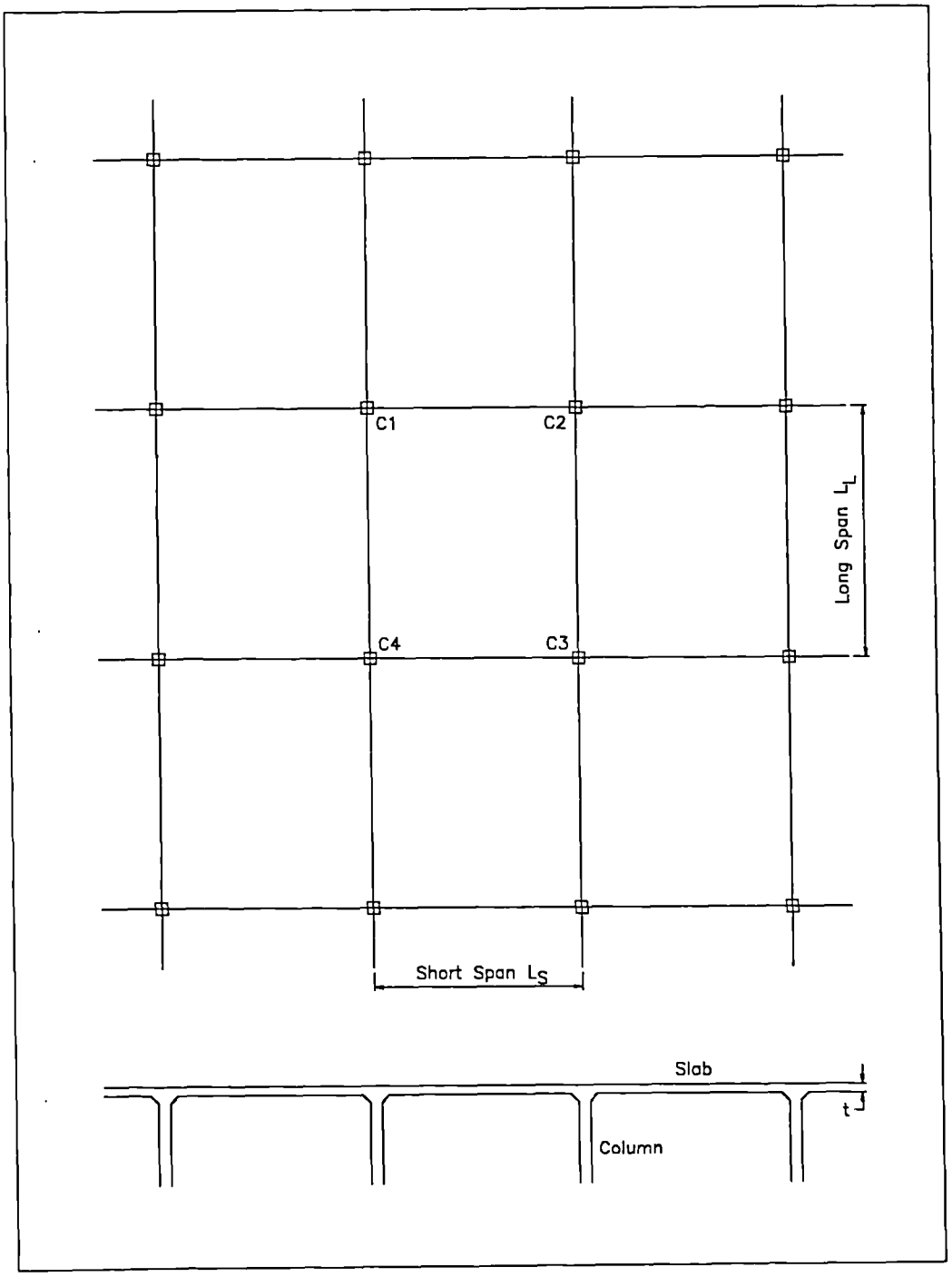

Figure 3.6: Typical Plan Layout and Cross-Section

3.2.1 Vantage West Car Park

Structure Description (see Figure 3.6)

Location	:	Hammersmith
Typical panel	:	$L_S = 7.2$ m, $L_L = 8.4$ m
Slab	:	t = 225 mm
Columns	:	C1 = C2 = C3 = C4 = 360 mm x 360 mm
Finishing	:	None
Test date	:	Friday 7 August 1992

Test Results

Fundamental natural frequency	:	8.1 Hz
Floor damping	:	4.6 % critical

Comments

The car park is close to the approach path of London's Heathrow Airport and motorway M4. Therefore, noise and vibrations due to the flying aeroplanes and road traffic have affected the results. The effect of noise is visible in the coherence function.

Measurements were taken when no vehicle was parked on the floor panel tested. The floor damping could not be estimated accurately due to the closely spaced modes and the interference due to noise in the data.

Graphs

Figure 3.7 shows the typical experimental inertance transfer function, corresponding phase diagram and coherence function plots.

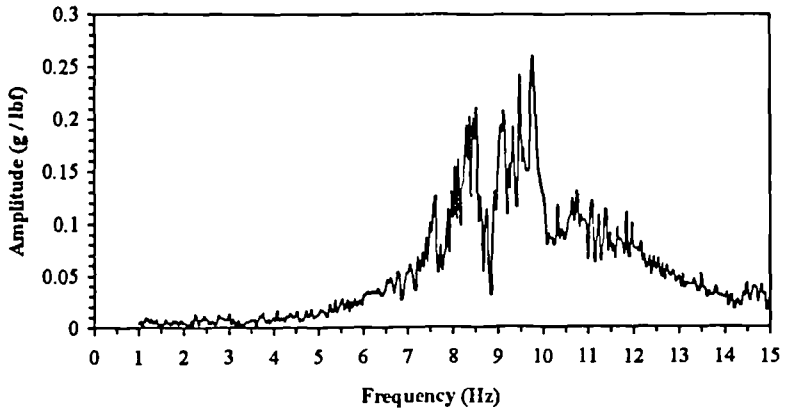

Transfer Function

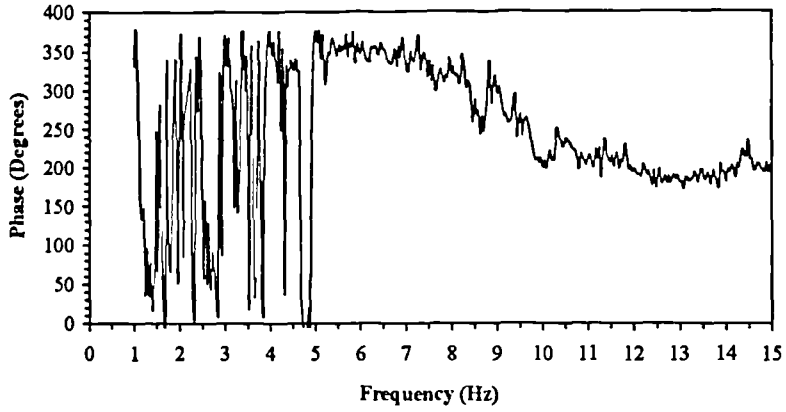

Phase

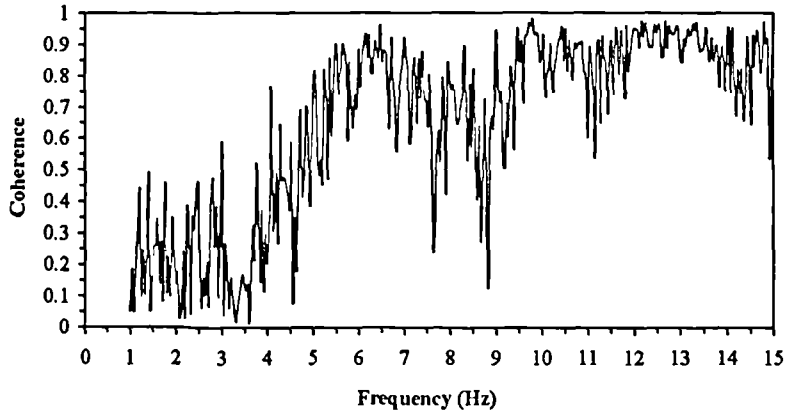

Coherence Function

Figure 3.7: Typical Transfer Function, Phase and Coherence Function

3.2.2 The Hart Shopping Centre Car Park, Level-2

Structure Description (see Figure 3.6)

Location	:	Fleet
Typical panel	:	L_S = 7.2 m, L_L = 10.7 m
Slab	:	t = 225 mm
Columns	:	C1 = C2 = C3 = C4 = 300 mm x 600 mm
Finishing	:	None
Test Date	:	Sunday 6 December 1992

Test Results

Fundamental natural frequency	:	5.9 Hz
Floor damping	:	6.5 % critical

Comments

The test on this roof level car park had to be repeated three times due to severe weather interruptions. The effect of strong wind on the test day is visible in the coherence function.

Measurements were taken when a few vehicles were parked near the floor panel tested. There were also disturbances due to vehicles moving on the floor for parking/exiting purposes. The high floor damping is due to the fact that the panel tested was close to the shopping mall below with walls etc. which acted as dampers. Also, the floor had suspended ceilings underneath.

Graphs

Figure 3.8 shows the typical experimental inertance transfer function, corresponding phase diagram and coherence function plots.

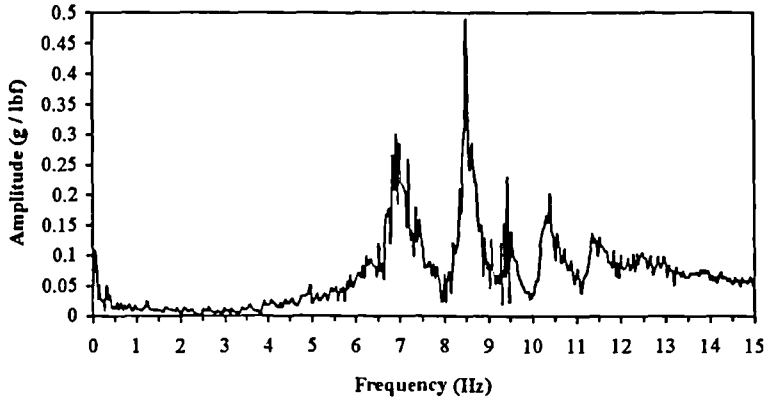

Transfer Function

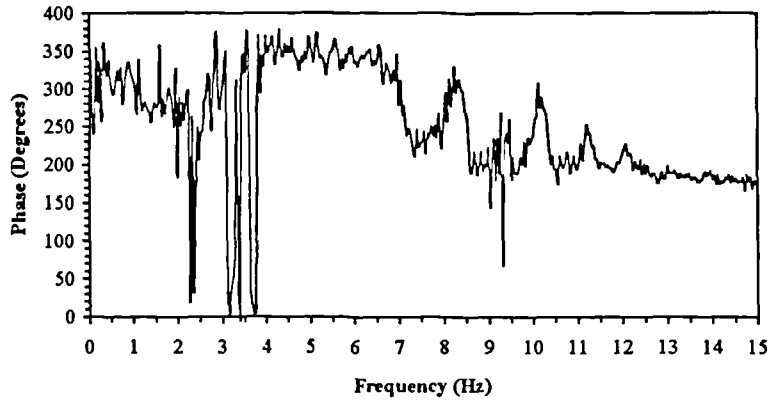

Phase

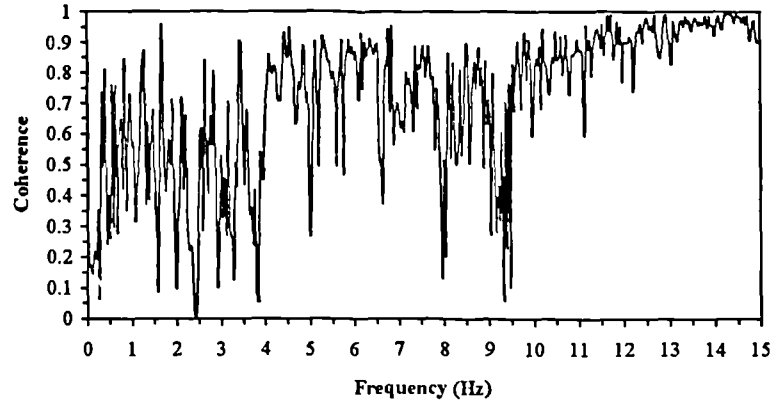

Coherence Function

Figure 3.8: Typical Transfer Function, Phase and Coherence Function

3.2.3 Nurdin & Peacock Office

Structure Description (see Figure 3.6)

Location	:	London
Typical panel	:	$L_S = 7.2$ m, $L_L = 7.2$ m
Slab	:	t = 225 mm
Columns	:	C1 = C2 = C3 = C4 = 450 mm x 450 mm
Finishing	:	False Floor
Test Date	:	Saturday 10 December 1994

Test Results

Fundamental natural frequency	:	10.1 Hz
Floor damping	:	7.1 % critical

Comments

This office floor was vacant at the time of the test. However, the office equipment, furniture, false floors and carpets etc. contributed to the values of frequency and damping. The results benefit from the quiet environment during the testing. This is reflected in the coherence function plot. However, the coherence function plot does not correspond to the grid point for which the transfer function and phase are given. This is due to the fact that only two plots could be stored at a time on the spectrum analyser and they were chosen as the transfer function and the corresponding phase diagram.

The spectrum analyser used for this test and all the remaining tests of this floor type (section 3.2), was newly bought and was different from the one used for earlier tests (sections 3.1, 3.2.1, and 3.2.2). The choice of this new spectrum analyser was the additional features required for other purposes in the laboratory.

Graphs

Figure 3.9 shows the typical experimental inertance transfer function, corresponding phase diagram and coherence function plots.

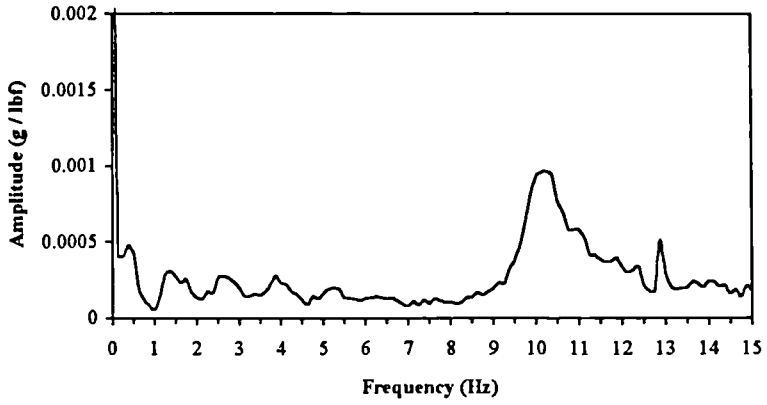

Transfer Function

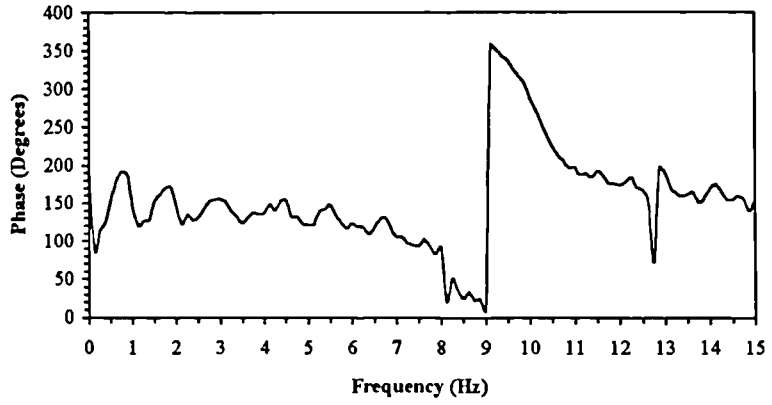

Phase

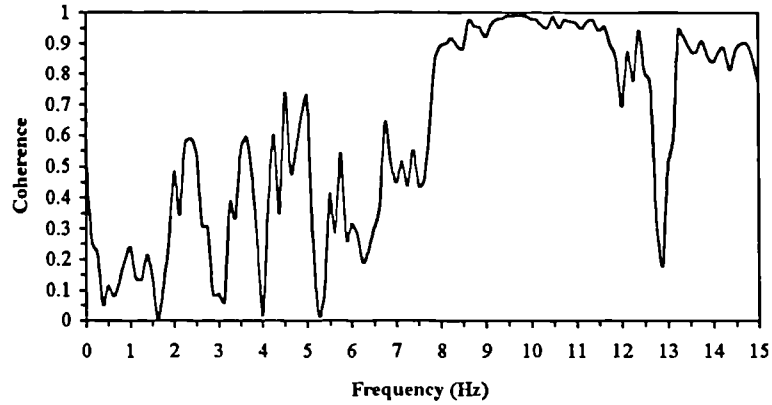

Coherence Function

Figure 3.9: Typical Transfer Function, Phase and Coherence Function

3.2.4 Crown Gate Shopping Centre, Chapel Walk, Service Deck

Structure Description (see Figure 3.6)

Location	:	Worcester
Typical panel	:	L_S = 8.0 m, L_L = 8.0 m
Slab	:	t = 375 mm
Columns	:	C1 = C2 = C3 = C4 = 400 mm x 400 mm
Finishing	:	Asphalt layer
Test Date	:	Wednesday 14 December 1994

Test Results

Fundamental natural frequency	:	12.7 Hz
Floor damping	:	1.0 % critical

Comments

This floor was tested at night time when no vehicle was present on the floor. During the test, the hammer impact tip broke down and another tip had to be used. The column locations could not be accurately located due to accessibility problems to the floor below. Therefore, some of the data was very poor possibly due to impact at or near column lines and also due to a strong breeze at the time of the test. The coherence function, therefore, shows a very poor floor response. The coherence function does not correspond to the grid point for which the transfer function and phase are given, for reasons given earlier in section 3.2.3.

The measured floor damping was below 1% of critical but was assumed as 1%. This low damping is due to the sharp first peak of the transfer function. It also shows that the presence of an asphalt layer has little contribution to floor damping. This has already been noted in section 3.1.3.

Graphs

Figure 3.10 shows the typical experimental inertance transfer function, corresponding phase diagram and coherence function plots.

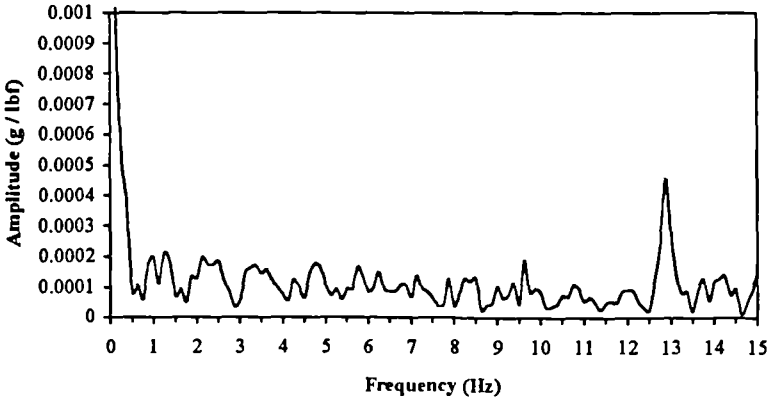

Transfer Function

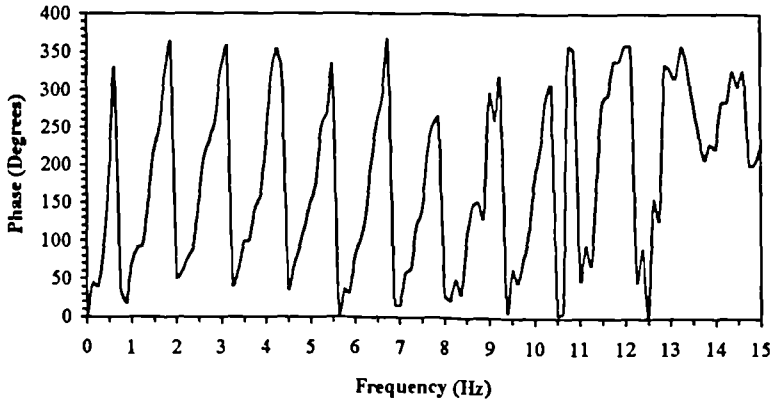

Phase

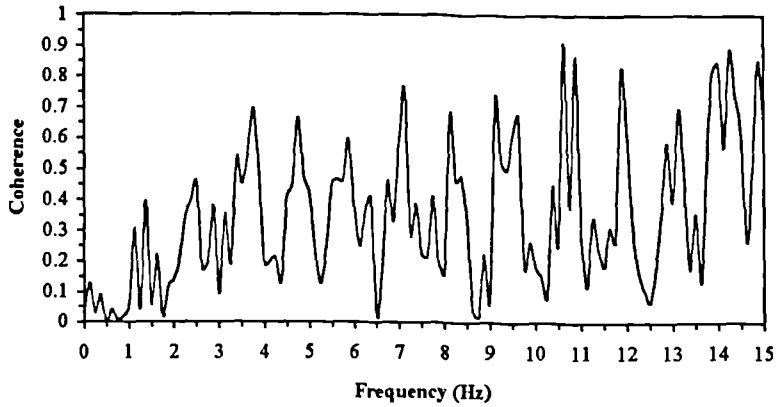

Coherence Function

Figure 3.10: Typical Transfer Function, Phase and Coherence Function

3.2.5 St. Martin's Gate Multi-Storey Car Park, Level-4

Structure Description (see Figure 3.6)

Location	:	Worcester
Typical panel	:	L_S = 7.2 m, L_L = 8.4 m
Slab	:	t = 250 mm
Columns	:	C1 = C2 = C3 = C4 = 450 mm x 450 mm
Finishing	:	None
Test Date	:	Saturday 28 January 1995

Test Results

Fundamental natural frequency	:	9.1 Hz
Floor damping	:	1.0 % critical

Comments

This floor was tested at a time when vehicles were moving out of the car park. Therefore, some of the data was very poor due to this disturbance. The floor is a liftslab type construction with special connections at the column locations. The floor damping measured was below 1% of critical but was assumed as 1%. The low floor damping is due to the non-monolithic column connections in addition to the not well defined peaks. The coherence function does not correspond to the grid point for which the transfer function and phase are given, for reasons given earlier in section 3.2.3. The coherence function shows the poor floor response due to the interference caused by the movement of vehicles.

Graphs

Figure 3.11 shows the typical experimental inertance transfer function, corresponding phase diagram and coherence function plots.

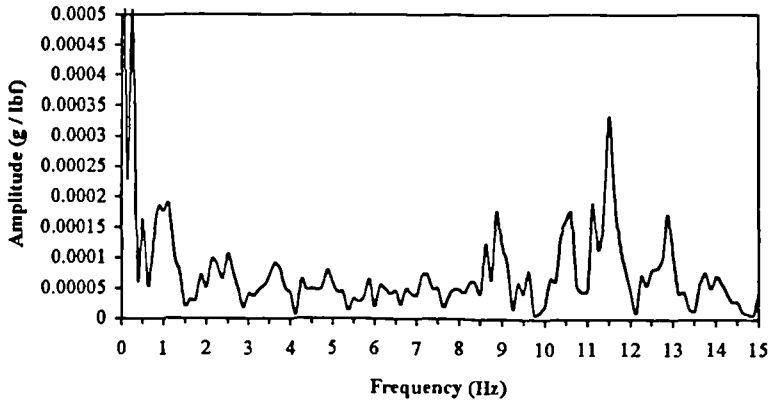

Transfer Function

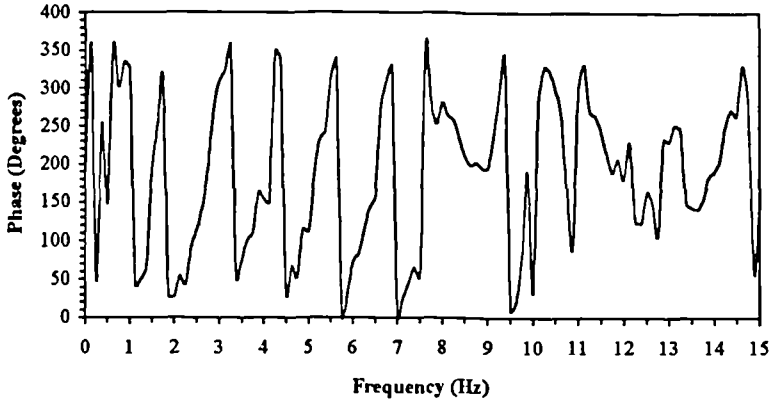

Phase

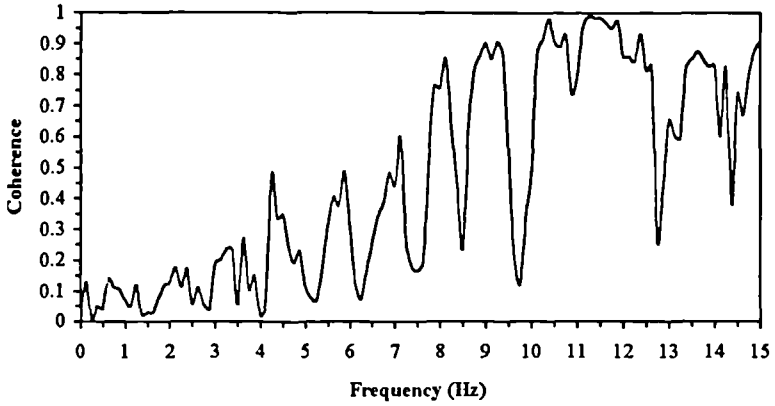

Coherence Function

Figure 3.11: Typical Transfer Function, Phase and Coherence Function

3.2.6 Brindley Drive Multi-Storey Car Park, Level-4

Structure Description (see Figure 3.6)

Location	:	Birmingham
Typical panel	:	$L_S = 7.2$ m, $L_L = 9.55$ m
Slab	:	t = 250 mm
Columns	:	C1 = C2 = C3 = C4 = 400 mm x 400 mm
Finishing	:	None
Test Date	:	Saturday 28 January 1995

Test Results

Fundamental natural frequency	:	7.2 Hz
Floor damping	:	1.4 % critical

Comments

This floor was tested in the evening when no vehicle was parked on the floor. However, there was a light breeze through the wall openings. The floor is a liftslab type construction with special connections at the column locations. The results were not very clear to interpret and, therefore, were analysed a number of times to obtain average values for frequency and damping. The low floor damping is due to the non-monolithic column connections. The coherence function, which shows the poor floor response, does not correspond to the grid point for which the transfer function and phase are given, for reasons given earlier in section 3.2.3.

Graphs

Figure 3.12 shows the typical experimental inertance transfer function, corresponding phase diagram and coherence function plots.

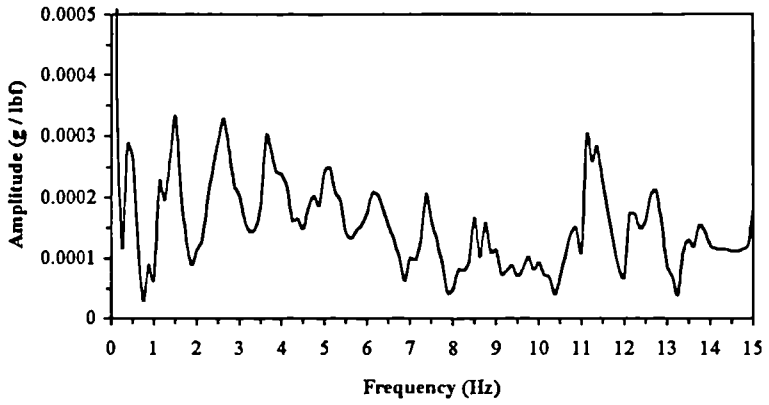

Transfer Function

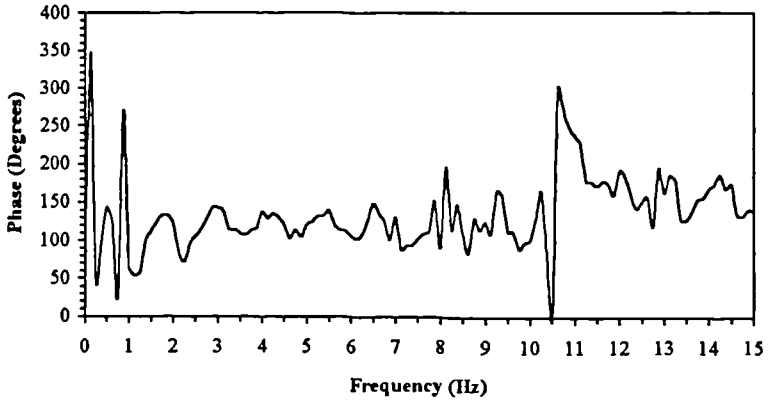

Phase

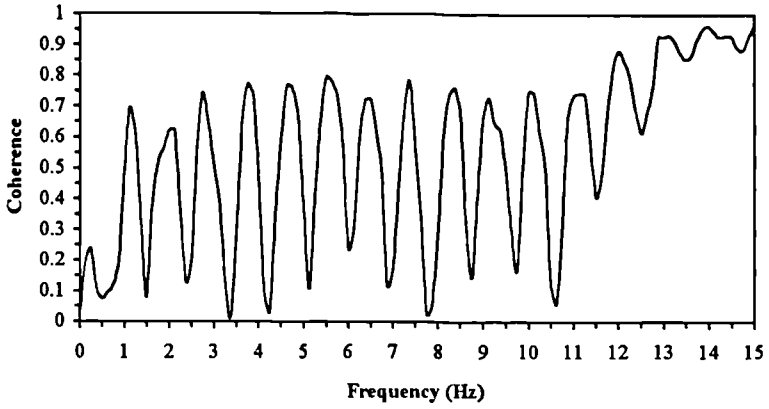

Coherence Function

Figure 3.12: Typical Transfer Function, Phase and Coherence Function

3.2.7 Snow Hill Re-Development Livery Street Multi-Storey Car Park, Level-1B

Structure Description (see Figure 3.6)

Location	:	Birmingham
Typical panel	:	L_S = 7.5 m, L_L = 8.0 m
Slab	:	t = 225 mm
Columns	:	C1 = C2 = C3 = C4 = 450 mm x 450 mm
Finishing	:	None
Test Date	:	Sunday 29 January 1995

Test Results

Fundamental natural frequency	:	8.6 Hz
Floor damping	:	1.0 % critical

Comments

This floor was tested at a time when no vehicle was parked on the floor. The car park is close to the main road and, therefore, there was continuous noise of the traffic. Some of the results were not very good and, therefore, they were analysed a few times before an average estimate of frequency and damping was obtained. The coherence function, which does not correspond to the grid points for which the transfer function and phase are given, for reasons given earlier in section 3.2.3, shows the effect of noise and light breeze across the car park.

The measured floor damping was below 1% of critical but was assumed as 1%. This is due to the fact that the tested panel was near the middle of this large car park with no partitions, suspended ceilings, and finishes etc.

Graphs

Figure 3.13 shows the typical experimental inertance transfer function, corresponding phase diagram and coherence function plots.

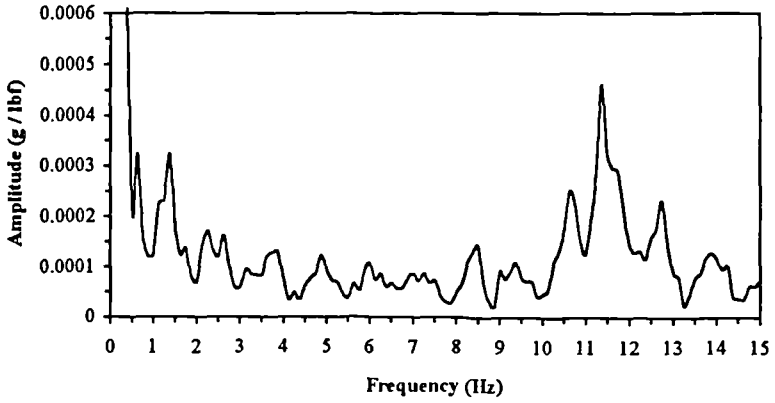

Transfer Function

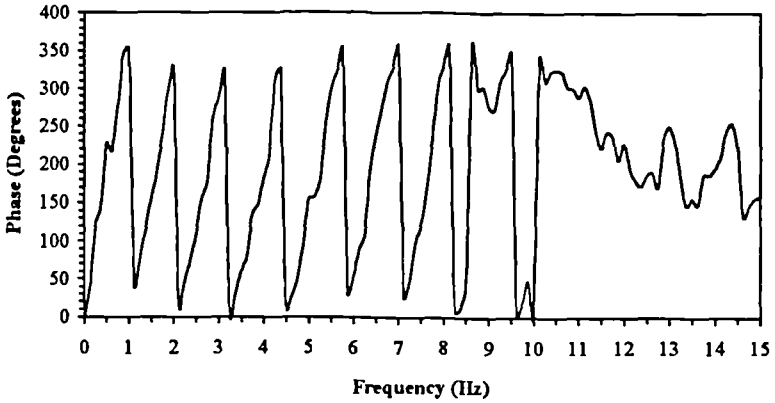

Phase

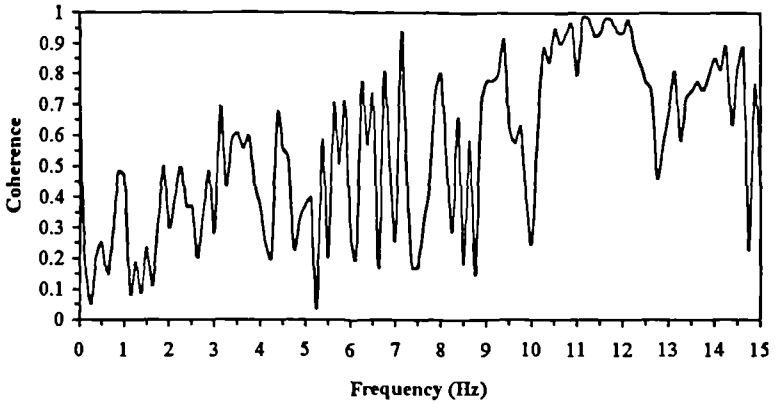

Coherence Function

Figure 3.13: Typical Transfer Function, Phase and Coherence Function

3.2.8 Snow Hill Re-Development Livery Street Multi-Storey Car Park, Level-1A

Structure Description (see Figure 3.6)

Location	:	Birmingham
Typical panel	:	L_S = 7.5 m, L_L = 8.0 m
Slab	:	t = 350 mm
Columns	:	C1 = C2 = C3 = C4 = 450 mm x 450 mm
Finishing	:	None
Test Date	:	Sunday 29 January 1995

Test Results

Fundamental natural frequency	:	12.7 Hz
Floor damping	:	1.6 % critical

Comments

This floor was tested at a time when no vehicle was parked on the floor. The floor is the next level below of the previous car park. The layout of the floor is identical to the previous floor except the slab thickness. This increased stiffness raised the frequency and also damping. The coherence function for this floor could not be measured due to the lack of memory space of the spectrum analyser which had just been used for the previous floor. Also, only a few grid points were measured for the same reason. The results were again not very good due to various disturbances discussed earlier in section 3.2.7.

Graphs

Figure 3.14 shows the typical experimental inertance transfer function and corresponding phase diagram plots. The coherence function for this test could not be measured due to lack of memory of the spectrum analyser.

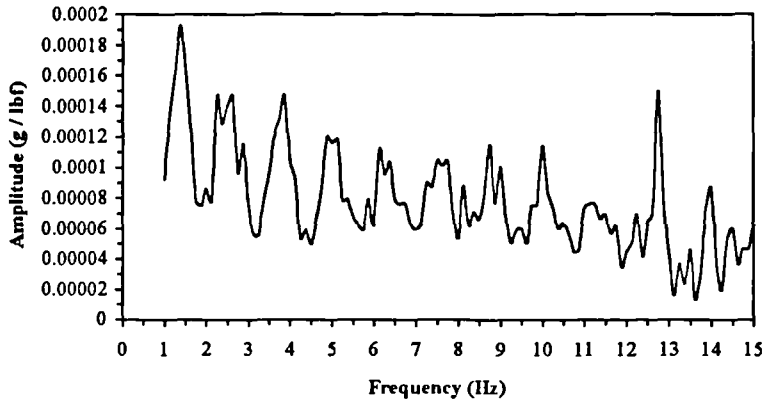

Transfer Function

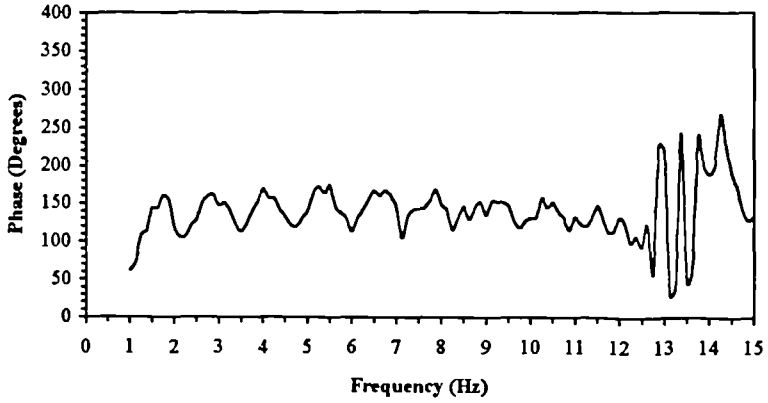

Phase

Figure 3.14: Typical Transfer Function and Phase

3.2.9 Island Site, Finsbury Pavement, Office, Level-4 (Flexible Panel)

Structure Description (see Figure 3.6)

Location	:	London
Typical panel	:	L_S = 9.0 m, L_L = 9.0 m
Slab	:	t = 300 mm
Columns	:	C1 = C2 = C3 = C4 = 600 mm Diameter (Assumed 600 mm x 600 mm)
Finishing	:	None
Test Date	:	Saturday 29 April 1995

Test Results

Fundamental natural frequency	:	8.4 Hz
Floor damping	:	1.0 % critical

Comments

This floor was tested at a time when construction work was in progress at the site. The site is located at the corner of a busy road junction. Therefore, the floor response was not accurately measured. The coherence function shows the quality of the measurements. Again, it does not correspond to the grid point for which the transfer function and phase are given, for reasons given earlier in section 3.2.3.

The floor panel tested is close to a central opening which caused a breakage in the continuous nature of the floor. The measured floor damping was less than 1% of critical but was assumed as 1%. The reason for low damping is the sharp peak in the transfer function.

Graphs

Figure 3.15 shows the typical experimental inertance transfer function, corresponding phase diagram and coherence function plots.

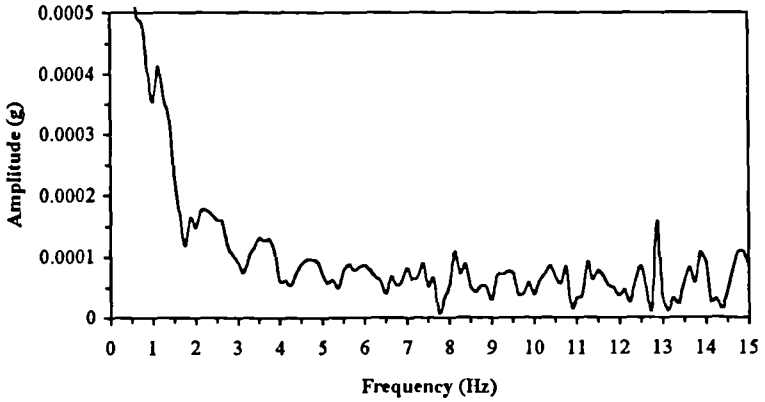

Transfer Function

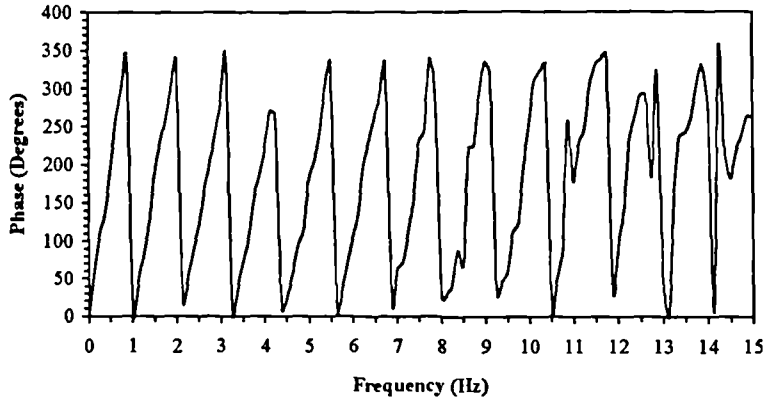

Phase

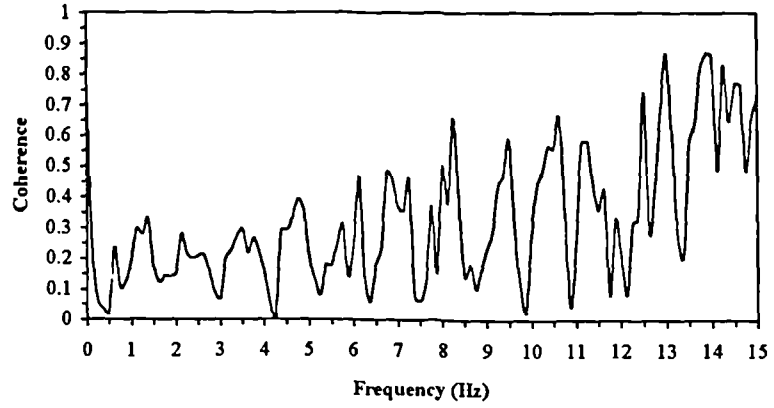

Coherence Function

Figure 3.15: Typical Transfer Function, Phase and Coherence Function

3.2.10 Island Site, Finsbury Pavement, Office, Level-4 (Stiff Panel)

Structure Description (see Figure 3.6)

Location	:	London
Typical panel	:	L_S = 7.5 m, L_L = 9.0 m
Slab	:	t = 300 mm
Columns	:	C1 = C2 = C3 = C4 = 600 mm Diameter
		(Assumed 600 mm x 600 mm)
Finishing	:	None
Test Date	:	Saturday 29 April 1995

Test Results

Fundamental natural frequency	:	10.6 Hz
Floor damping	:	1.3 % critical

Comments

This floor panel is adjacent to the previous panel tested but away from the central floor opening. Therefore, the same comments apply here as for the previous floor in section 3.2.9.

Graphs

Figure 3.16 shows the typical experimental inertance transfer function, corresponding phase diagram and coherence function plots.

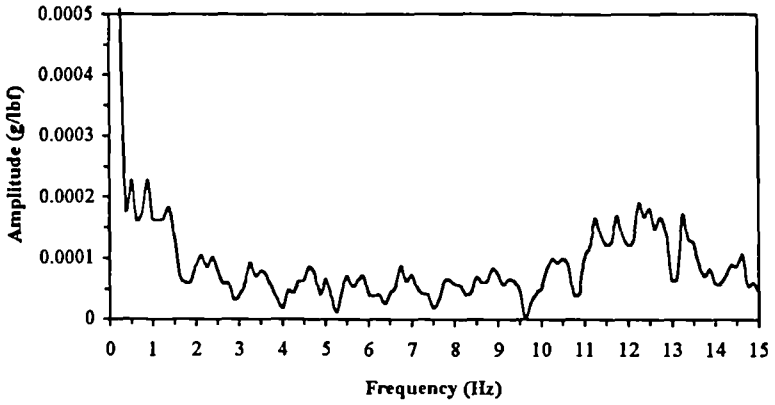

Transfer Function

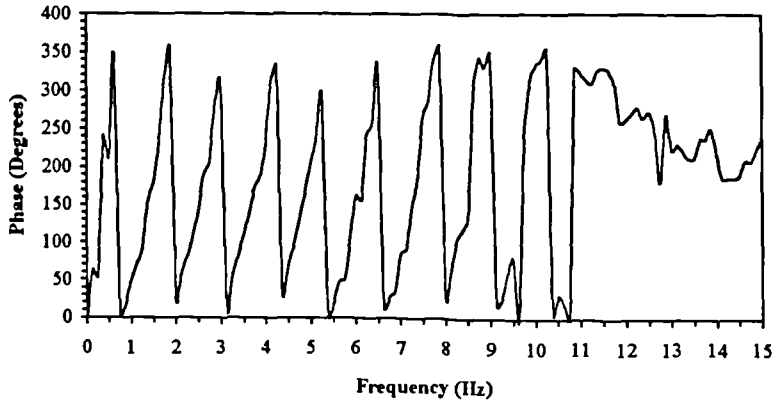

Phase

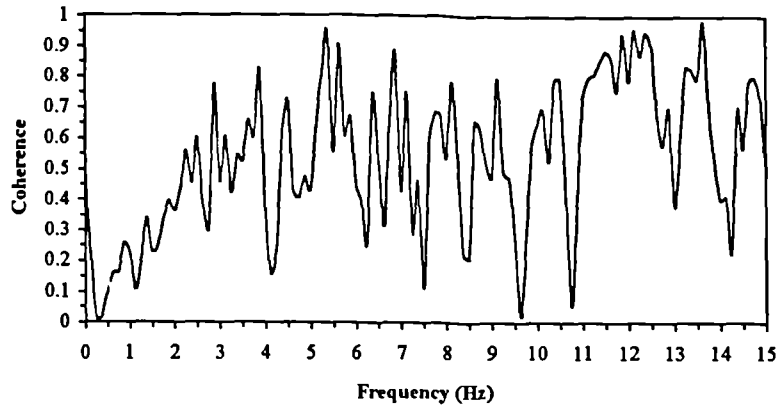

Coherence Function

Figure 3.16: Typical Transfer Function, Phase and Coherence Function

3.2.11 Friars Gate Multi-Storey Car Park, Level-5

Structure Description (see Figure 3.6)

Location	:	Winchester
Typical panel	:	$L_S = 6.0$ m, $L_L = 7.5$ m
Slab	:	t = 200 mm
Columns	:	C1 = C2 = C3 = C4 = 250 mm x 450 mm
Finishing	:	None
Test Date	:	Wednesday 3 May 1995

Test Results

Fundamental natural frequency	:	10.3 Hz
Floor damping	:	1.5 % critical

Comments

This car park is located near the city centre. However, the test was carried out when the car park had been closed. The only disturbance that occurred was due to the light breeze through the car park. Therefore, results are better and the quality of measurements is reflected in the coherence function. The coherence function does not correspond to the grid point for which the transfer function and phase are given, for reasons given earlier in section 3.2.3.

The floor panel tested is part of the floor constructed as an extension of the existing car park. The two floors are separated by a 50 mm expansion joint. The low damping is due to the absence of any partitions, finishes and suspended ceilings etc.

Graphs

Figure 3.17 shows the typical experimental inertance transfer function, corresponding phase diagram and coherence function plots.

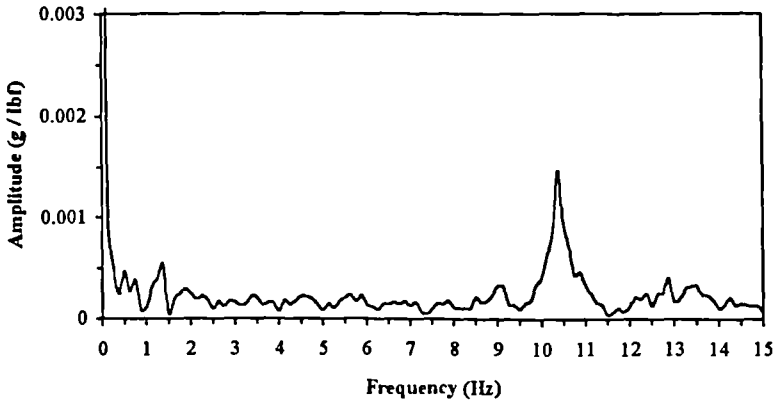

Transfer Function

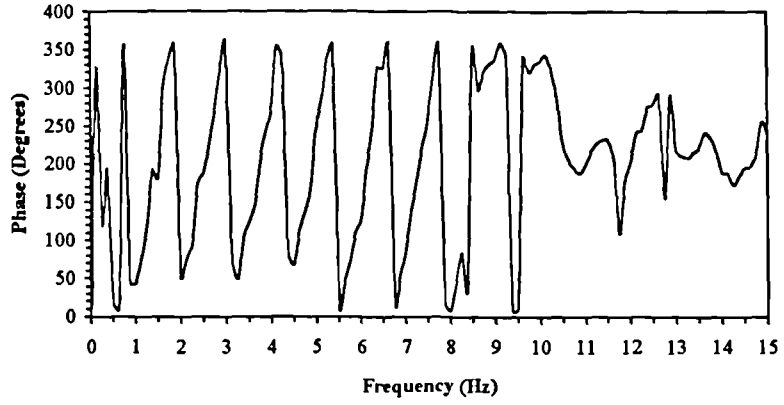

Phase

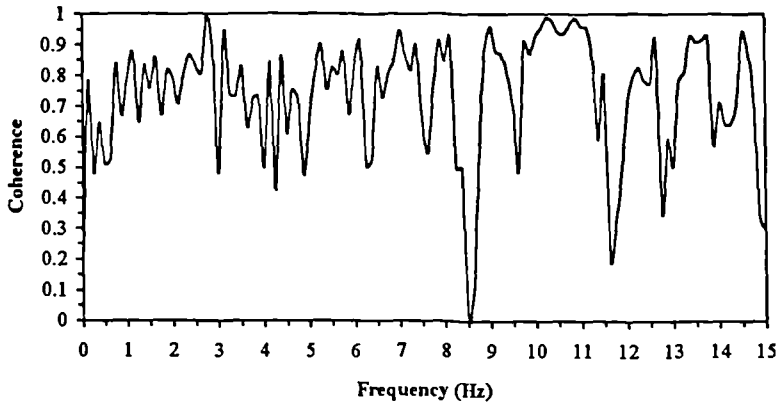

Coherence Function

Figure 3.17: Typical Transfer Function, Phase and Coherence Function

3.2.12 Tower Street Car Park

Structure Description (see Figure 3.6)

Location	:	Winchester
Typical panel	:	$L_S = 8.0$ m, $L_L = 9.0$ m
Slab	:	t = 275 mm
Columns	:	C1 = C2 = C3 = C4 = 450 mm x 450 mm
Finishing	:	None
Test Date	:	Wednesday 3 May 1995

Test Results

Fundamental natural frequency	:	8.5 Hz
Floor damping	:	2.8 % critical

Comments

This car park is located near the city centre and close to a busy traffic roundabout. The car park is open 24 hours and there was some vehicular movement throughout testing. However, due to time constraints, the test had to be carried out. Every effort was, however, made to record measurements when no vehicle moved on the floor panels nearby. The coherence function shows the effect of disturbances due to vehicle movement, noise on the adjacent road and strong breeze through the car park. The coherence function does not correspond to the grid point for which the transfer function and phase are given, for reasons given earlier in section 3.2.3.

Graphs

Figure 3.18 shows the typical experimental inertance transfer function, corresponding phase diagram and coherence function plots.

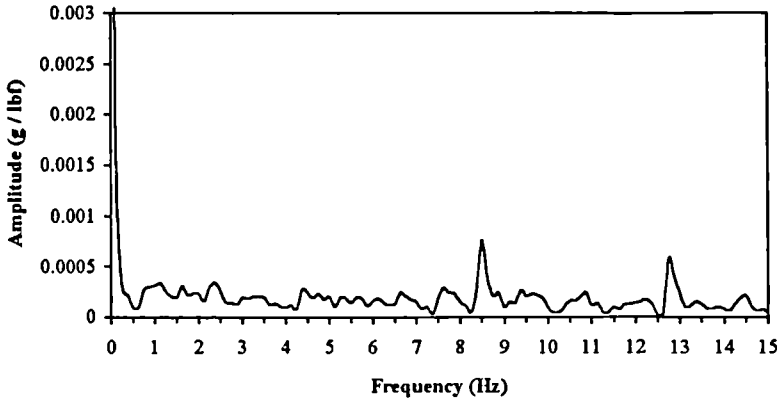

Transfer Function

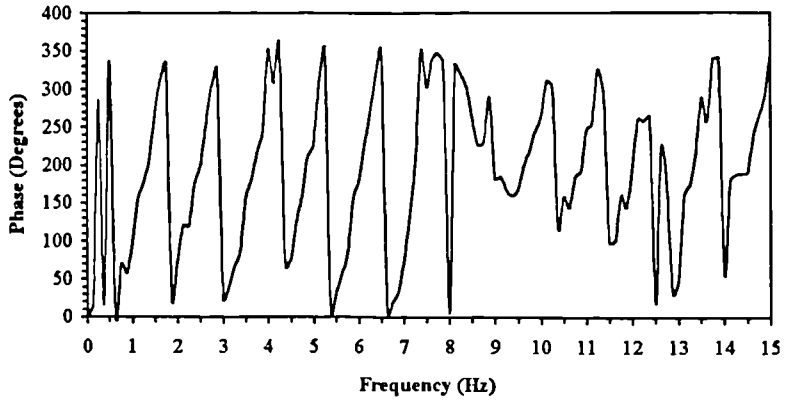

Phase

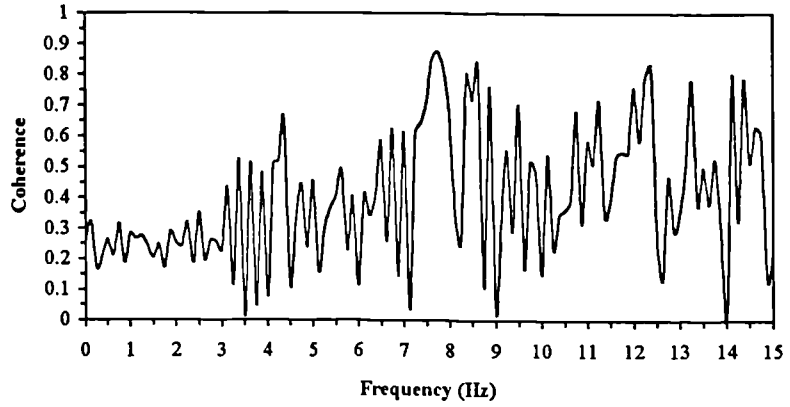

Coherence Function

Figure 3.18: Typical Transfer Function, Phase and Coherence Function

3.3 Pre-Tensioned Concrete Double-T Beam Floors

Only five (5) floors of this type could be tested. All of them consisted of double-T beams supported on L-girders or inverted T-beams on neoprene bearing pads. Figure 3.19 shows a general layout for this floor type with a typical cross-section (see also Appendix A). Specific dimensions are given for each floor individually.

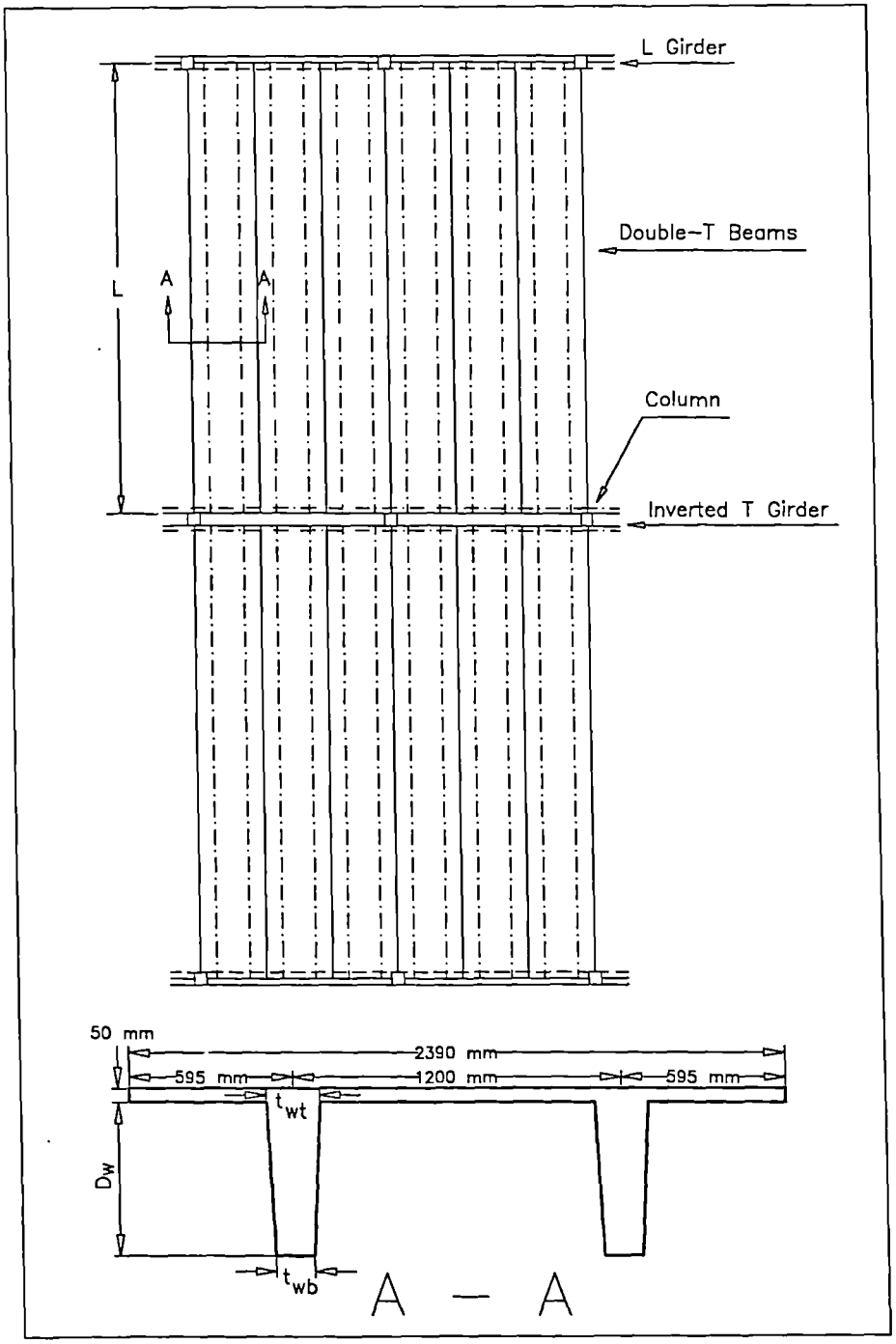

Figure 3.19: Typical Plan Layout and Cross-Section

3.3.1 Trigonos Phase V Multi-Storey Car Park, Level-6

Structure Description (see Figure 3.19)

Location	:	Swindon
Column Spacing	:	7.2 m
Beam Size	:	D_w = 550 mm, t_{wt} = 185 mm, t_{wb} = 130 mm
Beam Length	:	L = 16.045 m
Finishing	:	75 mm screed; 50 mm asphalt
Test date	:	Monday 27 July 1992

Test Results

Fundamental natural frequency	:	4.9 Hz
Floor damping	:	2.1 % critical

Comments

At the time of the test, there was a strong breeze on this roof floor. This caused some ambient vibrations and, therefore, the accelerometer sensitivity had to be increased. The coherence function indicates the effect of this disturbance.

Measurements were taken when no vehicles were parked on the floor. The floor frequency was low due to its long span. There were many closely spaced modes and the data had to be analysed a number of times to obtain an average estimate of the floor frequency and damping.

Graphs

Figure 3.20 shows the typical experimental inertance transfer function, corresponding phase diagram and coherence function plots.

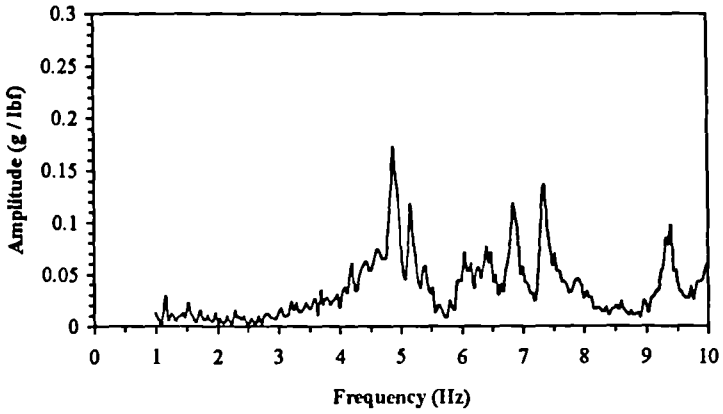

Transfer Function

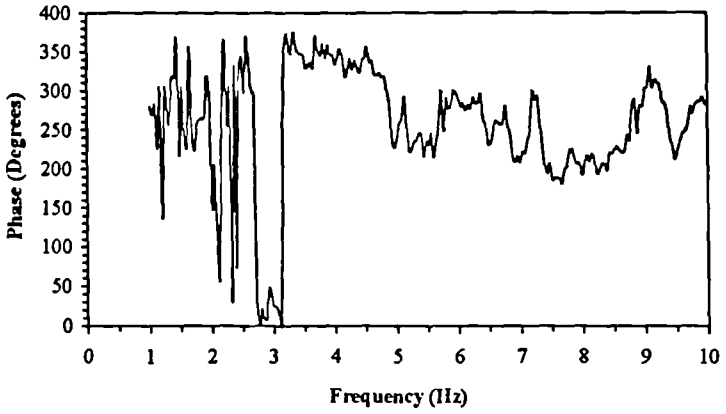

Phase

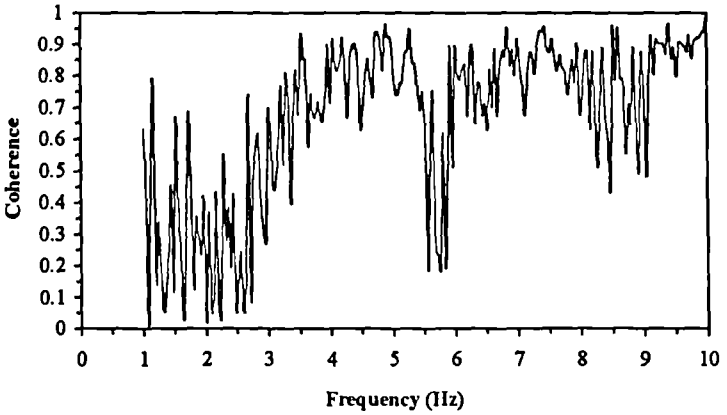

Coherence Function

Figure 3.20: Typical Transfer Function, Phase and Coherence Function

3.3.2 Reading Station Re-Development Multi-Storey Car Park, Level-10

Structure Description (see Figure 3.19)

Location	:	Reading
Column Spacing	:	7.2 m
Beam Size	:	D_w = 550 mm, t_{wt} = 195 mm, t_{wb} = 140 mm
Beam Length	:	L = 15.4 m
Finishing	:	75 mm screed
Test date	:	Sunday 19 March 1995

Test Results

Fundamental natural frequency	:	5.6 Hz
Floor damping	:	1.0 % critical

Comments

Measurements were taken when no vehicle was parked on the floor. The floor frequency was low due to its long span. This frequency was estimated after a number of analysis of the data. The quality of the data was very poor due to interferences caused by wind and noise. Also, floor damping could not be accurately estimated for the same reasons. It was evaluated at a value below 1.0 % of critical but was assumed as 1.0 % critical. The results have also been affected by the poor construction of the floor which showed leakages at the beam junctions.

The spectrum analyser used for this test and all the remaining tests of this floor type (section 3.3), was newly bought and was different from the one used for earlier tests (sections 3.1, 3.2.1, 3.2.2 and 3.3.1). The reasons have already been discussed in section 3.2.3.

Graphs

Figure 3.21 shows the typical experimental inertance transfer function, corresponding phase diagram and coherence function plots.

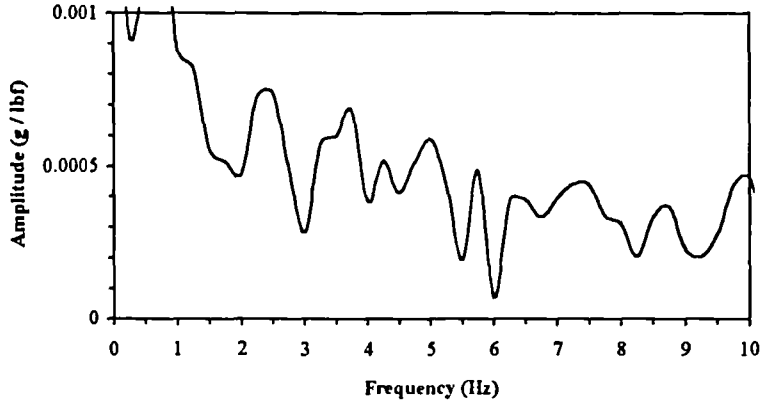

Transfer Function

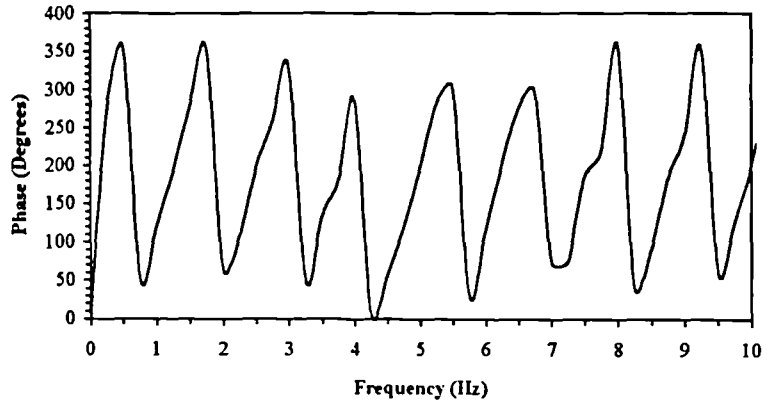

Phase

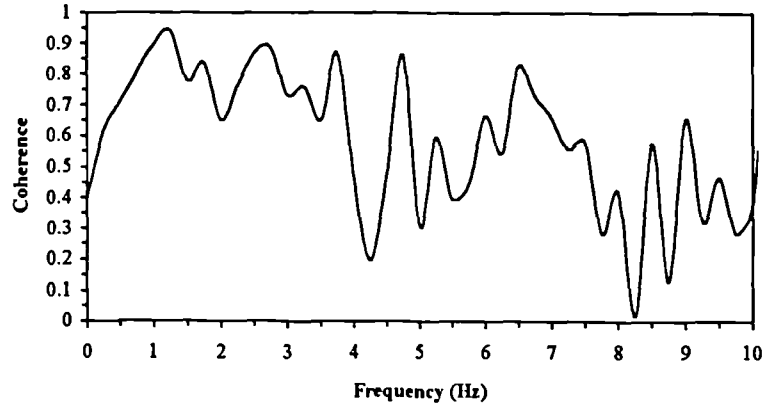

Coherence Function

Figure 3.21: Typical Transfer Function, Phase and Coherence Function

3.3.3 Safeway Superstore Car Park

Structure Description (see Figure 3.19)

Location	:	Sutton
Column Spacing	:	7.2 m
Beam Size	:	D_w = 550 mm, t_{wt} = 225 mm, t_{wb} = 170 mm
Beam Length	:	L = 15.6 m
Finishing	:	75 mm screed
Test date	:	Sunday 23 April 1995

Test Results

Fundamental natural frequency	:	5.5 Hz
Floor damping (average)	:	1.0 % critical

Comments

At the time of the test, there was a strong breeze on this roof floor. Also, light rain started towards the end of the test. This caused some ambient vibrations and, therefore, the accelerometer sensitivity had to be increased. The coherence function indicates the effect of this disturbance. It, however, does not correspond to the grid point for which the transfer function and phase are given, for reasons given earlier in section 3.2.3. The quality of floor construction also affected the results, as discussed in section 3.3.2.

Measurements were taken when no vehicle was parked on the floor. The floor frequency was low due to its long span. The reasons for low damping are the same as for the previous floor (section 3.3.2).

Graphs

Figure 3.22 shows the typical experimental inertance transfer function, corresponding phase diagram and coherence function plots.

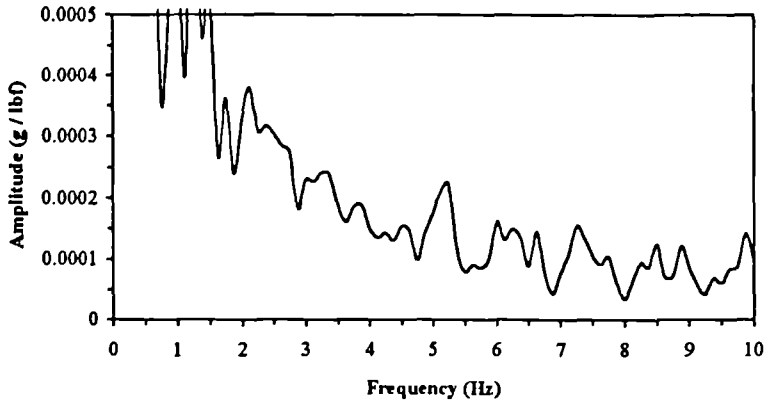

Transfer Function

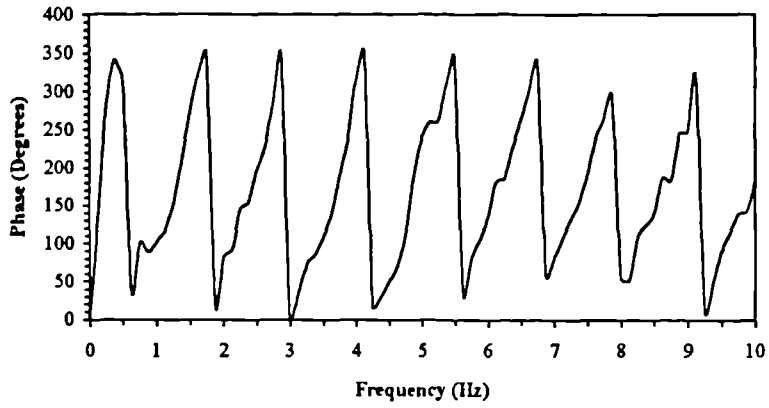

Phase

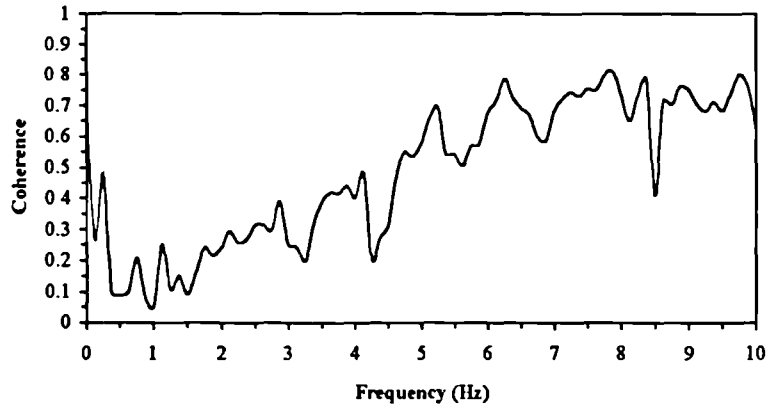

Coherence Function

Figure 3.22: Typical Transfer Function, Phase and Coherence Function

3.3.4 Toys R Us Multi-Storey Car Park # 4, Level-7

Structure Description (see Figure 3.19)

Location	:	Basildon
Column Spacing	:	7.2 m
Beam Size	:	D_w = 450 mm, t_{wt} = 265 mm, t_{wb} = 208 mm
Beam Length	:	L = 15.7 m
Finishing	:	100 mm screed
Test date	:	Wednesday 26 April 1995

Test Results

Fundamental natural frequency	:	4.6 Hz
Floor damping	:	3.4 % critical

Comments

Measurements were taken when no vehicle was parked on the floor. However, the odd vehicle did move along the adjacent bay for entering/exiting purposes. The floor frequency was low due to its long span. Damping estimate was higher than other floors of this type. This was due to the closely spaced modes. Again, the quality of data was poor due to the interferences caused by a light breeze and traffic noise. The poor floor construction has also affected the results.

The coherence function does not correspond to the grid point for which the transfer function and phase are given, for reasons given earlier in section 3.2.3. The quality of measurements is reflected in the coherence function.

Graphs

Figure 3.23 shows the typical experimental inertance transfer function, corresponding phase diagram and coherence function plots.

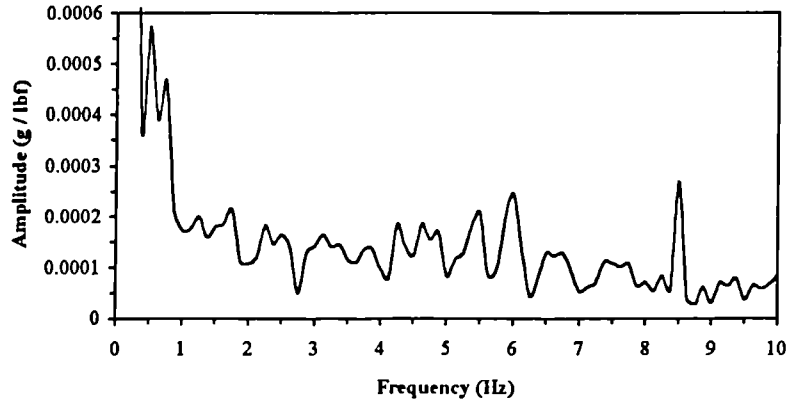

Transfer Function

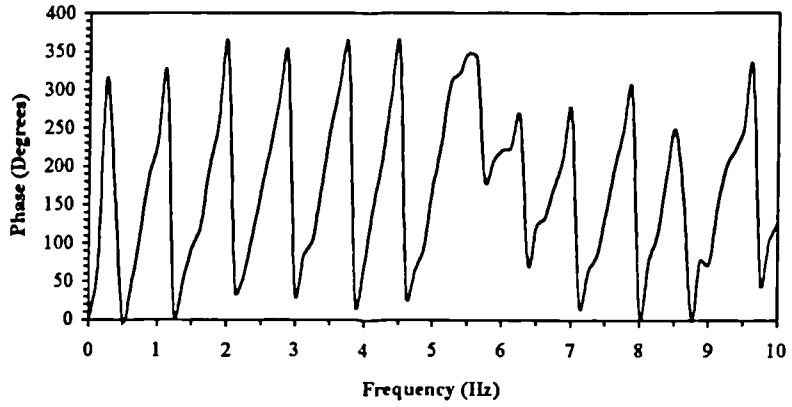

Phase

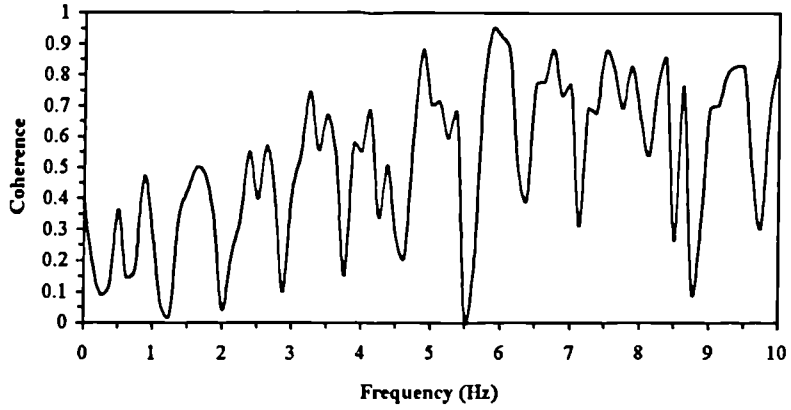

Coherence Function

Figure 3.23: Typical Transfer Function, Phase and Coherence Function

3.3.5 Royal Victoria Place Multi-Storey Car Park, Level-3

Structure Description (see Figure 3.19)

Location	:	Tunbridge Wells
Column Spacing	:	7.2 m
Beam Size	:	D_w = 550 mm, t_{wt} = 195 mm, t_{wb} = 140 mm
Beam Length	:	L = 15.4 m
Finishing	:	75 mm screed
Test date	:	Sunday 30 April 1995

Test Results

Fundamental natural frequency	:	5.8 Hz
Floor damping (average)	:	1.0 % critical

Comments

Measurements were taken when no vehicle was parked on the floor. However, the odd vehicle did move along the adjacent bay for entering/exiting purposes. The floor frequency was low due to its long span. Damping estimate was lower than 1.0 % of critical but was assumed as 1.0 % critical. Again, the quality of data was poor. This is a particular feature for double-T car parks which have been investigated. The reason is thought to be caused by the floor construction techniques at the junction of two adjacent beams and also due to noise etc. The data was, therefore, analysed a number of times for reasonable estimates of the floor frequency and damping.

The coherence function does not correspond to the grid point for which the transfer function and phase are given, for reasons given earlier in section 3.2.3. It shows the quality of measurements.

Graphs

Figure 3.24 shows the typical experimental inertance transfer function, corresponding phase diagram and coherence function plots.

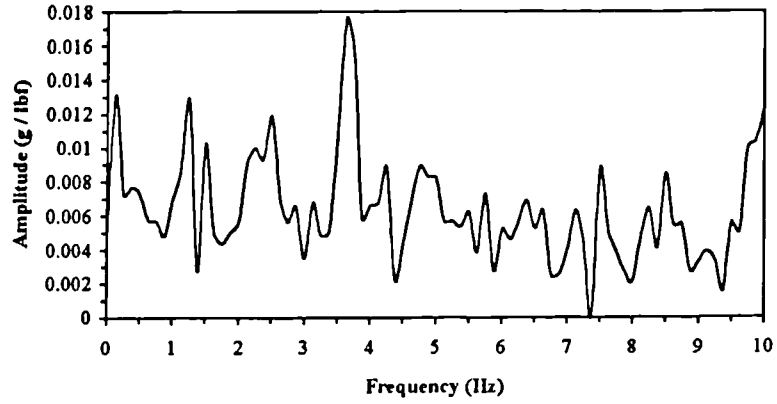

Transfer Function

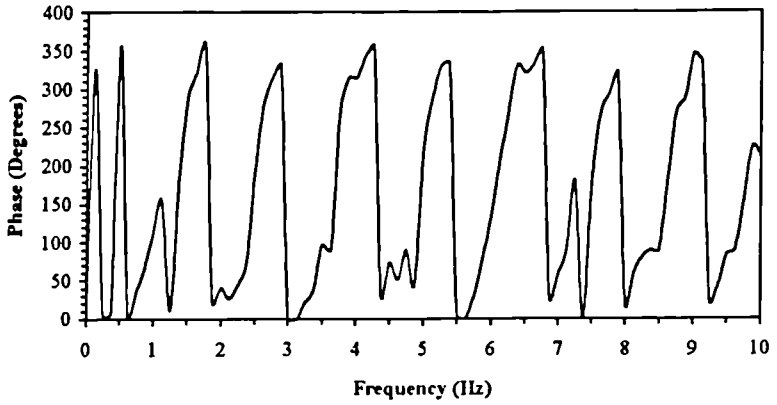

Phase

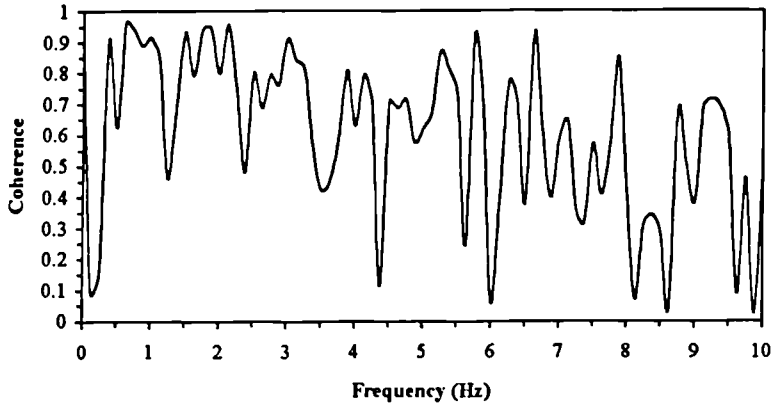

Coherence Function

Figure 3.24: Typical Transfer Function, Phase and Coherence Function

3.4 Composite Steel-Concrete Slab Floors

Only eight (8) floors of this type could be tested. All of them were continuous and supported on steel columns except the first floor, which was connected to reinforced concrete columns along the short span direction at the far side and steel columns at the near side. Figure 3.25 shows a general layout for this floor type with a typical cross-section (see also Appendix A). Specific dimensions are given for each floor individually.

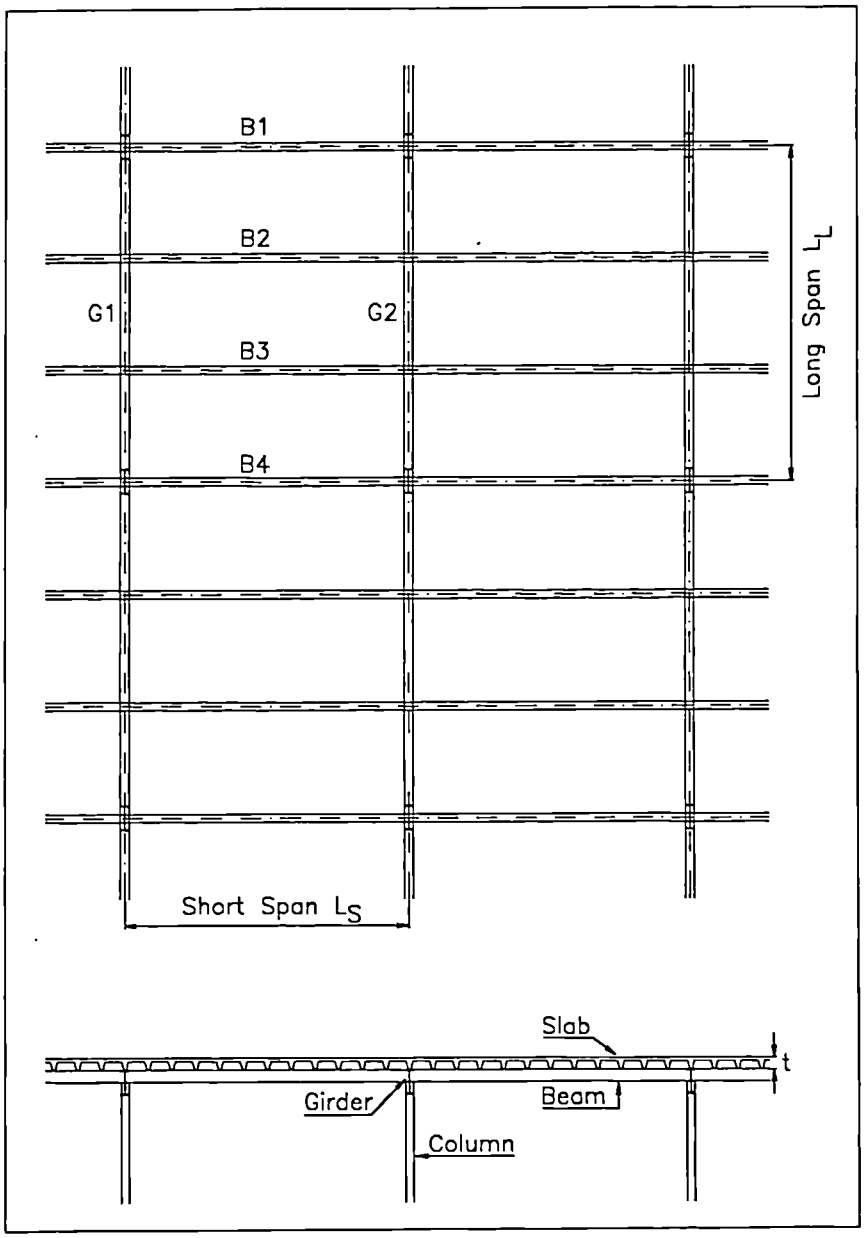

Figure 3.25: Typical Plan Layout and Cross-Section

3.4.1 The Millwall Football and Athletics Stadium, Senegal Fields, West Stand, Hospitality Level

Structure Description (see Figure 3.25)

Location	:	London
Typical Panel	:	L_S = 6.75 m, L_L = 8.3 m
Beams	:	B1 - UB610x229x101
		B2, B3 - UB356x127x33
		B4 - UB305x102x28
Girders	:	G1, G2 - UB610x229x101
Profile	:	CF70 (1.2)
Slab	:	t = 130 mm
Finishing	:	None
Test Date	:	Monday 7 December 1992

Test Results

Fundamental natural frequency	:	12.6 Hz
Floor damping	:	1.0 % critical

Comments

This stadium was under construction at the time of the test. Therefore, the test was carried out at night after the working shifts. However, the floor was wet at various locations and only a few selected grid points could be tested. The response of the floor was quite good as compared with many previous floors due to the quiet environment and absence of any other disturbances. This is visible in the coherence function.

The floor damping is quite low and therefore resulted in perceptible vibrations. It is mainly due to the sharp first peak of the transfer function, which in turn resulted due to the absence of any partitions, finishes and suspended ceilings etc.

Graphs

Figure 3.26 shows the typical experimental inertance transfer function, corresponding phase diagram and coherence function plots.

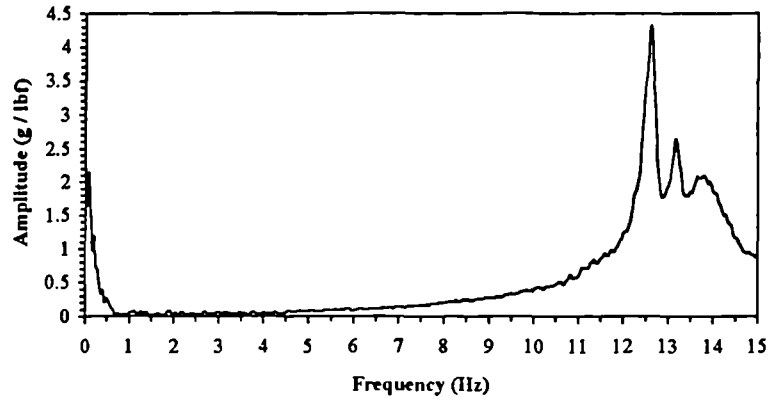

Transfer Function

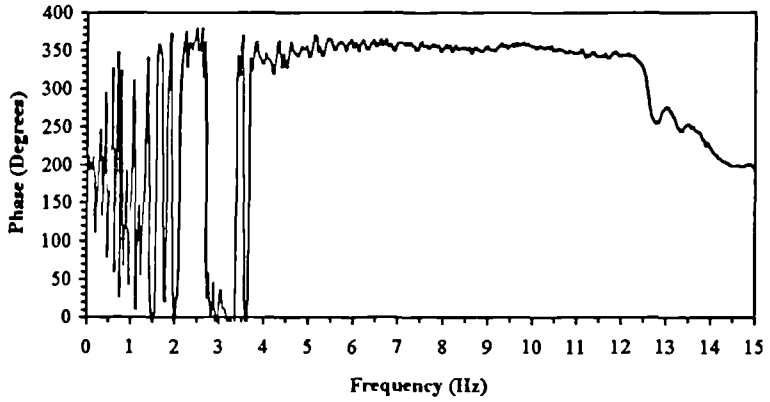

Phase

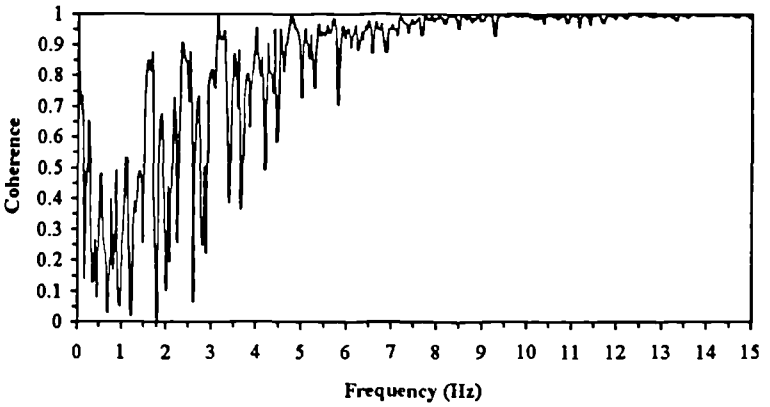

Coherence Function

Figure 3.26: Typical Transfer Function, Phase and Coherence Function

3.4.2 Worcester Central Development, Friary Walk Car Park, Level-2

Structure Description (see Figure 3.25)

Location	:	Worcester
Typical Panel	:	L_S = 7.2 m, L_L = 8.0 m
Beams	:	B1 - UB914x305x253
		B2, B3 - UB610x229x101
		B4 - UB914x419x388
Girders	:	G1, G2 - UB610x229x101
Profile	:	CF60 (1.2)
Slab	:	t = 130 mm
Finishing	:	None
Test Date	:	Thursday 15 December 1994

Test Results

Fundamental natural frequency	:	8.1 Hz
Floor damping	:	3.2 % critical

Comments

This car park was tested after the business hours. However, the floor panel tested was close to the shopping mall where most of the shops were closing down and caused considerable disturbance, which can be observed in the coherence function. The coherence function does not correspond to the grid point for which the transfer function and phase are given, for reasons given earlier in section 3.2.3. The floor frequency was obtained from an average sample of data due to poor quality. The floor damping is relatively high when compared with the previous floor of this type. The main reason for this was the nearby mall with shops at the lower levels which acted as dampers.

The spectrum analyser used for this test and all the remaining tests of this floor type (section 3.4), was newly bought and was different from the one used for earlier tests (sections 3.1, 3.2.1, 3.2.2, 3.3.1 and 3.4.1). The reasons have already been discussed in section 3.2.3.

Graphs

Figure 3.27 shows the typical experimental inertance transfer function, corresponding phase diagram and coherence function plots.

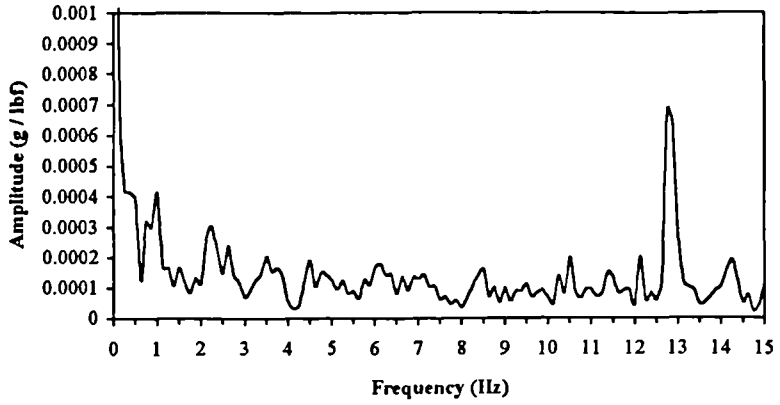

Transfer Function

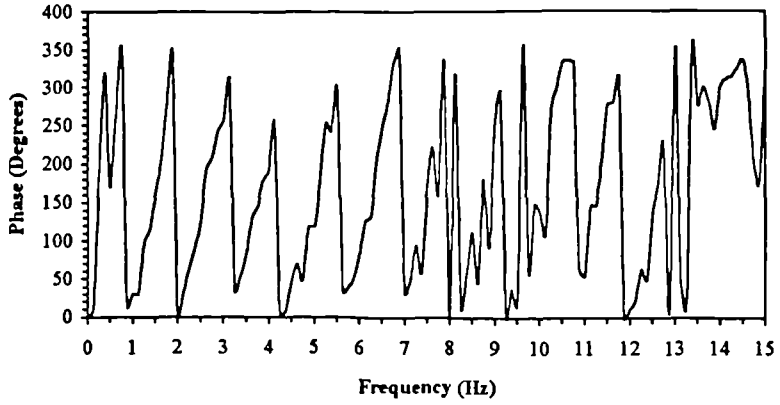

Phase

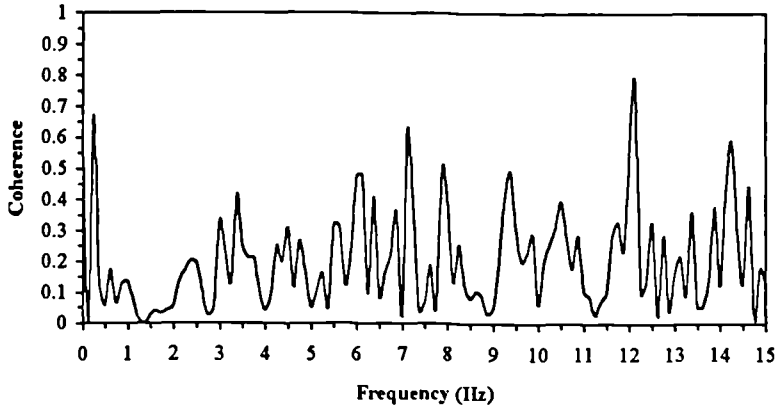

Coherence Function

Figure 3.27: Typical Transfer Function, Phase and Coherence Function

3.4.3 Braywick House Office

Structure Description (see Figure 3.25)

Location	:	Maidenhead
Typical Panel	:	$L_S = 9.0$ m, $L_L = 9.0$ m
Beams	:	B1, B4 - Cellform650x152x60
		B2, B3 - Cellform650x152x52
Girders	:	G1 - UB610x305x238
		G2 - UB610x229x140
Profile	:	CF51 (1.2)
Slab	:	t = 130 mm
Finishing	:	None
Test Date	:	Friday 24 February 1995

Test Results

Fundamental natural frequency	:	8.8 Hz
Floor damping	:	2.0 % critical

Comments

This floor was tested during construction hours. The floor was partly loaded with construction material and some patchy water. Effects of noise and breeze are visible in the coherence function plot. The coherence function does not correspond to the grid point for which the transfer function and phase are given, for reasons given earlier in section 3.2.3.

The floor response was more accurately measured than the previous floor (section 3.4.2) due to an increase in the sensitivity of the accelerometer. The floor damping is quite low and, therefore, resulted in perceptible vibrations. It may increase when the construction has finished due to the presence of planned suspended ceilings and boundary walls.

Graphs

Figure 3.28 shows the typical experimental inertance transfer function, corresponding phase diagram and coherence function plots.

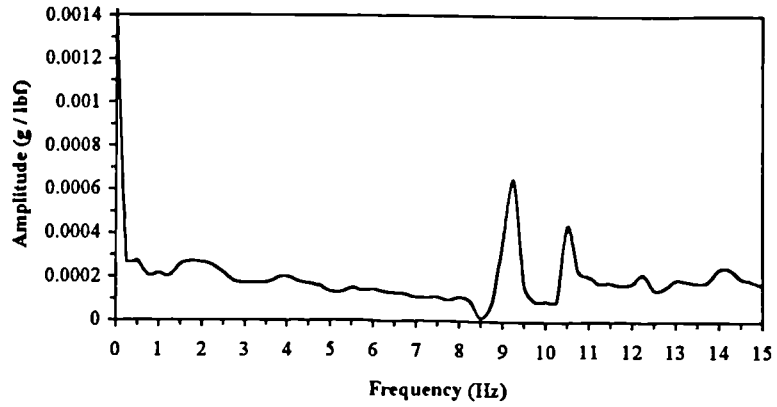

Transfer Function

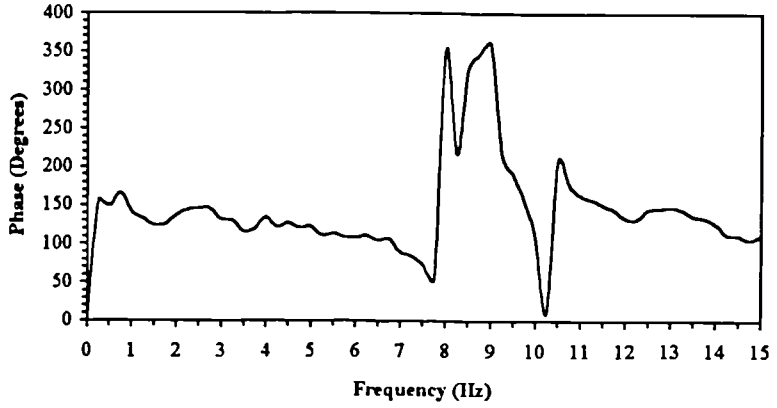

Phase

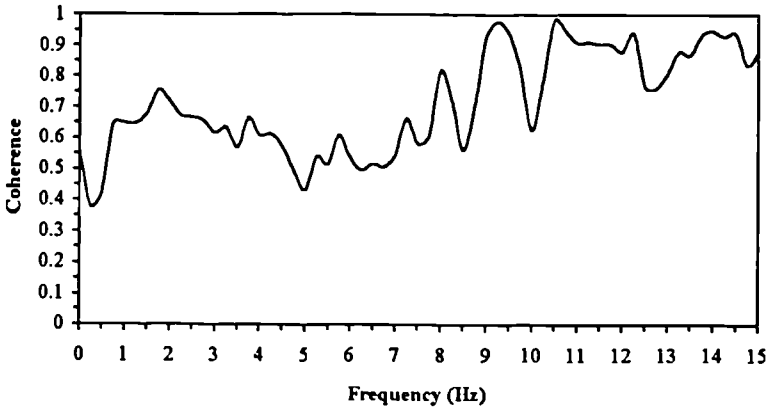

Coherence Function

Figure 3.28: Typical Transfer Function, Phase and Coherence Function

3.4.4 Premium Products Office

Structure Description (see Figure 3.25)

Location	:	Heathrow
Typical Panel	:	$L_S = 6.0$ m, $L_L = 9.0$ m
Beams	:	B1, B3 - UB356x127x33
		B2 - UB406x140x39
Girders	:	G1, G2 - UB533x210x92
Profile	:	CF70 (1.2)
Slab	:	t = 130 mm
Finishing	:	False Floor
Test Date	:	Thursday 2 March 1995

Test Results

Fundamental natural frequency	:	9.1 Hz
Floor damping	:	11.4 % critical

Comments

This building is located inside a cargo hanger near London's Heathrow Airport Terminal-4. This newly built floor was being furnished. The floor had false flooring and was carpeted recently. There were some partition walls being added. The test was carried out after the working hours in an enclosed and quiet environment. However, most of the furnishings and equipment was lying on the floor near the panel tested. The floor response was measured by removing a flooring panel and placing the accelerometer on the bare concrete. The floor damping is unexpectedly quite high due to the false floor and carpets and partitions underneath.

The coherence function does not correspond to the grid point for which the transfer function and phase are given, for reasons given earlier in section 3.2.3. It shows a good floor response.

Graphs

Figure 3.29 shows the typical experimental inertance transfer function, corresponding phase diagram and coherence function plots.

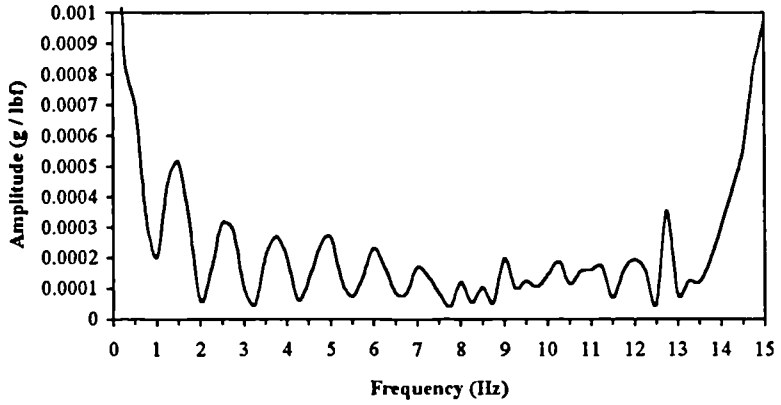

Transfer Function

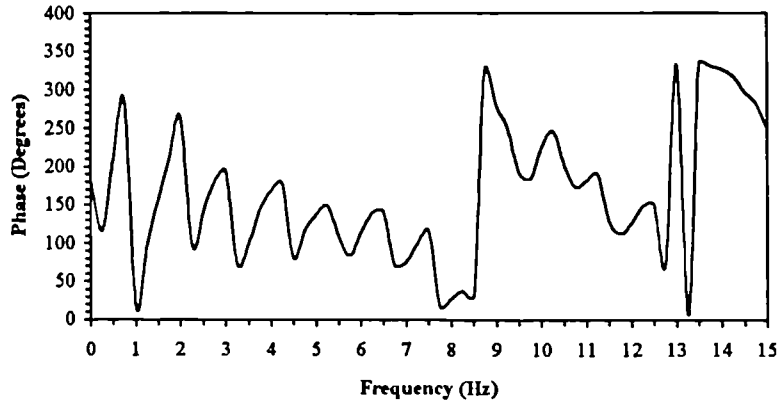

Phase

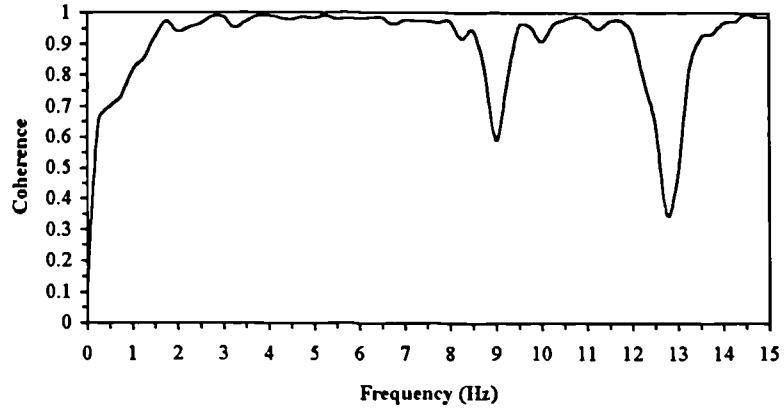

Coherence Function

Figure 3.29: Typical Transfer Function, Phase and Coherence Function

3.4.5 Tattersalls Grandstand Windsor Racing Stadium

Structure Description (see Figure 3.25)

Location	:	Windsor
Typical Panel	:	L_S = 6.0 m, L_L = 7.75 m
Beams	:	B1, B2, B3 - UB406x140x39
Girders	:	G1, G2 - UB406x140x39
Profile	:	CF70 (1.2)
Slab	:	t = 130 mm
Finishing	:	None
Test Date	:	Friday 3 March 1995

Test Results

Fundamental natural frequency	:	10.6 Hz
Floor damping	:	6.4 % critical

Comments

This floor was under construction and partly loaded with construction material. The test was carried out after the working hours. The high floor damping is mainly due to the partitions underneath and the close spacing of the beams.

The coherence function does not correspond to the grid point for which the transfer function and phase are given, for reasons given earlier in section 3.2.3.

Graphs

Figure 3.30 shows the typical experimental inertance transfer function, corresponding phase diagram and coherence function plots.

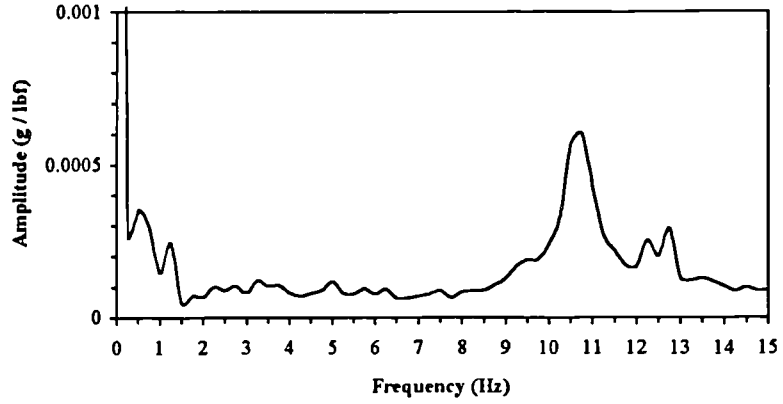

Transfer Function

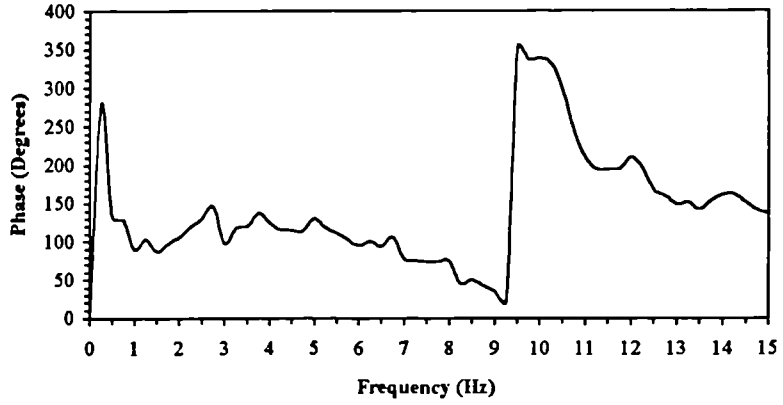

Phase

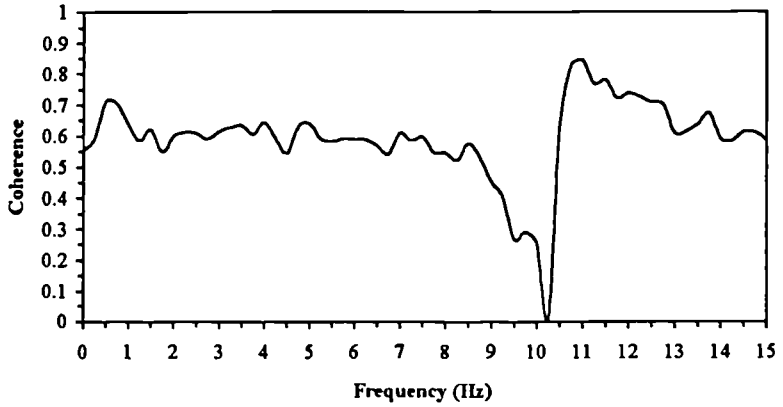

Coherence Function

Figure 3.30: Typical Transfer Function, Phase and Coherence Function

3.4.6 St. George's RC Secondary School Office

Structure Description (see Figure 3.25)

Location	:	London
Typical Panel	:	L_S = 7.0 m, L_L = 7.37 m
Beams	:	B1, B2, B3 - UB533x210x101
Girders	:	G1, G2 - UB533x210x101
Profile	:	CF70 (1.2)
Slab	:	t = 200 mm
Finishing	:	None
Test Date	:	Friday 17 March 1995

Test Results

Fundamental natural frequency	:	14.0 Hz
Floor damping	:	2.7 % critical

Comments

This floor was under construction and partly loaded with construction material. Some rain water was also coming in through the side walls at the time of the test. The results were, therefore, affected and this can be observed in the coherence function. The high floor frequency was primarily due to the heavy stiff beams and girders.

Graphs

Figure 3.31 shows the typical experimental inertance transfer function, corresponding phase diagram and coherence function plots.

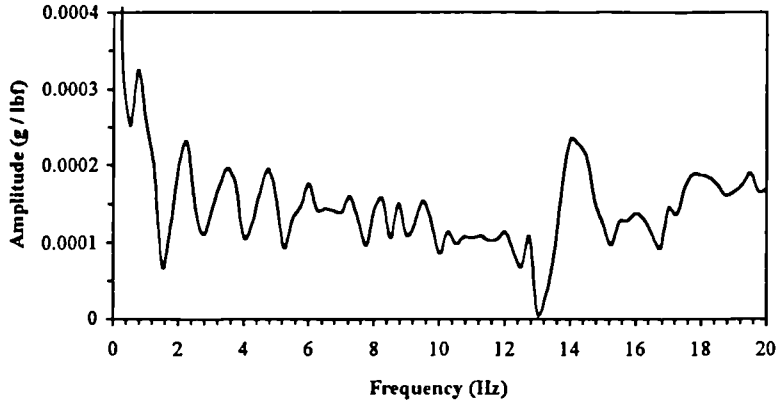

Transfer Function

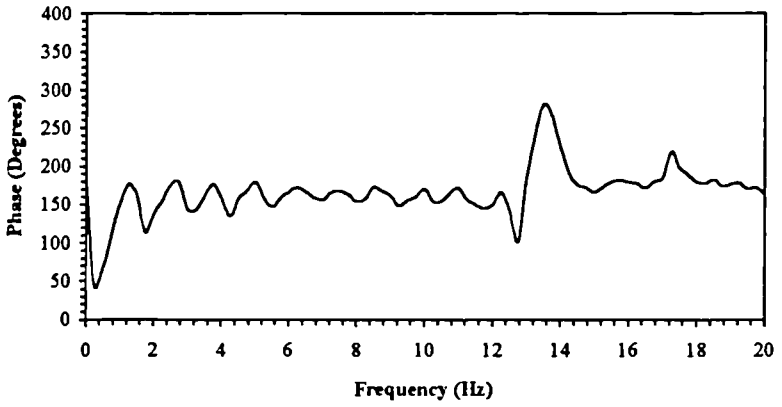

Phase

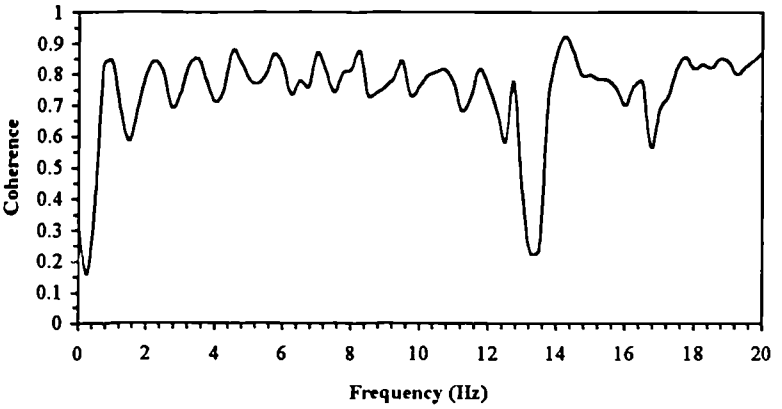

Coherence Function

Figure 3.31: Typical Transfer Function, Phase and Coherence Function

3.4.7 BRE's Large Building Test Facility, Level-5

Structure Description (see Figure 3.25)

Location	:	Cardington
Typical Panel	:	$L_S = 9.0$ m, $L_L = 9.0$ m
Beams	:	B1, B2, B3, B4 - UB305x165x40
Girders	:	G1 - UB356x171x51
		G2 - UB610x229x101
Profile	:	CF70 (1.2)
Slab	:	t = 130 mm
Finishing	:	None
Test Date	:	Monday 3 April 1995

Test Results

Fundamental natural frequency	:	6.4 Hz
Floor damping	:	3.6 % critical

Comments

This panel was the least cracked of the other panels on the floor. The floor had been subjected to excessive loading tests. These tests had caused cracking of concrete thereby reducing the overall moment of inertia of the slab. This, therefore, resulted in a lower first frequency and a slightly higher damping.

The coherence function does not correspond to the grid point for which the transfer function and phase are given, for reasons given earlier in section 3.2.3. The building is situated in a hanger and the testing environment was very quiet. However, a separate vibration test of the whole building was being carried out at the time of this test. This caused some disturbances which are visible in the coherence function.

Graphs

Figure 3.32 shows the typical experimental inertance transfer function, corresponding phase diagram and coherence function plots.

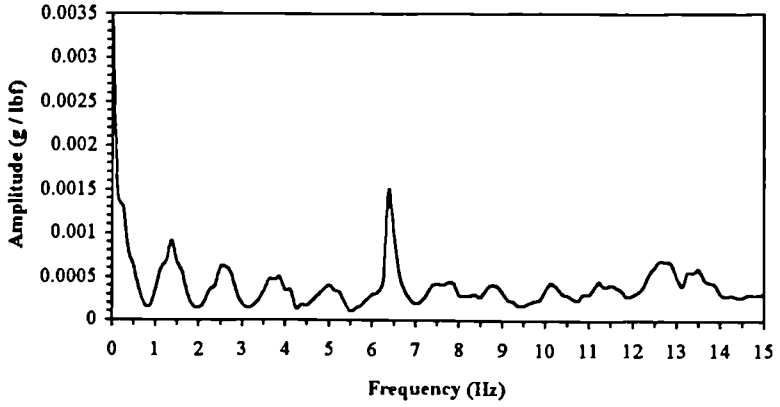

Transfer Function

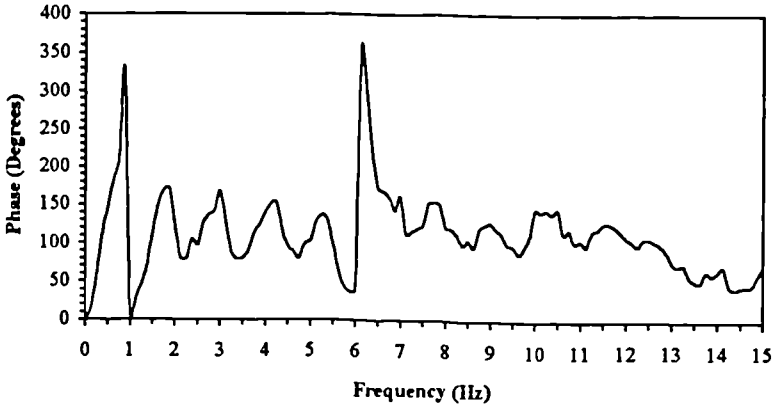

Phase

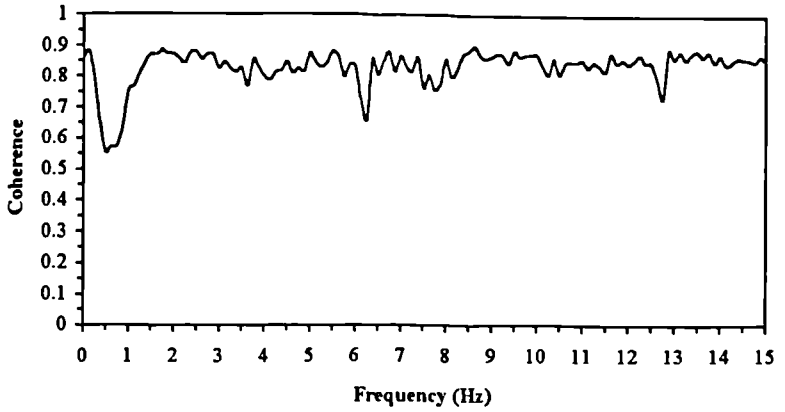

Coherence Function

Figure 3.32: Typical Transfer Function, Phase and Coherence Function

3.4.8 Guildford High School for Girls, Main Hall

Structure Description (see Figure 3.25)

Location	:	Guildford
Typical Panel	:	L_S = 2.95 m, L_L = 17.0 m
Beams	:	B1, B2 - UB610x229x140
Girders	:	Not supporting slab
Profile	:	CF70 (1.2)
Slab	:	t = 130 mm
Finishing	:	False Floor
Test Date	:	Tuesday 4 April 1995

Test Results

Fundamental natural frequency	:	8.6 Hz
Floor damping	:	3.8 % critical

Comments

This is a continuous floor supported on closely spaced long-span beams only. The floor had wooden false flooring and furniture for students. There were suspended ceilings underneath. The damping of the floor is, therefore, relatively high when compared with other floors of this type. The testing environment was ideal as it was carried out when the school had closed for vacation. However, since the accelerometer could not be placed on the bare concrete surface the results are not very good. This can be observed in the plot of the coherence function. The impact of hammer on the wooden floor also produced noise which has affected the results as visible from the coherence function plot. The coherence function does not correspond to the grid point for which the transfer function and phase are given, for reasons given earlier in section 3.2.3.

The frequency of the floor was estimated after careful and repeated analysis of the data due to its poor quality. This floor has also been tested by Westok Structural Services Ltd. Their measurements indicated a fundamental frequency of 7.8 Hz, WSSL (1995). They had connected the accelerometer to the steel beams which explains the difference in frequencies.

Graphs

Figure 3.33 shows the typical experimental inertance transfer function, corresponding phase diagram and coherence function plots.

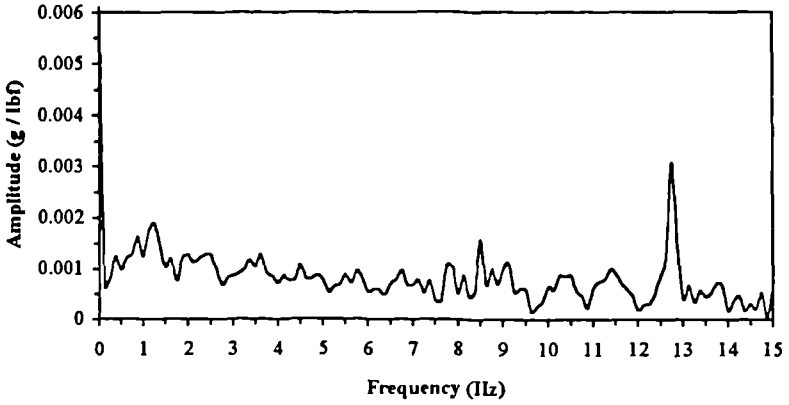

Transfer Function

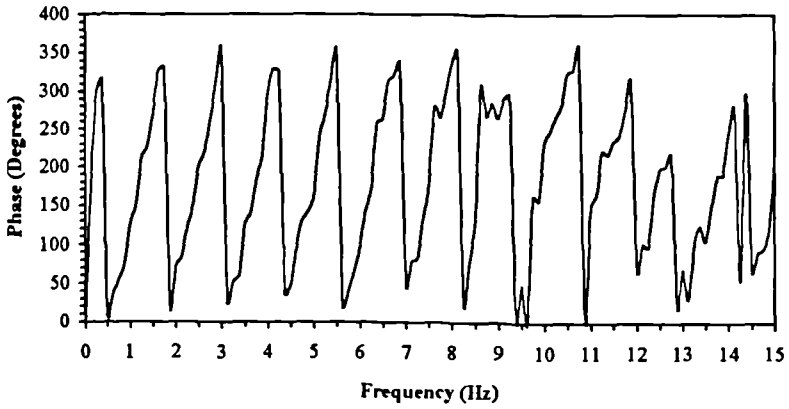

Phase

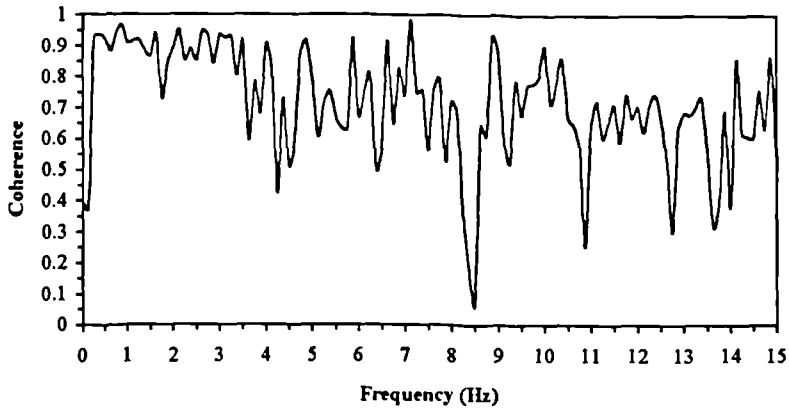

Coherence Function

Figure 3.33: Typical Transfer Function, Phase and Coherence Function

Chapter 4 FINITE ELEMENT MODELLING

This Chapter presents the results of finite element (FE) modelling of all the floor slabs tested in the experimental programme. Four different models are discussed according to each category of floors which have been mentioned in Chapter 3. Material properties pertinent to each floor category are given. Figures of typical models showing the boundary conditions are given for each floor category with corresponding modelling details. FE results for each floor are given individually along with the experimental fundamental natural frequency. Since the main theme of the research was the estimation of fundamental frequency, only this is used in all comparisons and discussions. A parametric study of the models leading to various curves for the control of natural frequency and deflections is also given. These curves were used to modify the SDOF system formula for the estimation of frequency using static deflections ($f = \frac{1}{2\pi}\sqrt{\frac{g}{\Delta_s}}$, see section 1.2.3) for each floor type and this is discussed for each floor category.

4.1 Post-Tensioned Concrete 1-Way Spanning Solid Floor Slabs With Beams

The FE modelling of the four floors of this type was carried out using the I-DEAS and ANSYS software packages. All these floors are continuous in both directions with variable beam and column dimensions and span lengths in both directions. However, the study was limited to 3x3 adjacent panels only (see Figure 3.1), to study the effect of continuity of the floor on fundamental natural frequency and if a more detailed model resulted in any accuracy. Models in steps of a single panel and upto 3x3 panels where possible were, therefore, analysed. The High Wycombe car park floor could only be studied upto 3x1 panels with the cantilever portion of slab. The Ilford car park floor could be studied with an upto 2x2 panel model due to the unsymmetric layout and other layout restrictions. Major details of modelling are as follows:

Geometry

The as-built dimensions (measured on-site) were used in modelling the floors (for the reasons given in Chapter 3).

Boundary Conditions

The columns were modelled as fixed supports along their perimeter. This is the most realistic approach considering that columns are cast monolithic with the concrete slab.

Element Type

Linear isotropic quadrilateral elastic thin shell elements were used for the slab (in the horizontal plane) in the different models studied. The same shell elements (in the vertical plane) and elastic beam elements were used for the beams to study their effect. A brief discussion on both shell and beam elements follow. For full details, see I-DEAS and ANSYS manuals.

Shell Elements

The shell element has both bending and membrane capabilities. It has six degrees-of-freedom (DOF) at each node: translations in the nodal x, y and z directions and rotations about the nodal x, y and z axes. Both in-plane and normal loads are permitted. The element is defined by four nodes, four thicknesses and the orthotropic material properties. The element must not have a zero thickness or area. The four nodes defining the element should lie in an exact flat plane: however, a small out-of-plane tolerance is permitted so that the element may have a slightly warped shape. The shell element used is referred to as the Thin Shell Element in I-DEAS and Shell63 in ANSYS. Figure 4.1 shows the shell element.

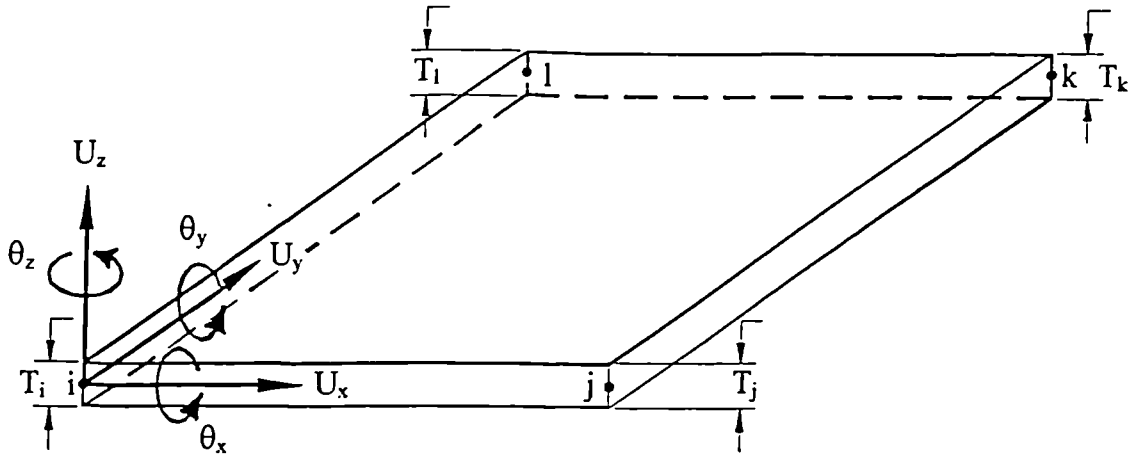

Figure 4.1: Shell Element

Beam Elements

The beam element is uniaxial with tension, compression, torsion and bending capabilities. It has six DOF's at each node: translations in the nodal x, y and z directions and rotations about the nodal x, y and z axes. The element is defined by two nodes, the cross-sectional area, two area moments of inertia (I_{yy} and I_{zz}), two thicknesses (t_y and t_z), an angle of orientation about the element x-axis, the torsional moment of inertia (I_{xx}) and the material properties. The beam element can have any cross-sectional shape for which the moments of inertia can be computed. However, the stresses are determined as if the distance between the neutral axis and the extreme fibre is one-half of the corresponding thickness. The element thicknesses are used only in the bending calculations. The beam element must lie in an X-Y plane and must not have a

zero length or area. The moments of inertia, however, may be zero. The beam element is slightly stiffer than the shell element because it allows bending in one direction only. The beam element used is referred to as the Beam Element in I-DEAS and 3-D Beam4 in ANSYS. Figure 4.2 shows the beam element.

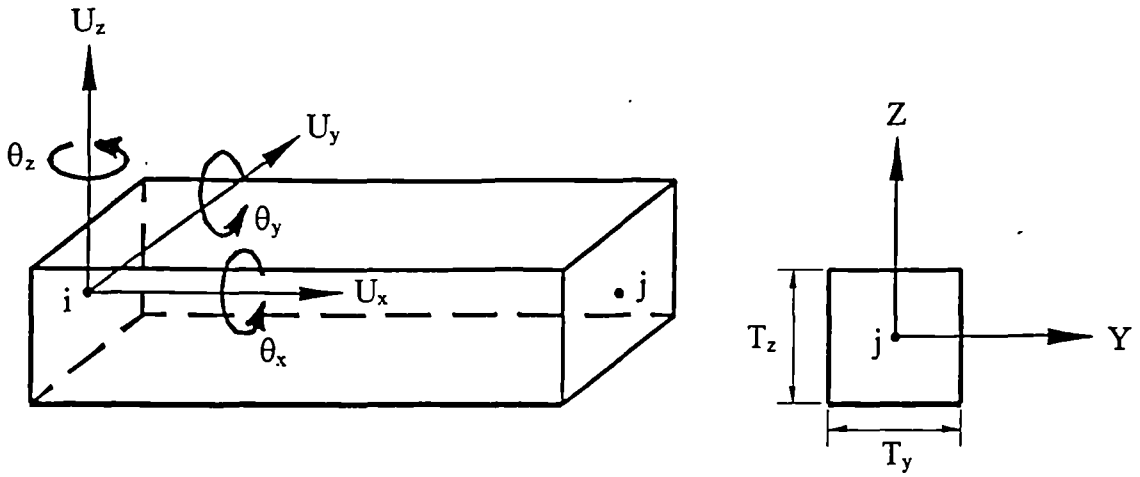

Figure 4.2: Beam Element

FE Modelling of Elements

The beams defined as shell elements of thickness B and depth D at the slab centroid O are shown in Figure 4.3. The centroid of the beams defined as beam elements of section BxD was translated in the vertical plane from O to O' to avoid any duplication of the area covered by the slab shell elements (see Figure 4.3). The centroids of the beam and slab elements were then connected by a rigid element between them to produce a reasonable constraint for their displacements (see Figure 4.3). This procedure establishes the simplest level of modelling that provides a reasonable representation of the dynamic characteristics of these floors.

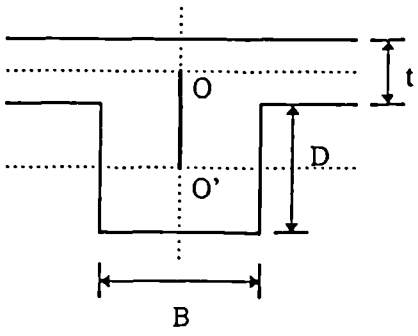

Figure 4.3: Beam Section Model

Material Properties

Assumptions regarding material properties had to be made for reasons which have given under "Geometry". Natural and normal weight aggregate concrete of Grade 40, normally used in prestressed construction, was assumed in the FE analyses. The following values for the material properties were used:

i)	Density of concrete (ρ_c)	:	2400 Kg/m^3
ii)	Compressive strength of concrete (f_{cu})	:	Grade 40 (i.e. 40 N/mm^2)
iii)	Modulus of elasticity of concrete (E_c)	:	34.79 KN/mm^2

The modulus of elasticity of concrete is the biggest uncertain variable in this type of dynamic analysis. There are a number of equations available for its estimation and none of them result in a single value, for example, Neville (1995), ACI (1994), etc. It depends, therefore, on the analyst to choose any value of the modulus based on his experience. However, in doing so, the following factors that would probably result in a higher value for the modulus than estimated by any equation, must be considered:

i) Effect of creep and shrinkage of concrete over time;
ii) Gain in compressive strength of concrete over time;
iii) Effects of post-tensioning (discussed later);
iv) High value for modulus in dynamic motion.

Moreover, in the case of post-tensioned floors, the service loads do not normally reach or exceed the design loads and, therefore, the concrete may be assumed uncracked.

The British Standards BS8110:Part-I (1985) provide the equation $E_c = 5.5\sqrt{f_{cu}}$ for the estimation of modulus. However, a range of 22-34 KN/mm^2 with an average of 28 KN/mm^2 is given in BS8110:Part-II (1985) for the modulus of Grade 40 concrete based on its 28-day strength. Since the 28-day compressive strength of Grade 40 concrete increases by 25% over 1-year, BS8110:Part-I (1985), this range, therefore,

becomes 24.6-38.0 KN/mm^2 with an average of 31.3 KN/mm^2. For simplicity of calculation and considering the above factors affecting E_c, the above equation was used to estimate E_c for these floor slabs. Since the dynamic modulus of elasticity is higher than the static by upto 21%, Chen and Aswad (1994), the results reported here, based on the above assumption, may be considered to be conservative.

Post-Tensioning

The effect of post-tensioning was not modelled in this study as this was not the main concern. However, it may be mentioned that post-tensioning enables the concrete section to resist tension due to applied loading without cracking, thus increasing the stiffness when compared with cracked sections which in turn would increase the frequencies. Post-tensioned floors may be assumed to be uncracked mainly because of the pre-compression and initial camber and the fact that the actual service loads are normally less than the design loads. The increases in modulus of elasticity due to strength gains, however, may be assumed to be offset by the prestress losses over time.

Since there are a large number of uncertainties in floor vibrations, it may be assumed that the modelling of post-tensioning will not lead to higher accuracies in frequency estimation as compared to using the accurate estimates of the modulus of elasticity, for example.

4.1.1 Single Panel vs Multi-Panel Models

It has been previously shown that a complete model of a composite floor leads to accurate estimates of all frequencies, Osborne and Ellis (1990). However, the floor analysed by Osborne and Ellis (1990) was a small building floor. In real life structures, the layout may not be easy to model. The floor may not be symmetric and may have different slab thicknesses and other structural element dimensions and properties. Also, the floor layout may be so large that it may become difficult to model the whole floor. Afterall, a very accurate analysis is not feasible in practice.

In order to develop simple analytical models, it is necessary to investigate more detailed models to ensure that accuracy is not jeopardised. However, it may be mentioned that most designers or consultants do not wish to spend extra time on detailed finite element modelling. Also, most floor arrangements tested in this research consisted of upto a maximum of three floor panels extending in one direction and several in the other direction (Figure 4.4). Therefore, the floors tested were modelled in steps of one panel and upto 3 x 3 panels only.

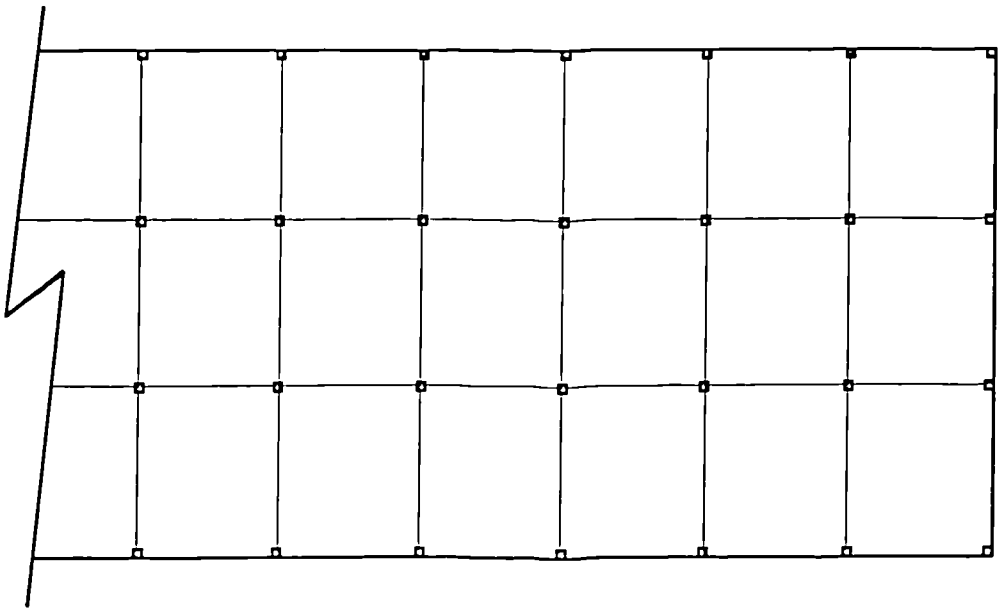

Figure 4.4: Typical Floor Layout

During modelling, the experimental results were used as a benchmark in order to achieve accuracy. This type of analyses, called model tuning, was carried out because it was not sure which element type or boundary condition would yield the closest results. Although the material properties of concrete were a major factor of uncertainty, these were kept constant throughout the analyses and for all the floors of this type so that every modelling effects could be studied.

Table 4.1 compares the measured fundamental natural frequency of these floors with the results of FE analyses for floor models with shell elements for both the slab and beams.

Table 4.1: FE and Measured Fundamental Frequencies

Site	Field Results (Hz)	Finite Element Results (Hz)		
		1 Panel	2 x 2 Panels	3 x 3 Panels
High Wycombe	10.2	10.13	9.85	10.08
Wimbledon	5.8	6.10	6.45	6.45
Fleet	11.2	11.53	7.34	N/A
Ilford	7.3	7.34	7.12	N/A

It can be seen from Table 4.1 that a single-panel model closely approximates the fundamental natural frequency of this floor type. Additional panels affect this frequency because of the differences in dimensions or boundary conditions.

The most important point to note from Table 4.1 is the results for the Fleet floor which has adjacent floor panels of different dimensions. Since it was not possible to test the most flexible panel, the fundamental frequencies using the 2 x 2 panel model do not match the experimental results. It may, therefore, be concluded that fundamental frequency is a localised property and will change from panel to panel. Because these low floor frequencies damp out quickly due to inherent damping, additional panels or a more complete floor model would, therefore, not affect the fundamental natural frequency significantly. Based on this conclusion, further studies were limited to a single panel model only.

The comparison of field and FE results for the single-panel FE model with shell elements is plotted in Figure 4.5.

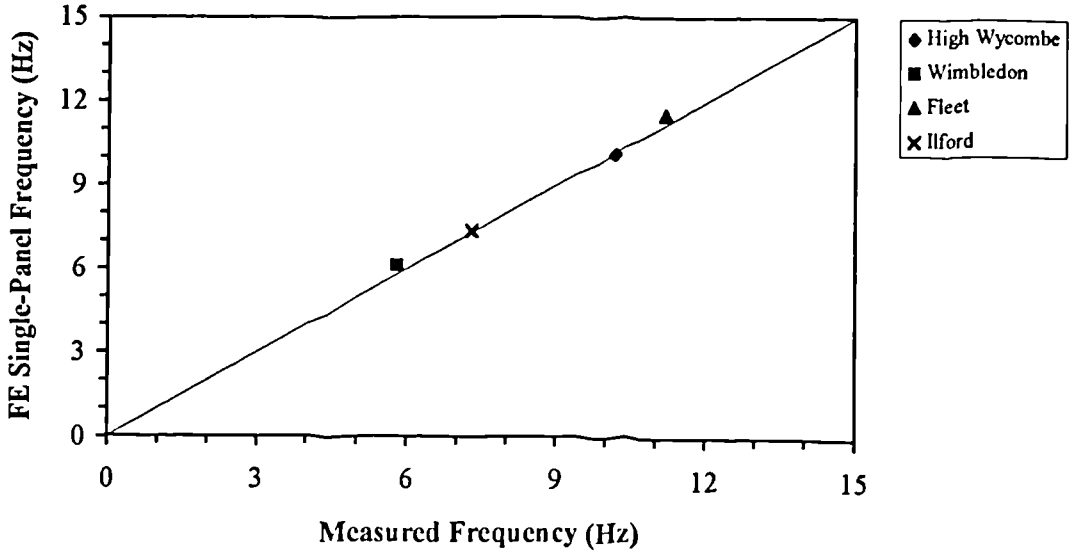

Figure 4.5: Field vs FE Frequency

Table 4.2 compares the measured fundamental natural frequency of these floors with the results of single panel FE analyses for floor models with shell elements for the slab and beam elements for the beams. These FE analyses were carried out using I-DEAS.

Table 4.2: FE and Measured Fundamental Frequencies

Site	Field Results (Hz)	Finite Element Results (Hz)
High Wycombe	10.2	10.35
Wimbledon	5.8	6.95
Fleet	11.2	11.48
Ilford	7.3	7.61

It can be seen from Table 4.2 that using a beam element for the beams of this floor type results in a stiffer model and, therefore, higher frequencies. Thus, it may be concluded that beams in this type of floors behave as part of the floor and not as supports.

Therefore, a single panel FE model with shell elements for both the slab and beams (i.e. model using one element type) achieve true representative conditions for the dynamic motion of these slabs and provides the best results. This model can, therefore, be used reliably to estimate the fundamental frequency of this type of floors. The

model also allow the beams to bend in both orthogonal directions which is more realistic because of their longer spans. Further studies have, therefore, been based on this model.

Figures 4.6 to 4.8 below shows the typical 1-panel, 2-panel and 3-panel models for the floor type under consideration.

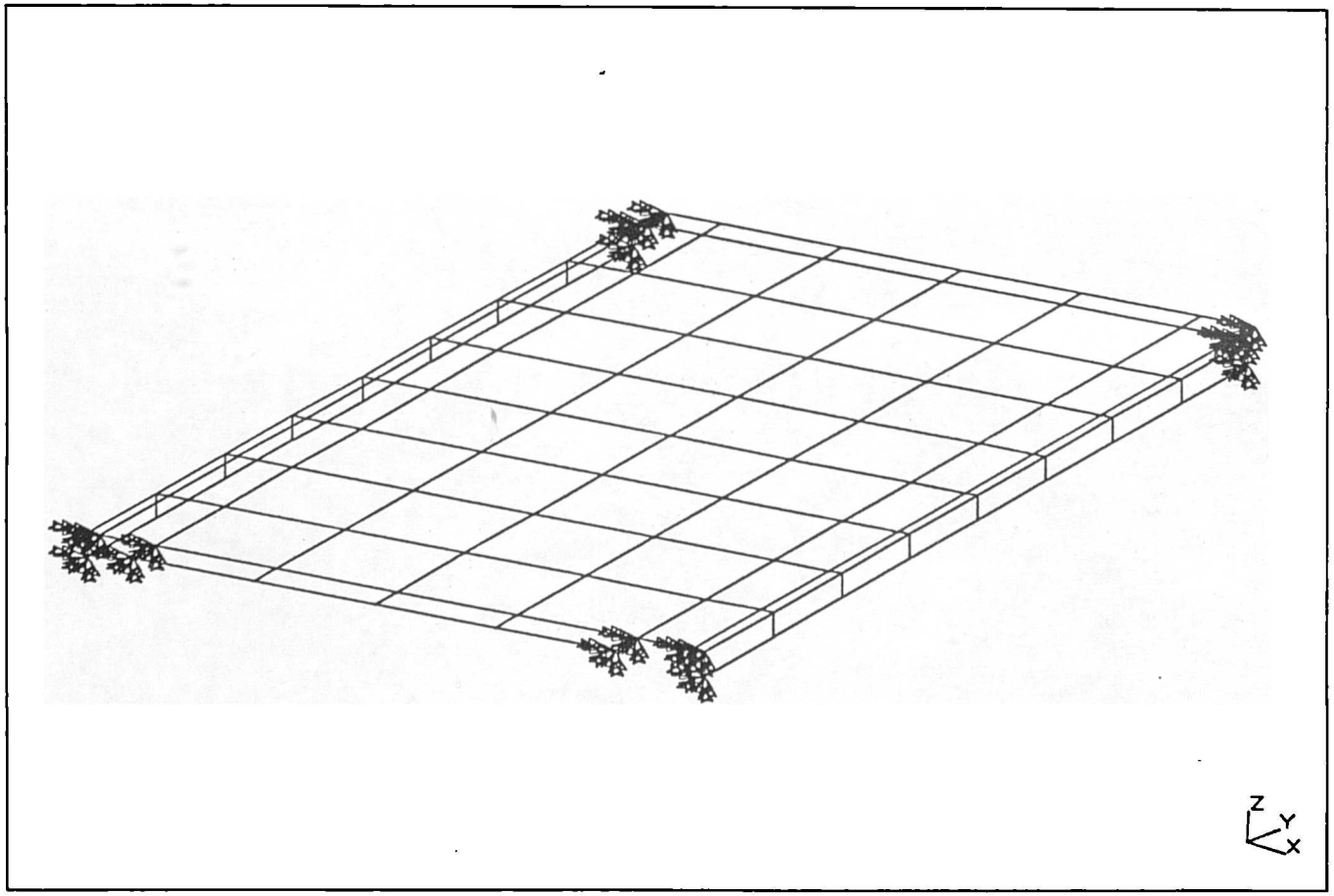

Figure 4.6: A Typical FE 1-Panel Model

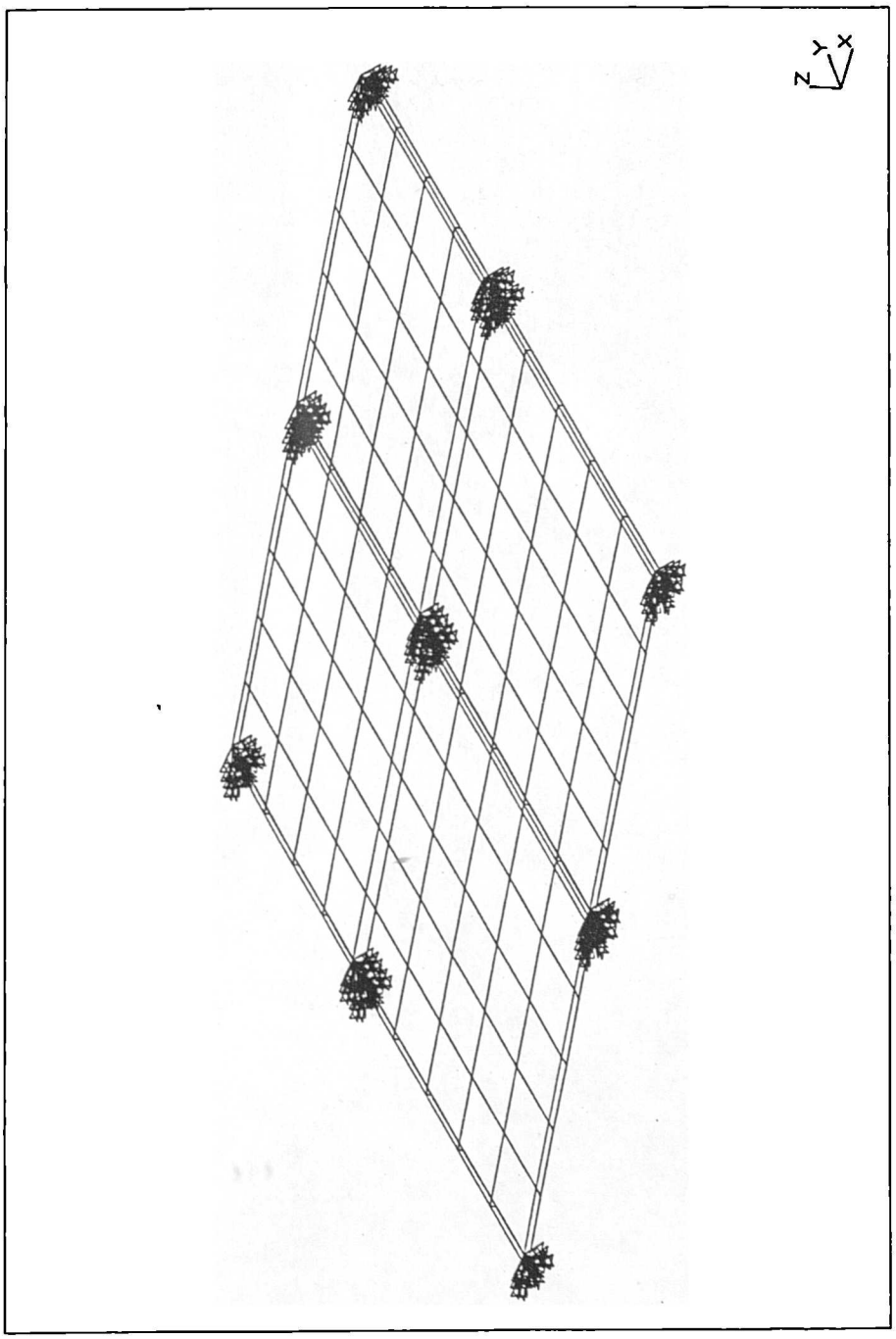

Figure 4.7: A Typical FE 2-Panel Model

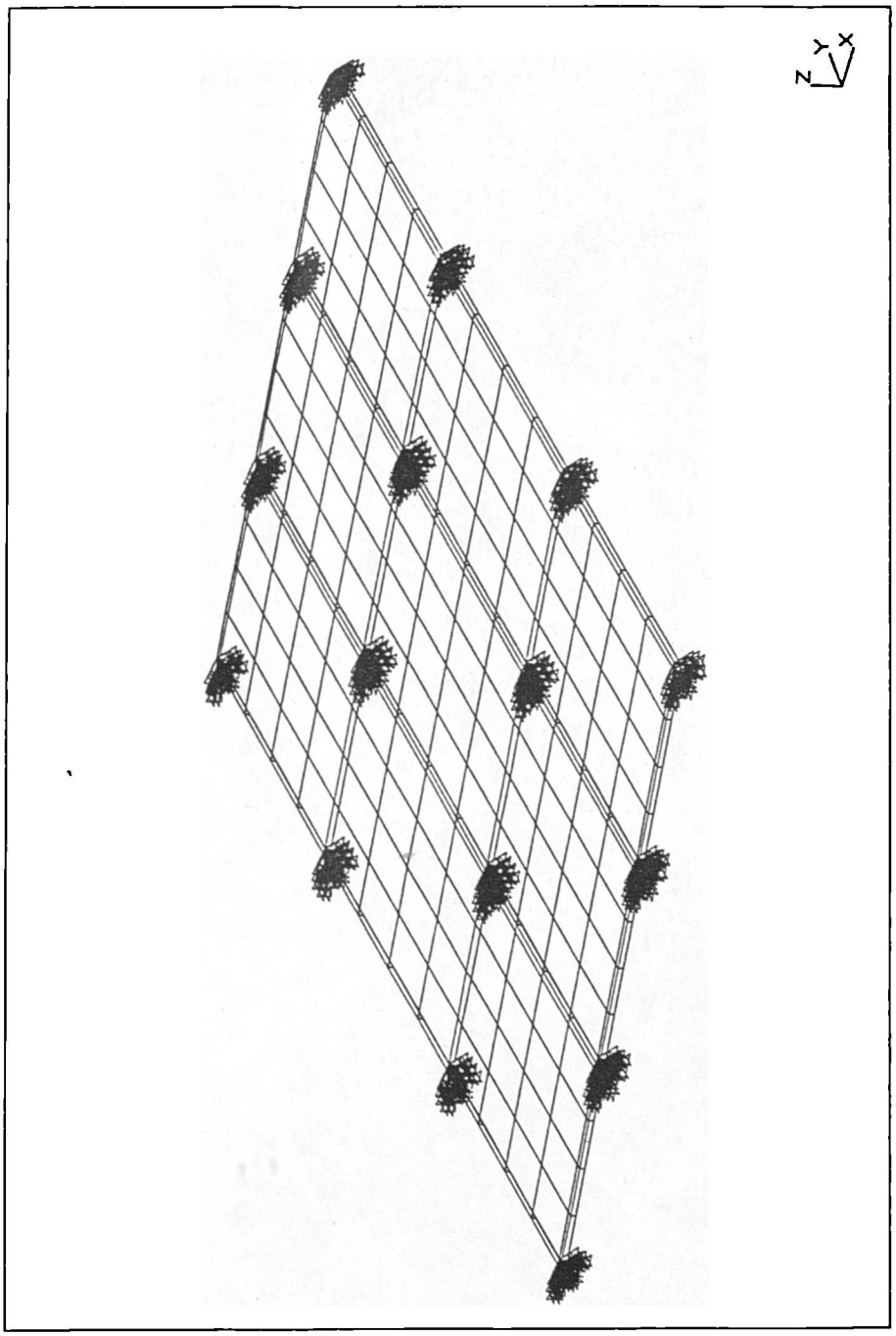

Figure 4.8: A Typical FE 3-Panel Model

4.1.2 Parametric Studies

The single panel FE model was used to study the variation of fundamental frequency with the span/depth ratios in both directions of the floor slab; and the maximum static deflections. The thickness of the slab was the only variable changed in the model. Static and dynamic analyses of the model then yielded maximum static deflections and floor frequencies for each slab thickness, respectively. These analyses were carried out for self-weight only and no super-imposed load was considered. In practice, any extra loading would reduce the frequencies and increase the deflections. However, in the FE analyses the inclusion of these loads would only affect the frequencies if they are modelled as an equivalent slab thickness of density equal to that of concrete. This, however, would also increase the stiffness and thus raise the frequencies. Thus, the effect of modelling the super-imposed loads in this way are negligible and were, therefore, not considered.

The analyses were restricted to a maximum frequency range of interest of 15 Hz and, therefore, slab thicknesses which resulted in higher frequencies were not used in studying these variations. The analyses were, however, carried out below the minimum frequency limits only to establish these limits. However, a minimum slab thickness of 125 mm was used for all the floors to achieve lower frequencies. The upper limit of slab thickness resulting in the maximum frequencies of 15 Hz was variable for all the floors, depending on their span/depth ratios in each direction.

Since the Canadian Code, CSA (1985, 1989), requires a full dynamic analysis for floors with fundamental frequencies below 6 Hz, this frequency was used as a minimum in the parametric studies.

4.1.2.1 Frequency vs Span/Depth Ratios

Figures 4.9 and 4.10 shows the variation of floor frequency with the short and long span/depth ratios, respectively.

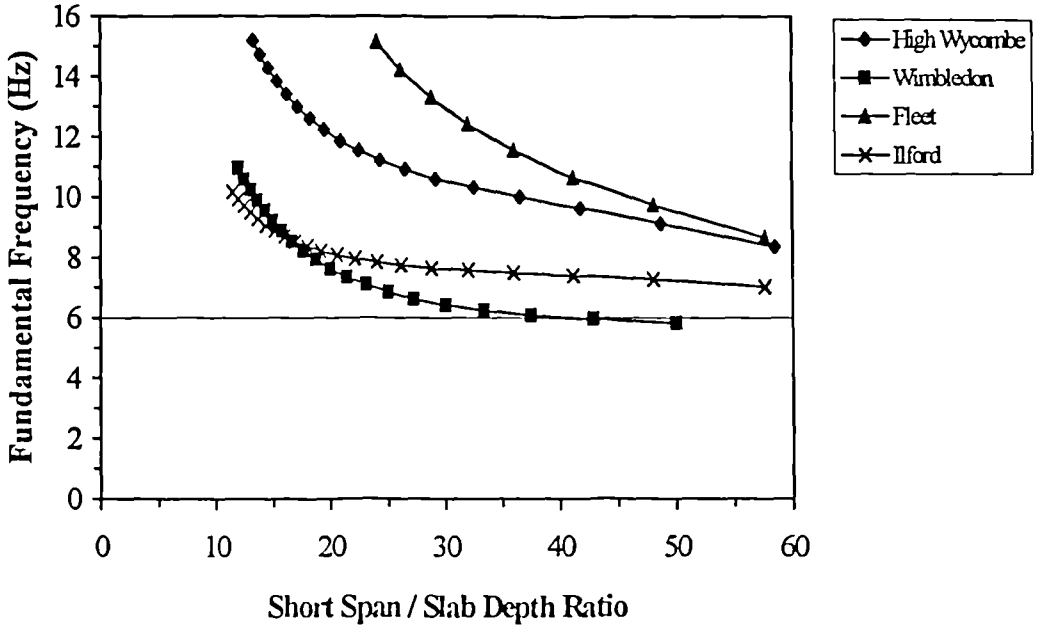

Figure 4.9: Frequency vs Short Span/Depth Ratio

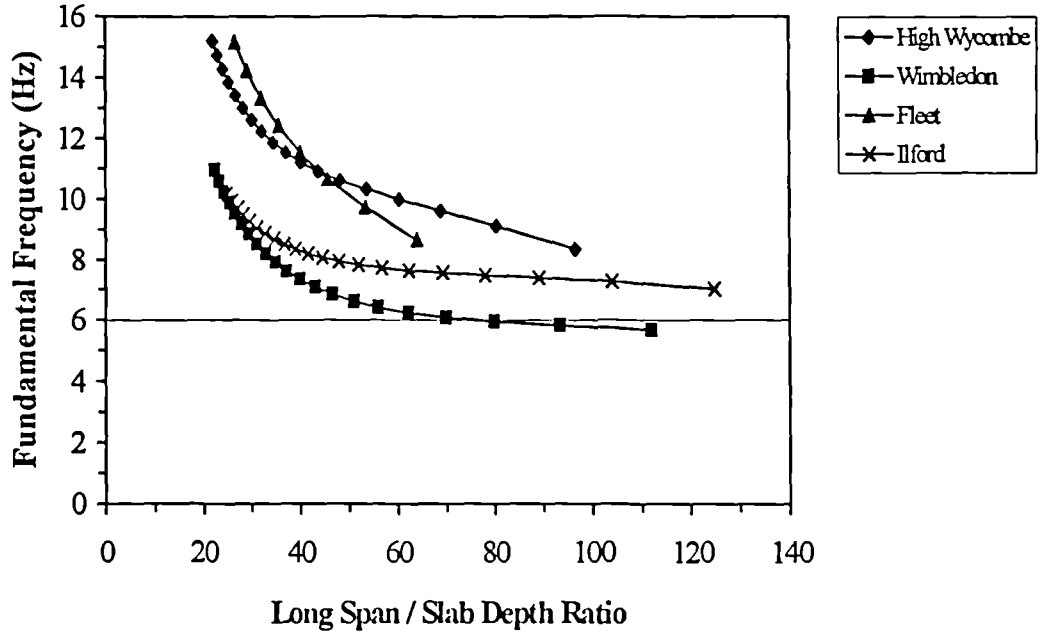

Figure 4.10: Frequency vs Long Span/Depth Ratio

From Figures 4.9 and 4.10, it may be noted that the graphs of span/depth ratios against floor fundamental frequencies follow a general trend but differ in shape due to the different dimensions of the beams. The difference in the ordinates, however, is due to the different stiffnesses caused by the span/depth ratios and beam and column dimensions of each floor.

It is clear from Figures 4.9 and 4.10 that a maximum span/depth ratio of 42 for the slab's short span direction (normal to beams) and 78 for the slab's long span direction (along beams), respectively, would ensure a minimum fundamental frequency of 6 Hz for this floor type. It may be noted, therefore, that the Ilford floor donot satisfy this requirement (see Table 4.3).

Assuming that the fundamental frequencies of the single-panel FE model are correct, it can be concluded that all the floors tested satisfy the minimum frequency requirement. However, the high frequency of Ilford floor even for higher short and long span/depth ratios is due to the contribution of beams and the extra stiffness provided by columns. It has been shown previously that beams behave as part of the floors and not as supports but they increase local stiffness which plays an important role in using high span/depth ratios for the slab. Generally, a lower span/depth ratio is obtained for a floor with a wide beam of large cross-section area and a higher span/depth ratio is obtained for a floor with a narrow beam of small cross-section area (see Table 4.1, Figures 4.9 and 4.10 and Table 4.3).

Table 4.3: Span/Depth Ratios of the Tested Floors

Site	Short Span/Depth Ratio	Long Span/Depth Ratio
High Wycombe	34.8	57. 4
Wimbledon	37.5	70.0
Fleet	36.0	40.0
Ilford	45.0	97.5

4.1.2.2 Frequency vs Deflection Relationship

Figures 4.11 shows the variation of floor frequency with maximum static deflections.

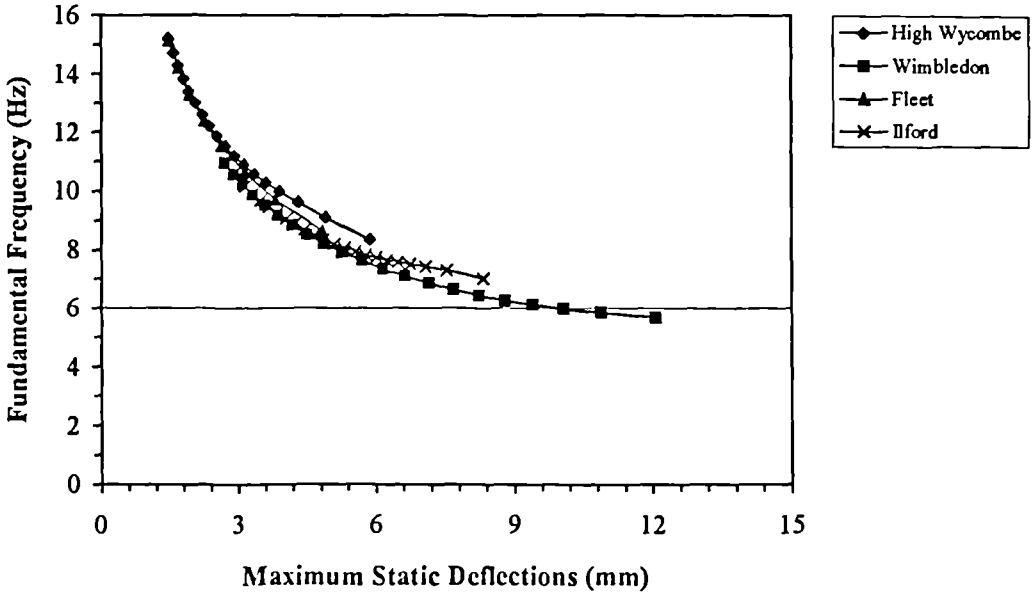

Figure 4.11: Frequency vs Static Deflections

Figure 4.11 shows that the variation of static deflections against corresponding floor frequency generally follows a consistent trend. The difference in the shape of these curves is due to the different dimensions of the beams. A trendline least-squares curve-fit shows that these relationships are of the following form:

$$f = \frac{K}{\sqrt{\Delta_s}} \tag{4.1}$$

Equation 4.1 is a modified form of the more well-known formula $f = \frac{1}{2\pi}\sqrt{\frac{g}{\Delta_s}}$ for a SDOF spring-mass system (see also section 1.2.3). The constant K as determined by curve-fitting is given in Table 4.4 below:

Table 4.4: FE Single Panel Deflections and Constant K

Site	Maximum Static Deflection (mm)	Constant K
High Wycombe	3.78	17.714
Wimbledon	9.40	17.065
Fleet	2.64	18.197
Ilford	7.32	15.524
Average		17.125

It may be noted from Table 4.4 that the constant K varies from 15.524 to 18.197 (17.22% rise) for the four floors tested. An average value of this constant may be assumed as 17. It can, therefore, be assumed that the fundamental frequency of beam and slab type floors (distributed-mass i.e. MDOF system) can be closely approximated by the following relationship:

$$f = \frac{17}{\sqrt{\Delta_s}} \tag{4.2}$$

It may be noted that the value of K for a lumped-mass SDOF system is approximately 15.8 (i.e. $\frac{\sqrt{g}}{2\pi}$). Therefore, because of the limited number of tests on this floor type showing a wide range of variation for K, a lower bound limit for K should be taken as 15.8. This is also a very conservative limit because the frequency of a MDOF system will always be greater than that of a corresponding SDOF idealisation.

From Figure 4.11, it can also be seen that the minimum deflection for a minimum floor frequency of 6 Hz is about 10 mm. Therefore, limiting the deflections to 10 mm will ensure frequencies higher than 6 Hz. Alternatively, equation 4.2 can be used to estimate frequencies for a given deflection limit.

4.2 Post-Tensioned Concrete Solid Flat Slab Floors

The FE modelling of the twelve floors of this type was carried out using ANSYS software. All of these floors were continuous in both directions with variable column dimensions and span lengths in both directions (see Figure 3.6). However, the study was limited to 3x3 adjacent panels only, to study the effect of continuity of the floor on the fundamental frequency and if a more detailed model improves the accuracy of the result. Models in steps of a single panel and upto 3x3 panels where possible were, therefore, analysed. Major details of modelling of this floor type are the same as those discussed in section 4.1, except that in this case there are no beams to model.

4.2.1 Single Panel vs Multi-Panel Models

Table 4.5 compares the measured fundamental frequency of these floors with the results of FE analyses for floor models with shell elements for the slab.

Table 4.5: FE and Measured Fundamental Frequencies

Site	Fundamental Frequency (Hz)			
	Field Results	Finite Element Results		
		1 Panel	2 x 2 Panels	3 x 3 Panels
Hammersmith	8.1	8.41	9.25	9.81
Fleet	5.9	6.18	6.58	N / A
London	10.1	10.96	12.21	12.81
Worcester	12.7	14.19	15.90	16.69
Worcester	9.1	9.98	10.70	N / A
Birmingham	7.2	8.00	8.61	8.66
Birmingham	8.6	9.28	10.03	10.18
Birmingham	12.7	14.44	15.61	15.84
London	8.4	9.48	10.53	N / A
London	10.6	11.15	10.53	N / A
Winchester	10.3	10.32	10.81	N / A
Winchester	8.5	9.19	9.80	9.94

It can be seen from Table 4.5 that a single-panel model closely approximates the fundamental frequency of this floor type. This conclusion is identical to that given in section 4.1. Therefore, all other relevant comments in section 4.1.1 apply here as well.

Also, the 2 and 3-panel models show a consistent over-estimation of fundamental frequency. This is considered to be caused by the dimensions and boundary conditions of adjacent panels not always being the same.

The comparison of field and FE results for the single-panel FE model are plotted in Figure 4.12.

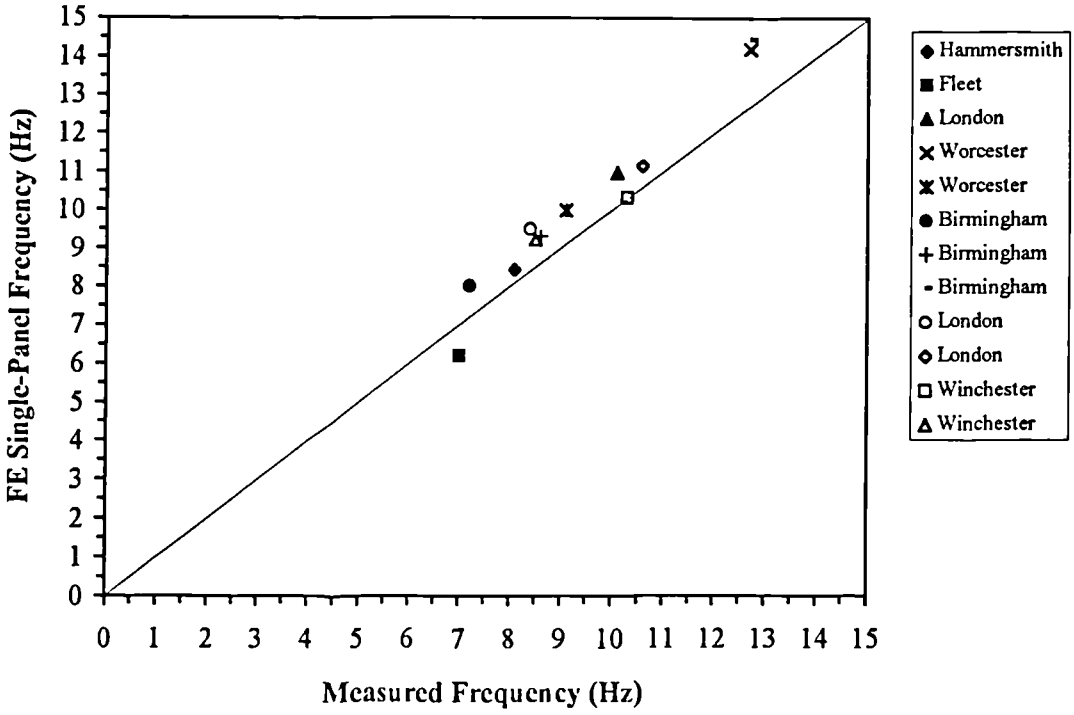

Figure 4.12: Field vs FE Frequency

Figures 4.13 to 4.15 below shows the typical 1-panel, 2-panel and 3-panel models of this floor type.

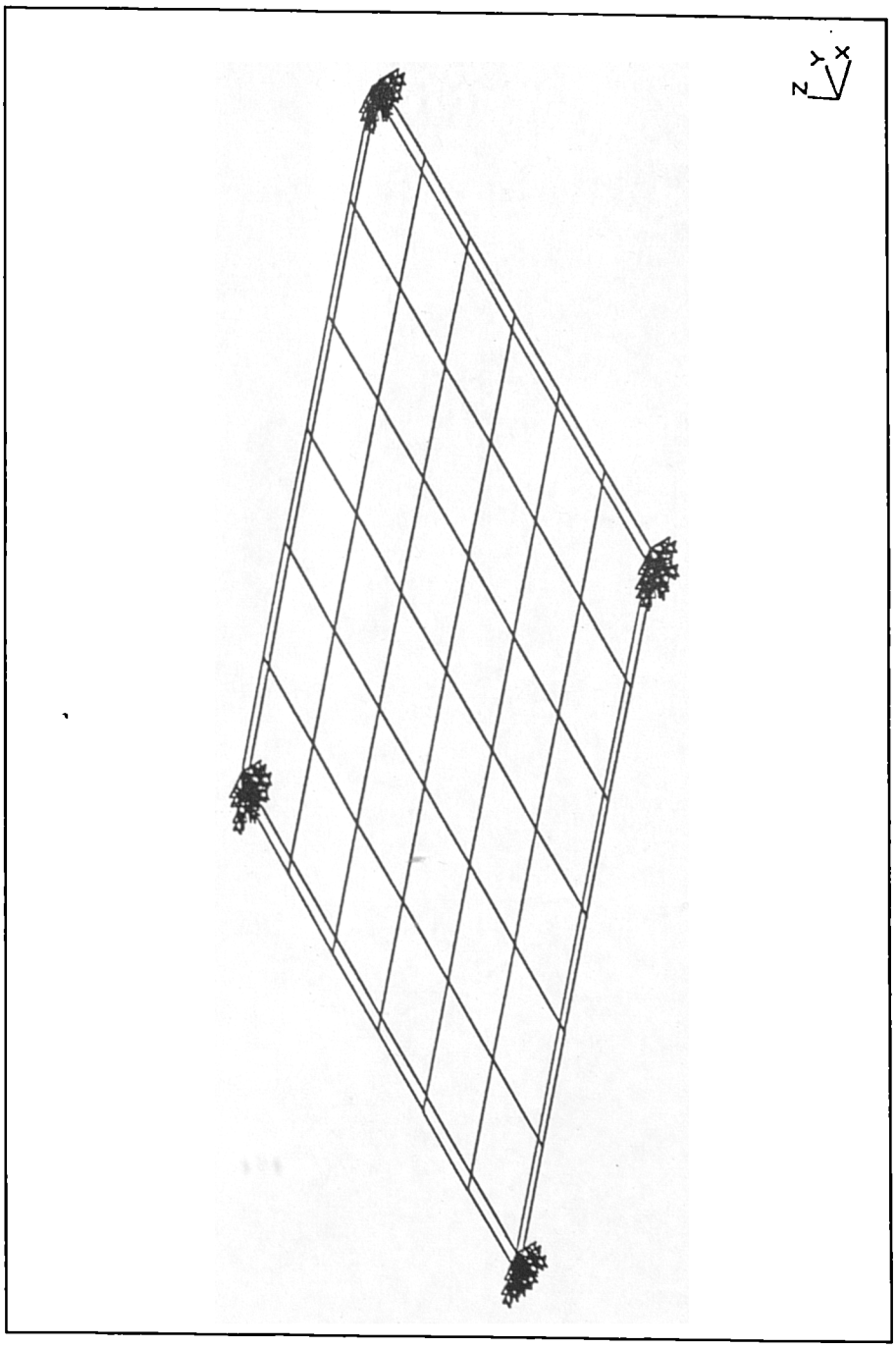

Figure 4.13: A Typical FE 1-Panel Model

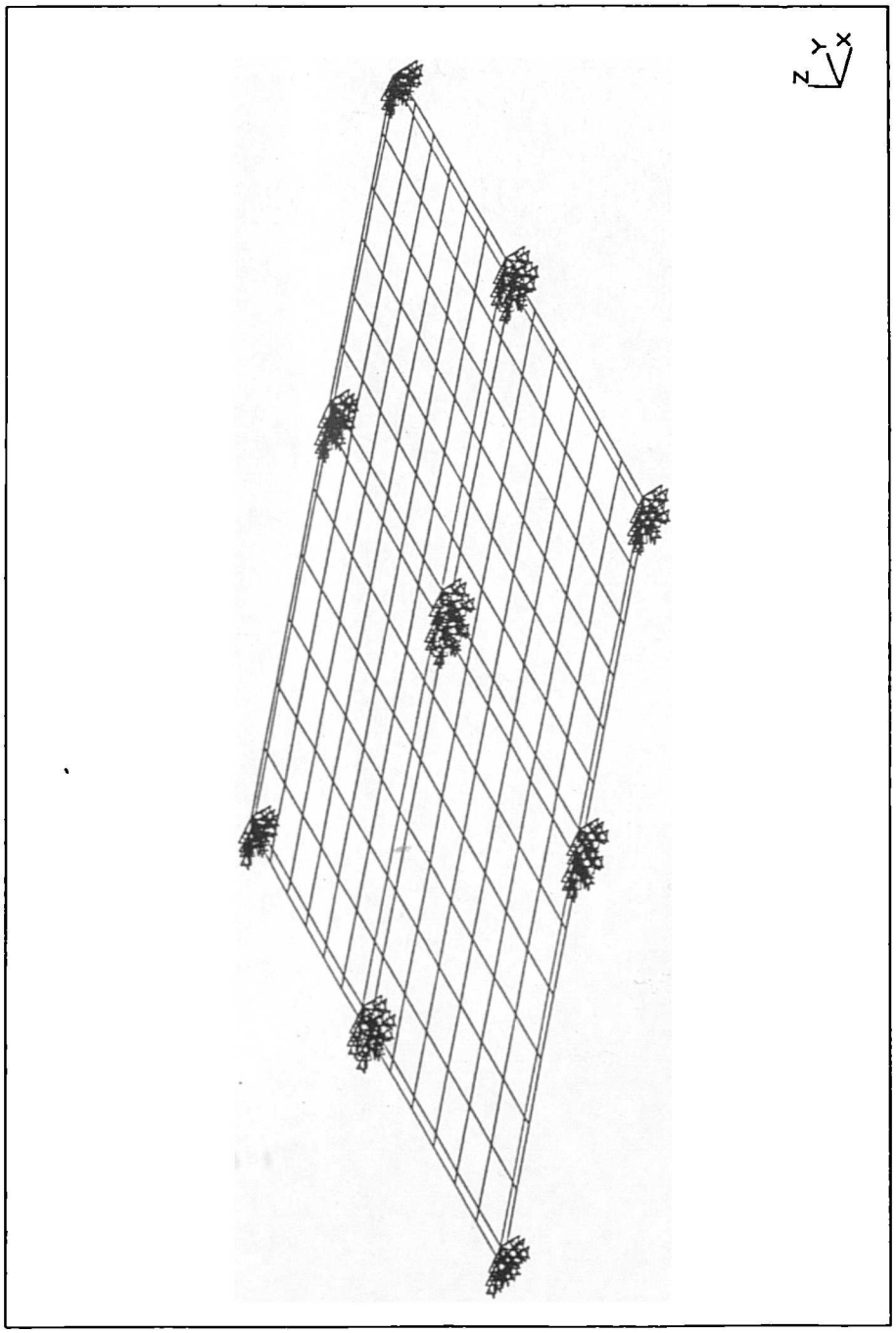

Figure 4.14: A Typical FE 2-Panel Model

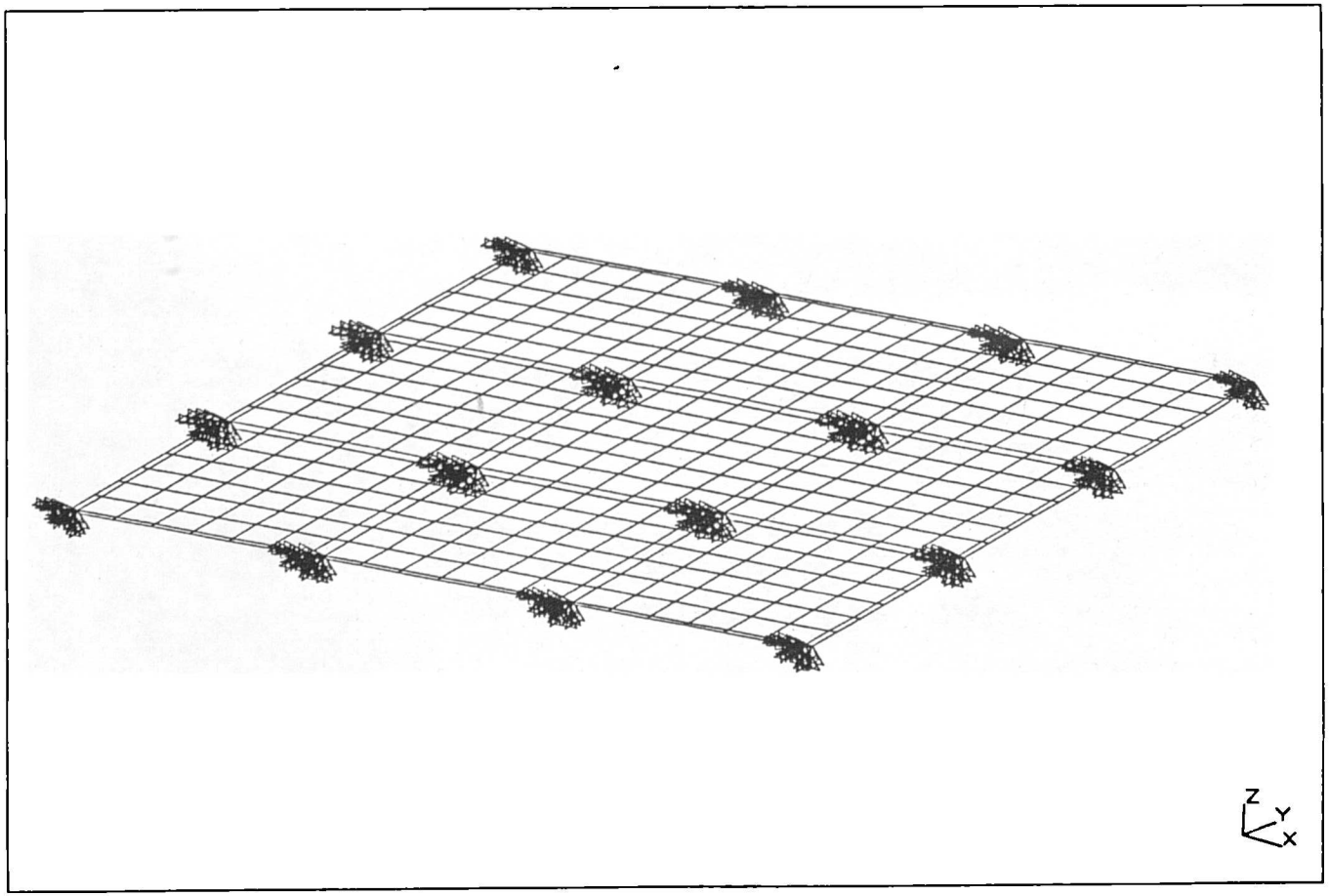

Figure 4.15: A Typical FE 3-Panel Model

4.2.2 Parametric Studies

The single panel FE model was used to study the variation of fundamental frequency with the span/depth ratios in both directions of the floor slab; and the maximum static deflections, in a manner similar to that given in section 4.1.2.

The thickness of slab only was varied in the model. Static and dynamic analyses of the model then yielded maximum static deflections and floor frequencies for each slab thickness, respectively.

4.2.2.1 Frequency vs Span/Depth Ratios

Figures 4.16 and 4.17 shows the variation of floor frequency with the short and long span/depth ratios, respectively.

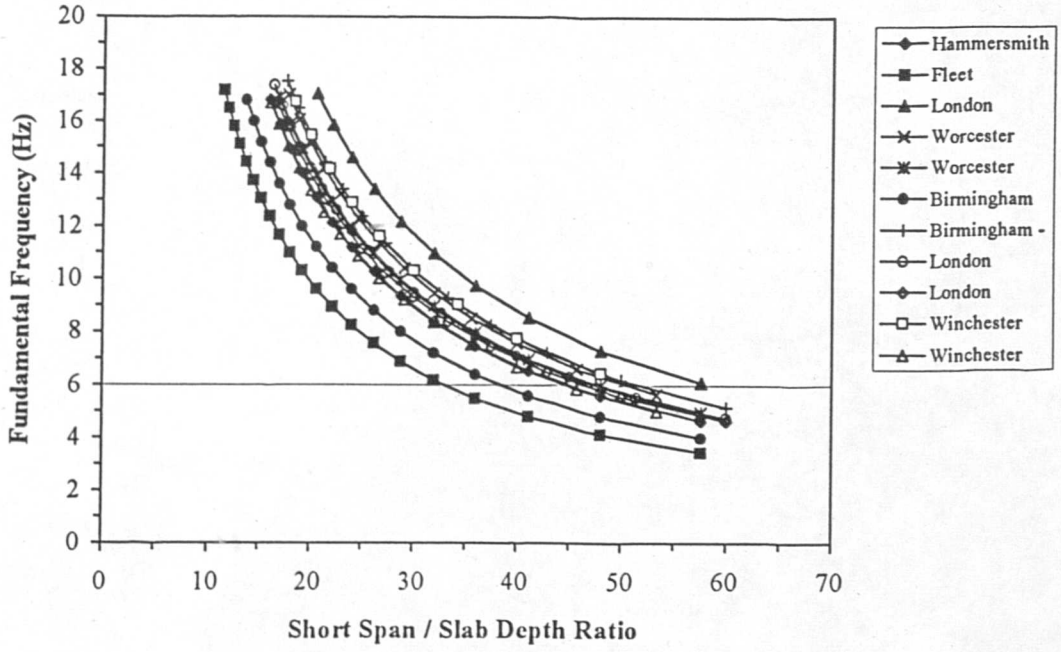

Figure 4.16: Frequency vs Short Span/Depth Ratio

It is clear from Figure 4.16 above that a maximum span/depth ratio of 33.5 for the short span direction will ensure frequencies above 6 Hz.

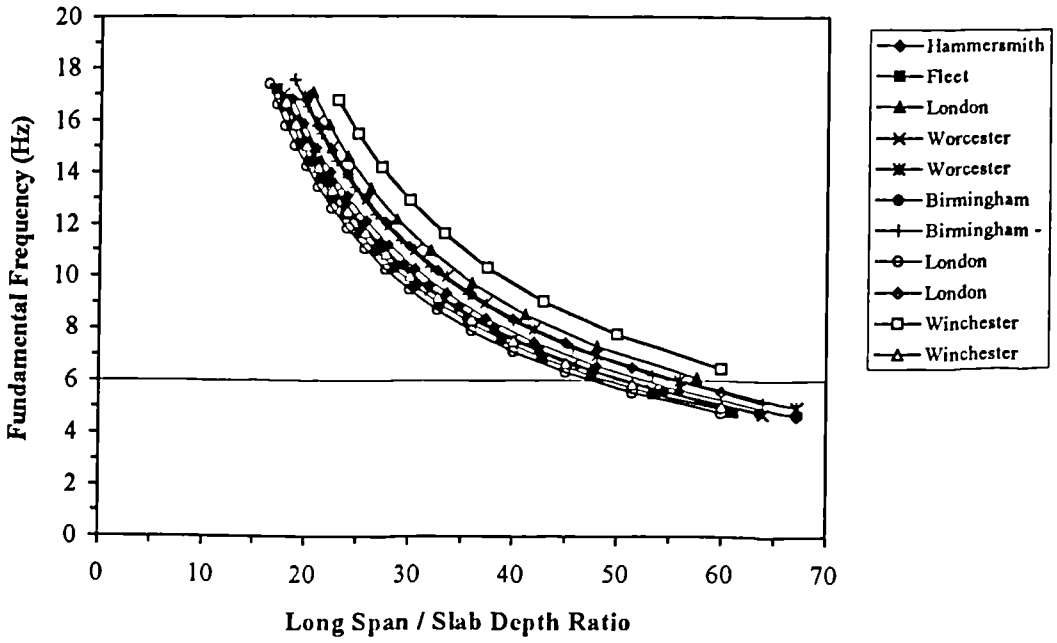

Figure 4.17: Frequency vs Long Span/Depth Ratio

It is clear from Figure 4.17 above that a maximum span/depth ratio of 47.8 for the long span direction will ensure frequencies above 6 Hz.

Figures 4.16 and 4.17 shows that the graphs of span/depth ratios against floor fundamental frequencies follow a general trend and similar shape. This is due to the homogeneous nature of the floor and absence of any beams. The difference in the ordinates, however, is due to the different stiffnesses caused by the span/depth ratios and column dimensions of each floor.

Therefore, in order to avoid fundamental frequencies below 6 Hz for this floor type, it is necessary to use span/depth ratios of upto 33.5 for the short span direction and 47.8 for the long span direction. It may be noted, therefore, that the Worcester floor (Test-4) donot satisfy this requirement (see Table 4.6).

Assuming that the fundamental frequencies of the single-panel FE model are correct, it can be concluded that all the floors tested satisfy the minimum frequency requirement. However, the high frequency of Worcester floor (Test-4) even for a higher short span/depth ratio is due to the extra stiffness provided by columns.

Table 4.6: Span/Depth Ratios of the Tested Floors

Site	Short Span/Depth Ratio	Long Span/Depth Ratio
Hammersmith	32.0	37. 3
Fleet	32.0	47.6
London	32.0	32.0
Worcester	35.6	35.6
Worcester	28.8	33.6
Birmingham	28.8	38.2
Birmingham	33.3	35.6
Birmingham	21.4	22.9
London	30.0	30.0
London	25.0	30.0
Winchester	30.0	37.5
Winchester	29.1	32.7

4.2.2.2 Frequency vs Deflection Relationship

Figures 4.18 shows the variation of floor frequency with maximum static deflections.

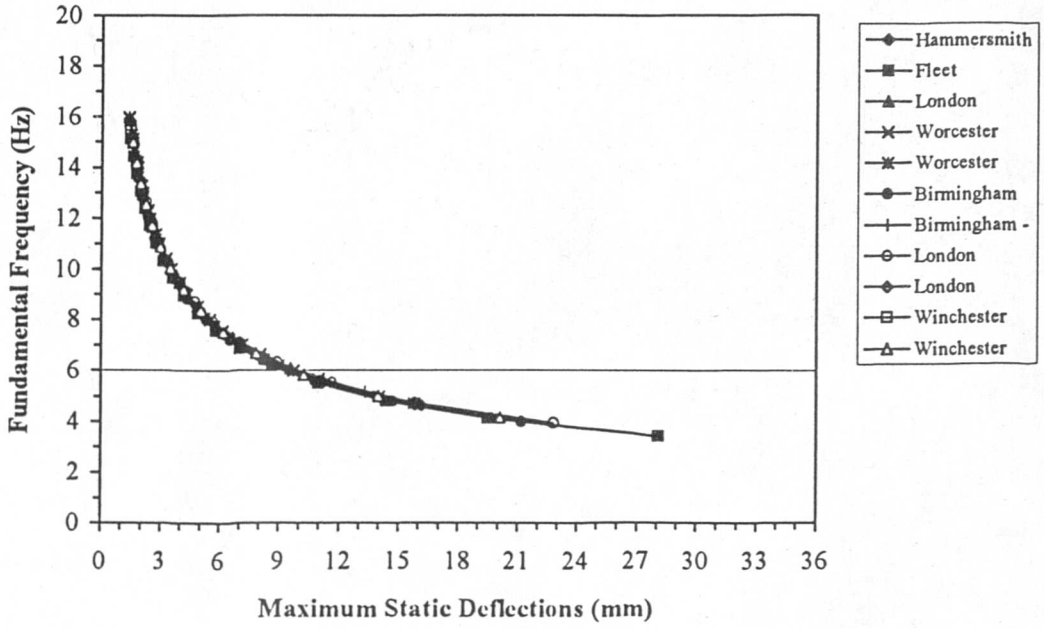

Figure 4.18: Frequency vs Static Deflections

Figure 4.18 shows that the variation of static deflections against corresponding floor frequency generally follows a consistent trend. A trendline least-squares curve-fit shows that these relationships are of the same form as equation 4.1 obtained earlier for the beam and slab type floors (see section 4.1.2.2). The constant K for these floors is given in Table 4.7 below:

Table 4.7: FE Single Panel Deflections and Constant K

Site	Maximum Static Deflections (mm)	Constant K
Hammersmith	4.89	18.607
Fleet	8.67	18.209
London	2.96	18.852
Worcester	1.75	18.795
Worcester	3.50	18.687
Birmingham	5.29	18.408
Birmingham	4.10	18.804
Birmingham	1.67	18.804
London	3.96	18.871
London	2.80	18.692
Winchester	3.24	18.573
Winchester	4.15	18.724
Average		18.669

It may be noted from Table 4.7 that the constant K varies from 18.209 to 18.871 (3.64% rise) for the twelve floors tested. An average value of this constant may be assumed as 18.7. It can, therefore, be assumed that the fundamental frequency of flat slab type floors can be closely approximated by the following relationship:

$$f = \frac{18.7}{\sqrt{\Delta_s}} \qquad (4.3)$$

It may be noted, however, that this constant depends on the type of floor (see section 4.1.2.2). The above results donot show a wide range of variation for K and, therefore, a conservative lower bound limit for K may be taken as 18.

From Figure 4.18, it can also be seen that the maximum deflection for a minimum floor frequency of 6 Hz is about 9 mm. Therefore, limiting the deflections to 9 mm will ensure frequencies higher than 6 Hz. Alternatively, equation 4.3 can be used to estimate frequencies for a given deflection limit.

4.3 Pre-Tensioned Concrete Double-T Beam Floors

The FE modelling of the five floors of this type was carried out using I-DEAS software. All floors are made of precast Double-T beams placed on inverted T or L-shaped girders. The topping in the form of screed or asphalt layer serves as a bond between these beams. Therefore, the FE modelling of this floor type included a single-beam model and upto ten adjacent beams to study the effect of adjacent beams on floor fundamental frequency and to determine if a more detailed model improves the accuracy of the results. Major details of modelling of this floor type are the same as those discussed in section 4.1, except the following:

Boundary Conditions

The beams were modelled as simply supported. This is the most realistic approach considering that these precast beams are placed on the girders supported by bearing pads.

Element Type

Linear isotropic quadrilateral thin shell elements were used for the flanges and linear isotropic beam elements were used for the webs in the different double-T models studied (see Figure 3.19). The webs of the double-T beams were approximated by a rectangular beam section. The beam and the shell elements were connected by rigid elements to define the correct restraint conditions for their displacements. This achieved true representative conditions for the dynamic motion of these simply supported long-span beams which essentially behave as one-way bending along the span.

Material Properties

Because these beams are manufactured with specific requirements, their material properties were easily available. The estimation of the modulus of elasticity of concrete, however, follow the same arguments as those given in section 4.1. The following values for material properties were used, Table 4.8:

Table 4.8: Material Properties

Site	Strength (GPa)	Modulus (GPa)	Density (kg/m^3)
Swindon	50	38.89	2500
Reading	52.5	39.85	2350
Sutton	50	38.89	2500
Basildon	52.5	39.85	2350
Tunbridge Wells	-do-	-do-	-do-

Pre-Tensioning

The effect of pre-tensioning was not modelled in this study. However, it may be mentioned that pre-tensioning enables the concrete section to resist tension due to applied loading without cracking, thus increasing the stiffness which in turn would increase the frequencies. Pre-tensioned floors may be assumed to be uncracked mainly because of the pre-compression and initial camber and the fact that the actual service loads are normally less than the design loads. However, the increases in modulus of elasticity due to strength gains may be assumed to be offset by the prestress losses over time.

4.3.1 Single Beam vs Multi-Beam Models

Chen and Aswad (1994) have studied a series of beams in a floor model for the estimation of frequencies. However, their studies are not based on experimental results. Since it has been established earlier that a single-panel floor model closely approximates the fundamental frequency of floors, this principle was applied to double-T beam type floors. Therefore, FE models for the Swindon floor with one double-T beam and upto ten adjacent double-T beams were studied for frequency estimation. In all FE models, the end nodes representing beam elements were assumed to be simply supported. All other nodes were free to move and rotate (see Figure 4.20). It was found that there was no effect of adjacent beams on fundamental frequency and that the 1-beam model closely approximates the fundamental frequency of the floor. Therefore, only the 1-beam model was studied for all the remaining floors of this type.

Table 4.9 gives the measured fundamental frequency of these floors along with the results of FE analysis.

Table 4.9: FE and Measured Fundamental Frequencies

Site	Fundamental frequency (Hz)	
	Field Results	FE Results
Swindon	4.9	4.6
Reading	5.6	5.2
Sutton	5.5	5.0
Basildon	4.6	4.4
Tunbridge Wells	5.8	5.2

It can be seen from Table 4.9 that a single-beam model closely approximates the fundamental frequency of this floor type. The addition of adjacent beams do not affect this frequency because they are of the same size. Because these low floor frequencies damp out quickly due to inherent damping, additional beams or a more complete floor model would, therefore, not affect the fundamental frequency significantly.

The comparison of field and FE results (Table 4.9) are plotted in Figure 4.19.

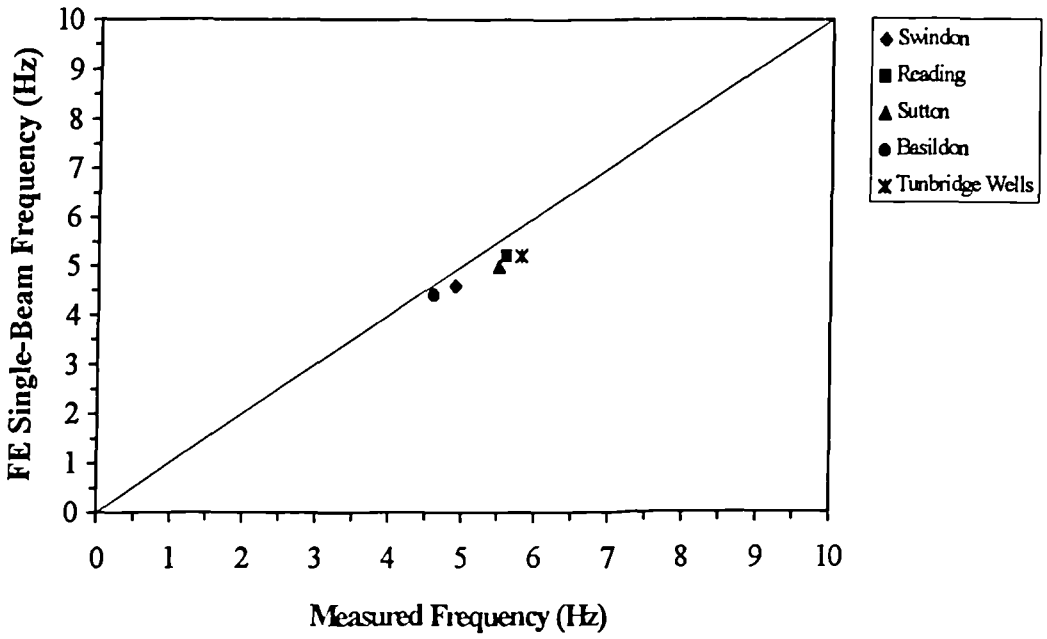

Figure 4.19: Field vs FE Frequency

Figure 4.19 above shows the close comparison of FE results with the experimental results. It may be noted, however, that all the FE frequencies are lower-bound and, therefore, conservative estimates.

Figure 4.20 and 4.21 shows the typical 1-beam and 10-beam models of this floor type.

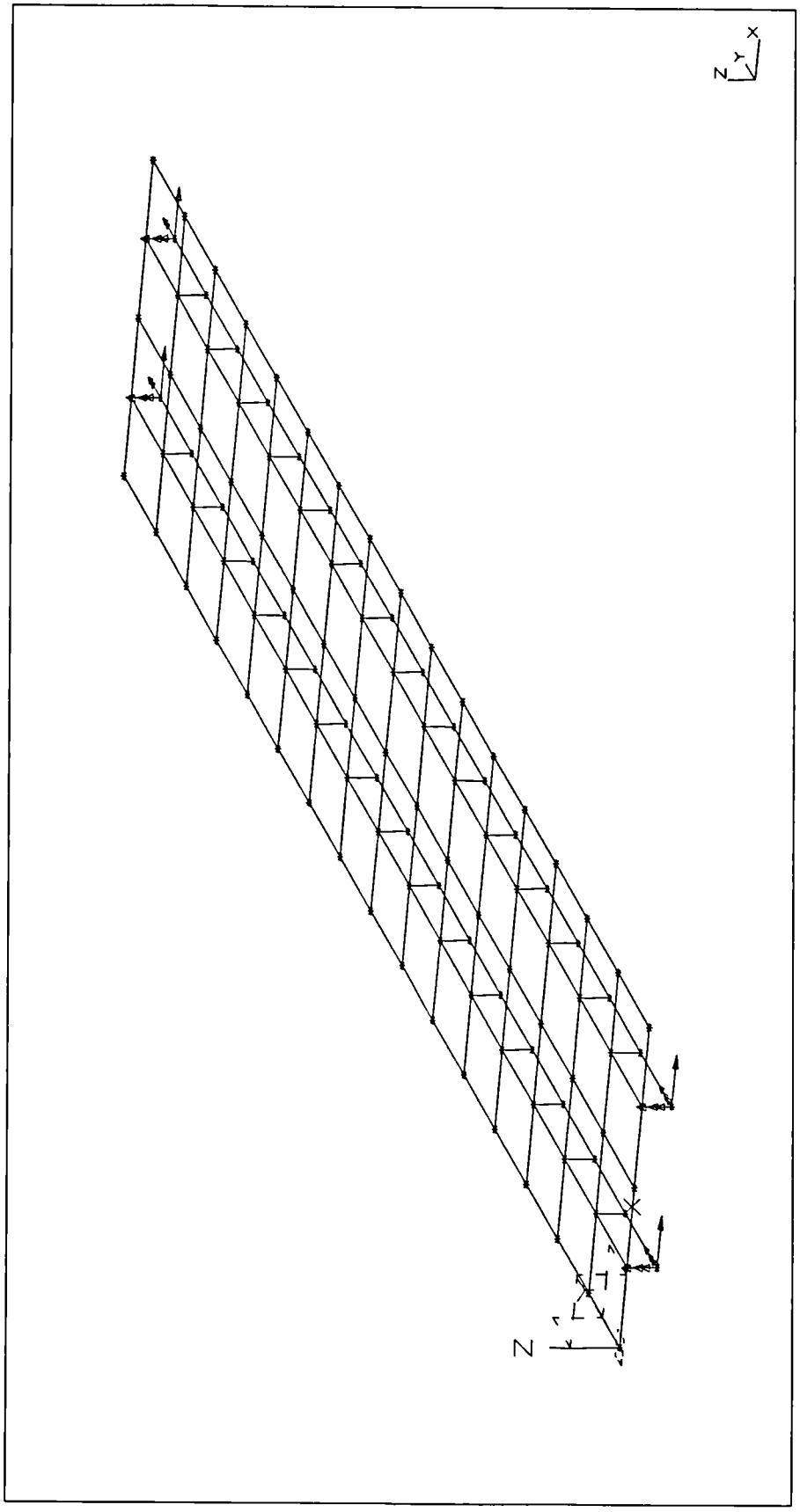

Figure 4.20: A Typical FE 1-Beam Model

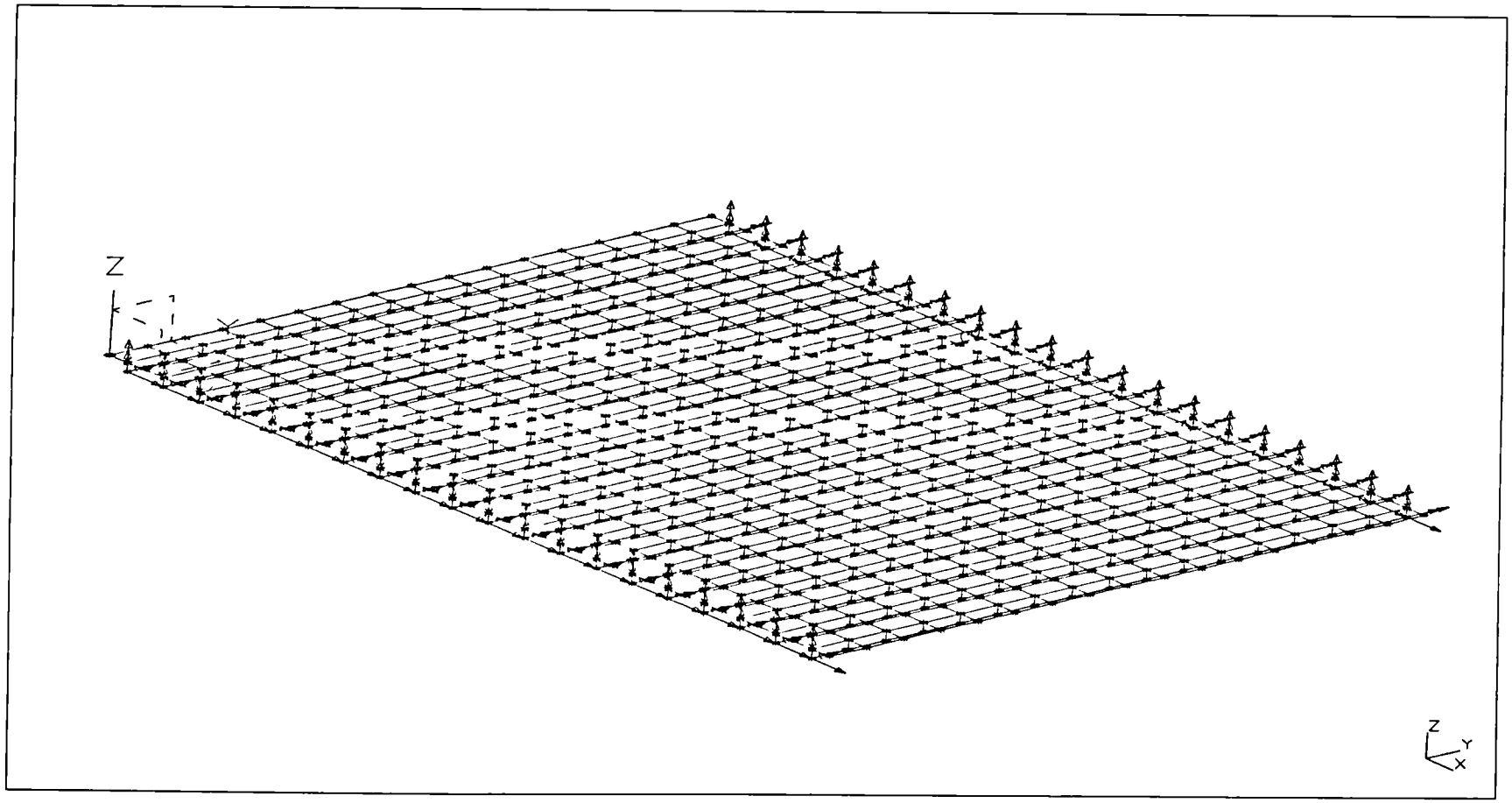

Figure 4.21: A Typical FE 10-Beam model

4.3.2 Parametric Studies

The single-beam FE model was used to study the variation of fundamental frequency with the beam length and the maximum static deflections, in a manner similar to that given in section 4.1.2. In this study, only the length of the beam was varied and fundamental frequency and static deflections evaluated.

Since the fundamental frequencies of double-T floors studied here were found to be below 6 Hz (Canadian Code requirement), a minimum fundamental frequency of 4.5 Hz was chosen for satisfactory vibration response. This frequency is more than twice the average walking frequency of 2 Hz and being not an exact multiple of walking frequency, is unlikely to be excited by people walking. Therefore, this frequency was used as a minimum in the parametric studies.

4.3.2.1 Frequency vs Beam Length

Figure 4.22 shows the variation of floor frequency with beam length.

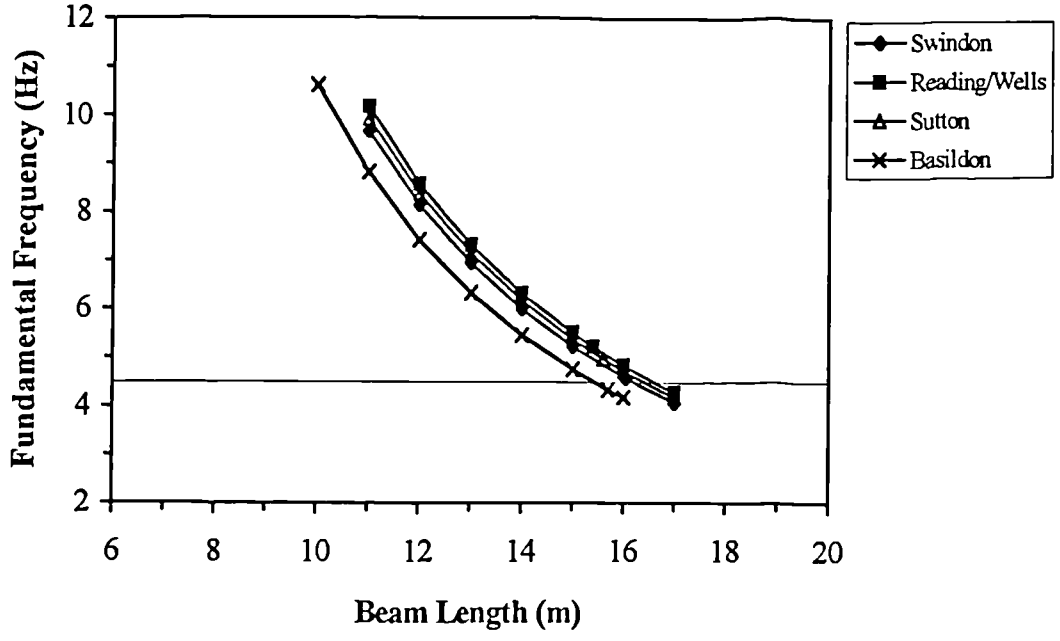

Figure 4.22: Frequency vs Beam Length

Table 4.10 gives the proposed span length limits based on a minimum fundamental frequency of 4.5 Hz. It may be noted, however, that the experimental fundamental frequency of the Basildon floor satisfy this requirement whereas its FE model result doesnot.

Table 4.10: Proposed Spans for the Tested Floors

Site	Original Span (m)	Proposed Span (m)
Swindon	16.045	16.2
Reading	15.4	16.6
Sutton	15.6	16.4
Basildon	15.7	15.4
Tunbridge Wells	15.4	16.6

4.3.2.2 Frequency vs Deflection Relationship

Figure 4.23 shows the variation of floor frequency with beam deflections.

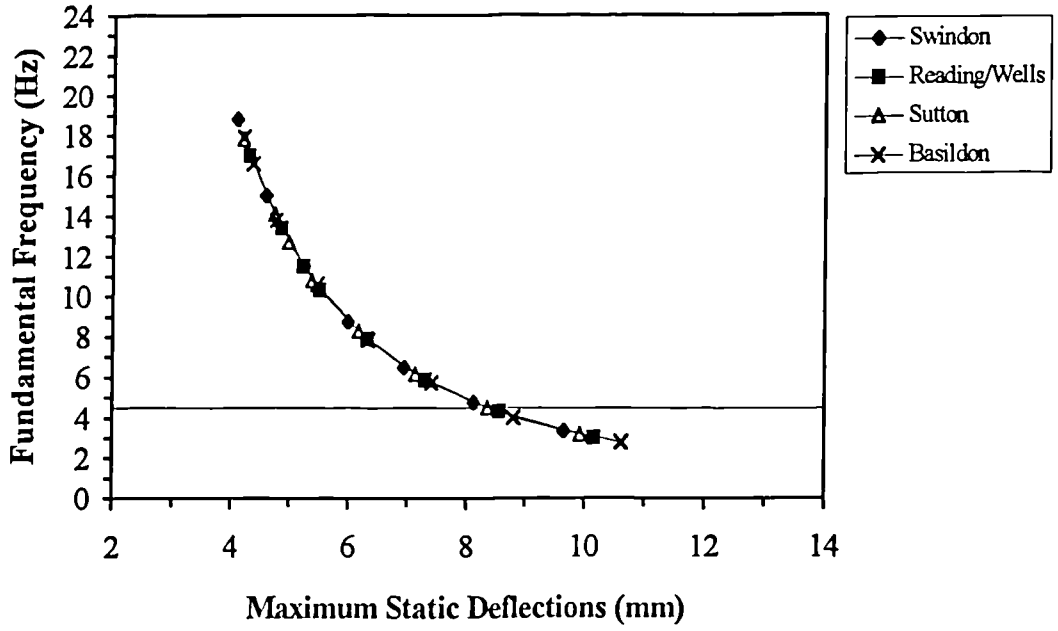

Figure 4.23: Frequency vs Static Deflections

Figure 4.23 shows a single curve following an average relationship of the form of equation 4.1, obtained earlier for beam and slab and flat slab type floors. The constant K is given in Table 4.11 below.

Table 4.11: FE Single Beam Deflections and Constant K

Site	Maximum Static Deflections (mm)	Constant K
Swindon	15.0	17.72
Reading	11.5	17.72
Sutton	12.7	17.73
Basildon	16.6	17.73
Tunbridge Wells	11.5	17.72
Average		17.72

It may be noted from Table 4.11 that the constant K varies from 17.72 to 17.73 (0.06% rise) for the five floors tested. An average value of this constant may be assumed as 17.7. Therefore, the fundamental frequency of double-T beam type floors can be closely approximated by the following relationship:

$$f = \frac{17.7}{\sqrt{\Delta_s}} \qquad (4.4)$$

Since the above results donot show a wide range of variation for K, a conservative lower bound limit for K may be taken as 17.5.

From Figure 4.23, it can also be seen that the maximum self-weight deflection for a minimum fundamental frequency of 4.5 Hz is about 8.5 mm. Therefore, limiting the deflections to 8.5 mm will ensure frequencies higher than 4.5 Hz. Alternatively, equation 4.4 can be used to estimate frequencies for a given deflection limit.

4.4 Composite Steel-Concrete Slab Floors

The FE modelling of the eight floors of this type was carried out using I-DEAS software. All of these floors are continuous in both directions and are made of concrete slabs supported on a steel profile which is welded to steel beams and girders (see Figure 3.25 and Appendix A.4). Based on previous floor modelling, only a single-panel of these floors was modelled. Major details of modelling of this floor type are the same as those discussed in section 4.1, except the following:

Boundary Conditions

The steel columns were modelled as simply supported at their centroid at the four corners of the single-panel FE model. This is the most realistic approach considering that the steel beams and girders are riveted to these columns. In the case of Millwall Stadium floor, however, the two north columns were encased in a concrete column of 780 mm diameter. These were, therefore assumed fixed at the perimeter of the column (assumed as 780 mm x 780 mm).

Element Type

Shell elements were used for the slab and beam elements were used for the beams and girders (see section 4.1). The slab was modelled in two different ways: of uniform slab thickness and of actual slab profile dimensions (for calculations, see Appendix B.4). In both cases shell elements were used. In the case of actual slab profile, however, the profile was modelled as shells in vertical plane (see section 4.1). The beam and girder elements were connected to the shell elements by rigid elements to represent the welded joints and define the correct constraint for their displacements.

Material Properties

Relevant data for the composite floors were taken from the brochures of Precision Metal Forming Limited on Composite Floor Decking Systems [71]. The following material properties were used in all calculations for these floors (see also section 4.1):

Concrete

Density (ρ_c)	:	1900 Kg/m^3
Compressive strength (f_{cu})	:	Grade 40 (i.e. 40 N/mm^2)
Modulus of elasticity (E_c)	:	22 KN/mm^2

The modulus of concrete (E_c) has been suggested by Wyatt (1989) as 22 KN/mm^2 for composite floors with light-weight concrete.

Steel

Density (ρ_s)	:	7820 Kg/m^3
Modulus of elasticity (E_s)	:	206.8 KN/mm^2

These values have been used as default for steel in I-DEAS and have, therefore, been assumed for all calculation purposes.

4.4.1 Single Panel Models

Table 4.12 compares the measured fundamental frequency of these floors with the results of single panel FE models. Results for both types of models studied are included.

Table 4.12: FE and Measured Fundamental Frequencies

Site	Fundamental Frequency (Hz)		
	Field	FE Results	
		Uniform Slab Thickness	Actual Slab Profile
London	12.6	11.0	10.5
Worcester	8.1	7.9	N / A
Maidenhead	8.8	9.9	8.6
Heathrow	9.1	10.4	8.8
Windsor	10.6	9.9	8.3
London	14.0	15.0	12.2
Cardington	6.4	7.2	6.4
Guildford	8.6	7.3	6.8

It can be seen from Table 4.12 that the single panel model closely approximates the fundamental frequency of this floor type. The results for the model with actual slab profile dimensions are lower than that with a uniform slab thickness for the floor. This is due to the increased flexibility of the model due to the profile dimensions. Both of these models may be used for frequency estimation. However, the model with actual slab profile dimensions consist of a large number of elements and is time consuming both from modelling and analysis point of view which may not be desirable for practical purposes. In any case, it has been shown previously that there is no need to modelling the floor in more detail to achieve higher accuracies in frequencies.

The comparison of field and FE results for the uniform slab thickness model are plotted in Figure 4.24.

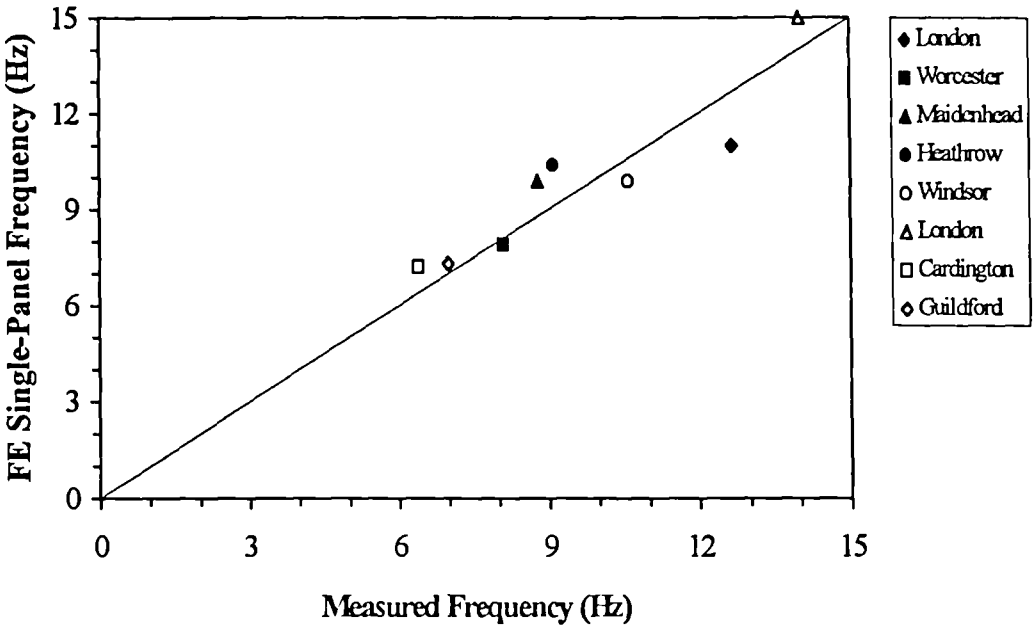

Figure 4.24: Field vs FE Frequency

Figures 4.25 and 4.26 shows typical 1-panel models based on a uniform slab thickness and the actual slab profile dimensions for this floor type, respectively.

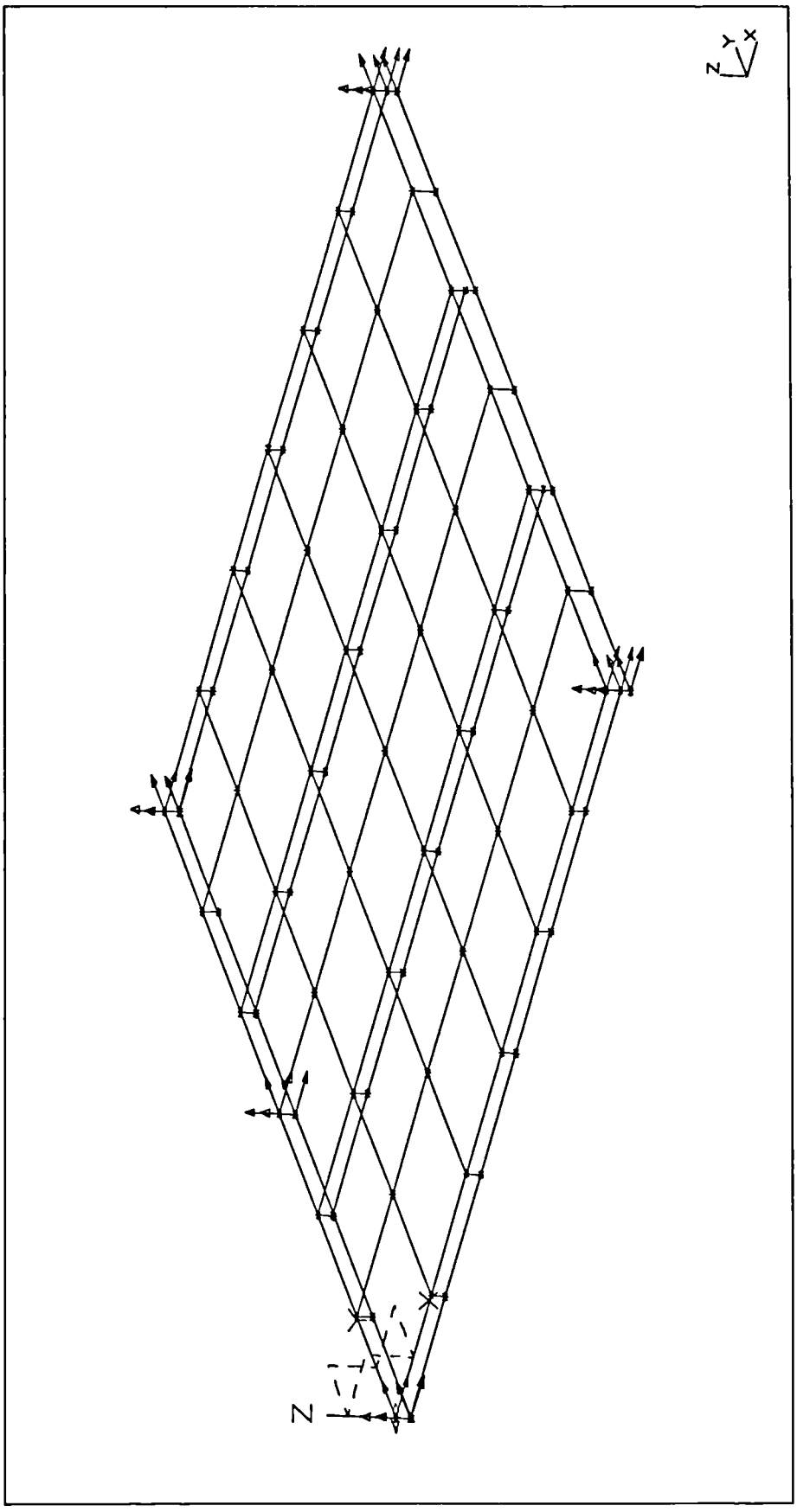

Figure 4.25: A Typical FE 1-Panel Model

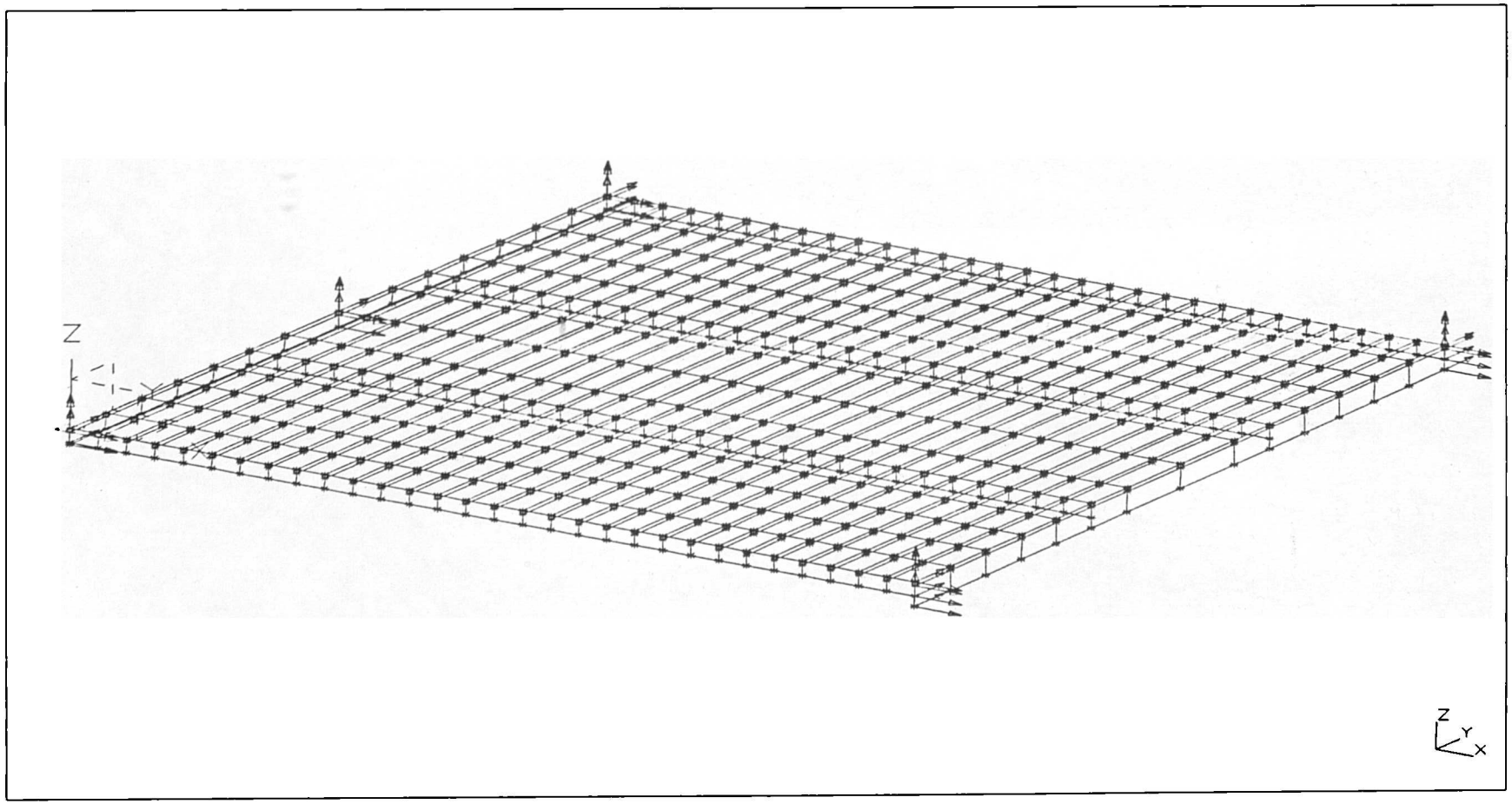

Figure 4.26: A Typical FE 1-Panel Model

4.4.2 Parametric Studies

The single panel FE model was used to study the variation of fundamental frequency with the depth of the composite slab and corresponding maximum static deflections, in a manner similar to that given in section 4.1.2. The slab depth was varied according to PMF (1994).

4.4.2.1 Frequency vs Slab Thickness

In the design of composite floors, only the slab thickness and/or beam or girder sections are varied, keeping their length constant, for a given design requirement. In the present study, however, only the slab thickness was varied to study their effect on the fundamental frequency of the floor. Figure 4.27 shows the variation of frequency versus slab thickness.

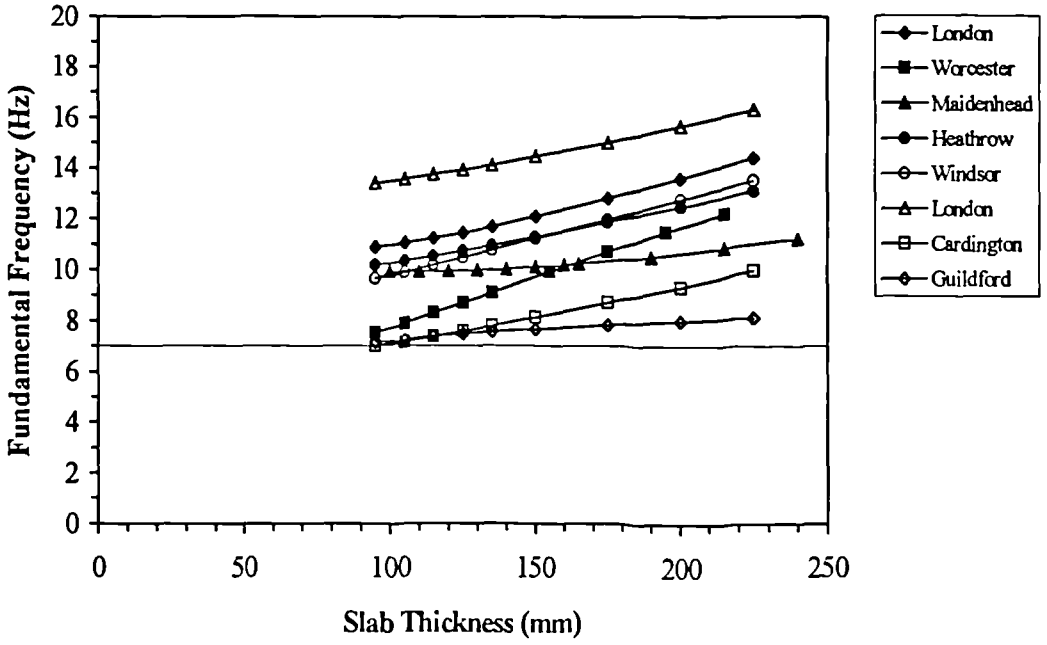

Figure 4.27: Frequency vs Slab Thickness

It is clear from Figure 4.27 that all the floors tested satisfy the minimum frequency limit of 7 Hz, Wyatt (1989), except the Cardington floor. The reasons for the low frequency of

Cardington floor has already been discussed in section 3.4.7. The figure shows that floor frequencies increase with increasing slab thickness. However, this increase is not high for most floors. Therefore, it may be concluded that increasing the slab thickness alone may not be a sufficient and economical solution to increase the fundamental frequency. However, changing the beam/girder section may lead to higher floor frequencies.

4.4.2.2 Frequency vs Deflection Relationship

Figure 4.28 shows the variation of frequency versus slab deflection.

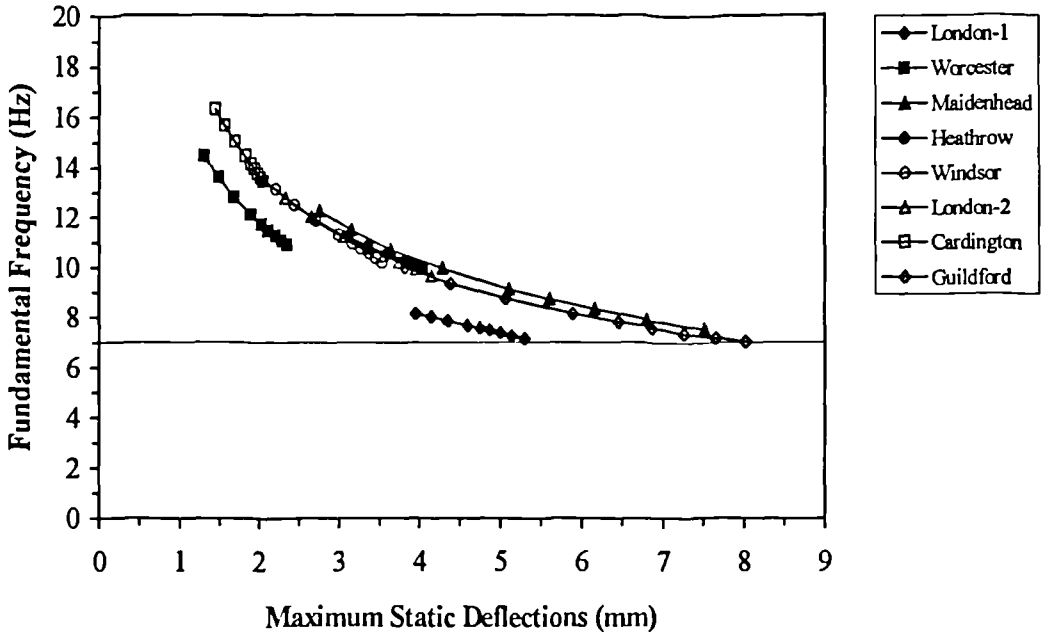

Figure 4.28: Frequency vs Static Deflections

Figure 4.28 shows that the variation of static deflections against corresponding floor frequency generally follows a consistent trend of the form of equation 4.1, obtained earlier for beam and slab, flat slab and double-T type floors. However, all the data points do not lie on a single curve. This is due to the difference in beam and girder sizes in addition to the profile shape and dimensions (see also section 4.1.2.2). The constant K is given in Table 4.13 below:

Table 4.13: FE Single Panel Deflections and Constant K

Site	Maximum Static Deflections (mm)		Constant K
	Uniform Slab Thickness	Actual Slab Profile	
London	2.28	2.41	14.996
Worcester	6.81	3.78	16.448
Maidenhead	4.04	8.60	19.982
Heathrow	3.45	8.78	19.437
Windsor	3.95	8.33	20.107
London	1.70	12.23	19.097
Cardington	7.65	6.59	20.087
Guildford	5.14	5.81	18.834
Average			18.624

It may be noted from Table 4.13 that the constant K varies from 14.996 to 20.107 (34.08% rise) for the eight floors tested. An average value of the constant K may be assumed as 18.6. It can, therefore, be assumed that the fundamental frequency of composite floors can be closely approximated by the following relationship:

$$f = \frac{18.6}{\sqrt{\Delta_s}} \tag{4.5}$$

The above results show a wide range of variation for K and since the minimum value of this constant for a MDOF system is 15.8 (see section 4.1.2.2), a conservative lower bound limit of K may be taken as 15.8.

From Figure 4.28, it can also be seen that the maximum deflection for a minimum floor frequency of 7 Hz is about 5.5 mm. Therefore, limiting the deflections to 5.5 mm will ensure frequencies higher than 7 Hz. Alternatively, equation 4.5 can be used to estimate frequencies for a given deflection limit.

Chapter 5 COMPARISONS

This Chapter presents the comparisons of the experimental fundamental frequency of all the floor slabs tested with the analytical methods given in Chapter 1. The results from only the methods appropriate to each category are compared. This is followed by brief comments on the use of each method. Typical calculations for each floor category are given in Appendix B.

5.1 Post-Tensioned Concrete 1-Way Spanning Solid Floor Slabs with Beams

Table 5.1 below compares the results obtained by the analytical methods with the experimental results for the four floors of this type. Typical calculations for the High Wycombe floor are given in Appendix B.1.

Table 5.1: Comparison of Results for Beam and Slab Floors

Site	Fundamental Frequency (Hz)									
	Field	EBM		PM		CSM		FEM (Single-Panel)	SDM	
		S.S.	F.S.	S.S.	C.S.	f_x	f_y		SDOF Formula (EBM Deflections)	Modified SDOF Formula (FEM Deflections)
									S.S.	F.S.	
High Wycombe	10.2	7.43	16.84	9.48	2.36	3.25	9.29	10.1	6.59	14.75	8.74
Wimbledon	5.8	4.21	9.55	8.06	1.70	1.82	6.33	6.1	3.74	8.37	5.55
Fleet	11.2	9.59	21.75	12.30	4.30	5.42	7.26	11.5	8.52	19.05	10.46
Ilford	7.3	4.96	11.25	6.60	1.09	1.24	5.61	7.3	4.41	9.85	6.28

S.S. = Simple Supports F.S. = Fixed Supports C.S. = Corner Supports

SDOF Formula: $f = \frac{1}{2\pi}\sqrt{\frac{g}{\Delta_s}}$ where $g = 9806.65$ mm/s^2

Δ_s = static deflection in mm $= \frac{5}{384}\frac{\rho A g L^4}{EI}$ (for a simply supported beam)

$= \frac{1}{384}\frac{\rho A g L^4}{EI}$ (for a fixed-ended beam)

Modified SDOF Formula: $f = \frac{K}{\sqrt{\Delta_s}}$ (Δ_s used here is the maximum static deflection of the single-panel/beam FE model)

(For K and Δ_s, see sections 4.1.2.2, 4.2.2.2, 4.3.2.2 and 4.4.2.2)

5.1.1 Discussion

Based on the results for the four floors given in Table 5.1 above, the estimation of fundamental frequency of this type of floor can be summarised as follows:

EBM: This method provides two estimates of the fundamental frequency. The simple support assumption for the equivalent beam always under-estimates the fundamental frequency whereas the fixed support assumption always over-estimates this frequency.

PM: This method provides two estimates of the fundamental frequency. The simple support assumption does not produce consistent estimates of the fundamental frequency whereas the corner support assumption always under-estimates this frequency.

CSM: This method offers two estimates. One estimate along the short span direction is always an under-estimate. The estimates using the long-span direction is not consistent.

FEM: This method offers the closest possible estimates.

SDM: This method provides three estimates of the fundamental frequency. The estimates may be based on the SDOF formula or the modified SDOF formula developed in this research. In the SDOF formula, deflections may be assumed for the EBM or PM approaches. For the EBM approach, the simple support deflections always under-estimate the fundamental frequency whereas the fixed support deflections always over-estimate this frequency. The PM deflections are difficult to estimate and, therefore, have not been used here. However, the modified SDOF formula using the maximum deflection from the static analysis of the single panel FE model provides the closest estimates.

5.1.2 Equivalent Beam Span Length

As noted in section 5.1.1, the EBM method for simple support conditions provide frequency estimates lower than the experimental results whereas the fixed support conditions provide higher estimates. Therefore, both the support conditions are not correct if EBM approach is to be used for frequency estimation. However, the EBM formula for simple supports could be used for frequency estimation if the beam span length taking part in vibrations is correctly identified. Figure 5.1 shows the relationship for the estimation of an equivalent span length for the EBM formula for simple supports for the estimation of fundamental frequency of the floor.

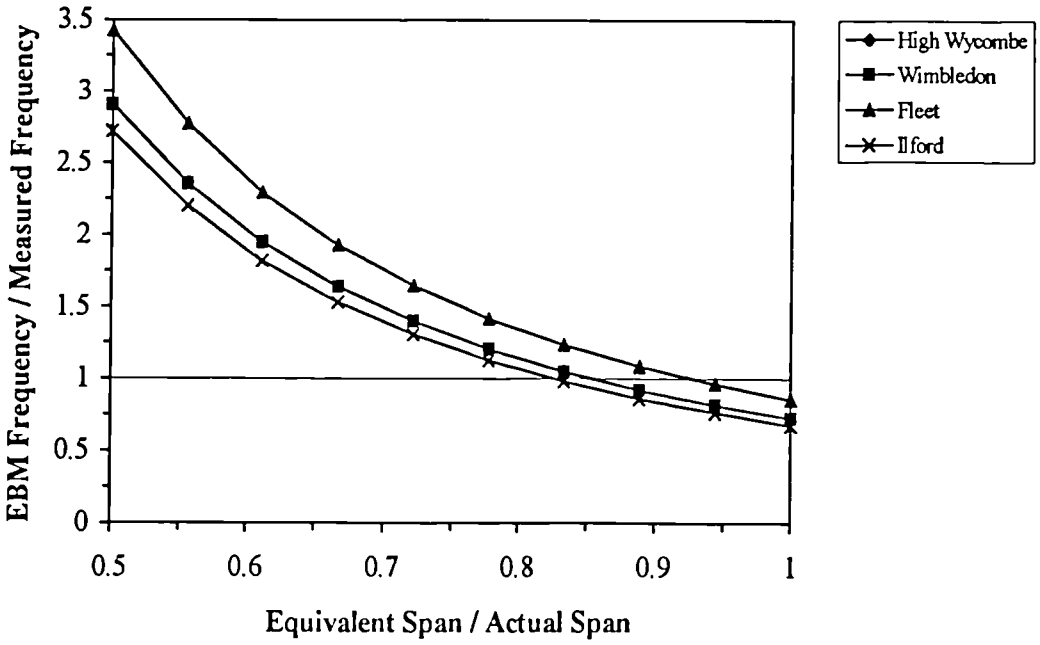

Figure 5.1: Estimation of Equivalent Span Length for EBM Formula

It may be noted from Figure 5.1 above that the EBM formula for the estimation of fundamental frequency may be used reliably if the span length of the beam is reduced by a factor between 0.825 and 0.925. The full length of the beam does not take part in vibrations due to restraints or end conditions at the column supports. It also depends on the slab thickness and beam cross-section area. Thus, if the EBM method is to be used instead of a single-panel FE model, the length of beam should be multiplied by a factor between 0.825 and 0.925. The choice is arbitrary because not enough experiments have

been carried out on this floor type. However, for conservative estimates, a factor of 0.925 or close to it may be used as a first approximation. Note, however, that the curves for the High Wycombe and Wimbledon floors overlap.

5.2 Post-Tensioned Concrete Solid Flat Slab Floors

Table 5.2 below compares the results obtained by the analytical methods with the experimental results for the twelve floors of this type. Typical calculations for the Hammersmith floor are given in Appendix B.2.

5.2.1 Discussion

Based on the results for the twelve tests given in Table 5.2 above, the estimation of fundamental frequency for this type of floor can be summarise as follows:

EBM: Same conclusions as in section 5.1.1.

PM: This method provides two estimates of the fundamental frequency. The simple support assumption always over-estimate the fundamental frequency whereas the corner support assumption generally under-estimates this frequency (except in the case of Test # 6).

CSM: Same conclusions as in section 5.1.1.

FEM: Same conclusions as in section 5.1.1.

SDM: Same conclusions as in section 5.1.1.

Table 5.2: Comparison of Results for Flat Slab Floors

Site	Fundamental Frequency (Hz)									
	Field	EBM		PM		CSM		FEM (Single-Panel)	SDM	
		S.S.	F.S.	S.S.	C.S.	f_x	f_y		SDOF Formula (EBM Deflections)	Modified SDOF Formula (FEM Deflections)
									S.S. F.S.	
Hammersmith	8.1	5.51	12.48	13.27	4.53	5.50	6.98	8.41	4.89 10.93	8.46
Fleet	5.9	3.39	7.69	11.11	3.12	3.48	6.50	6.18	3.01 6.74	6.35
London	10.1	7.49	16.99	15.30	5.52	7.09	7.61	10.96	6.65 14.88	10.87
Worcester	12.7	10.12	22.93	20.65	7.45	10.15	9.79	14.19	8.98 20.08	14.14
Worcester	9.1	6.12	13.87	14.74	5.03	5.82	8.38	9.98	5.43 12.15	10.00
Birmingham	7.2	4.73	10.73	13.33	8.52	4.68	7.80	8.0	4.20 9.40	8.13
Birmingham	8.6	6.07	13.76	13.24	7.48	6.12	6.54	9.28	5.39 12.05	9.24
Birmingham	12.7	9.44	21.40	20.60	7.31	9.33	10.34	14.44	8.38 18.75	14.47
London	8.4	6.39	14.49	13.05	4.71	6.35	6.13	9.48	5.68 12.70	9.40
London	10.6	6.39	14.49	15.92	5.35	6.47	8.24	11.15	5.68 12.70	11.18
Winchester	10.3	6.14	13.92	16.05	8.27	6.13	8.78	10.32	5.45 12.19	10.39
Winchester	8.5	5.86	13.29	13.55	4.71	5.72	7.19	9.19	5.20 11.64	9.18

5.2.2 Equivalent Beam Span Length

Following on the reasons given in section 5.1.2, Figure 5.2 shows the relationship for the estimation of an equivalent span length for the EBM formula for simple supports for the estimation of fundamental frequency of flat slab floors.

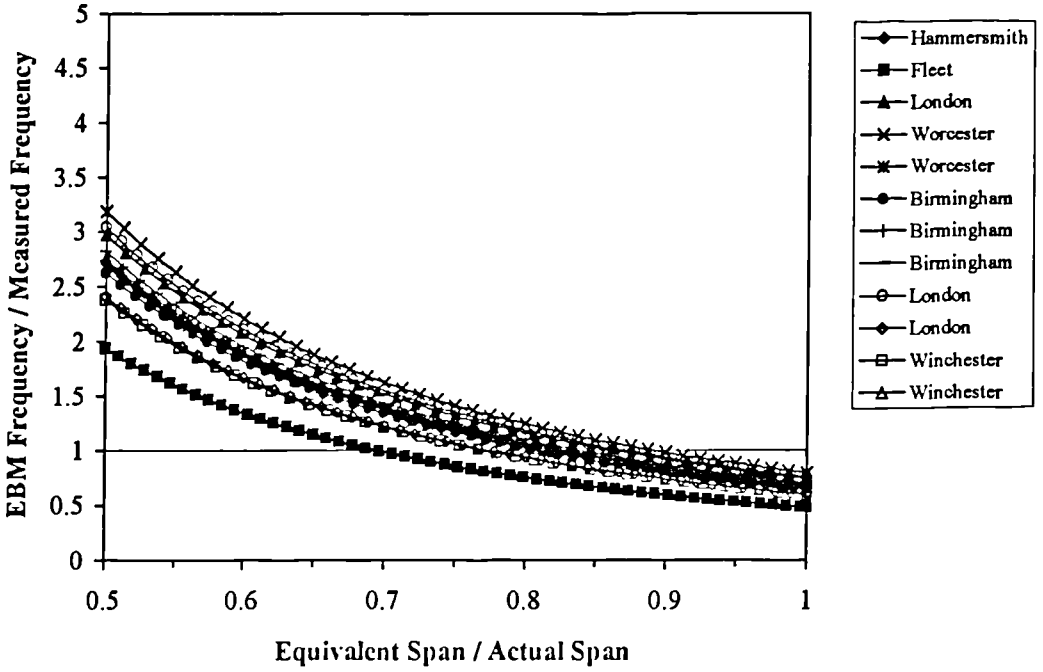

Figure 5.2: Estimation of Equivalent Span Length for EBM Formula

As in section 5.1.2, it may be noted from Figure 5.2 above that the EBM formula for the estimation of fundamental frequency may be used reliably if the span length of the beam is reduced by a factor between 0.7 and 0.9. This relatively wide range is due to the fact that these floor types do not have beams and are essentially 2-way slabs. The use of EBM formula for these floors is not directly applicable. However, it may still be used for quick and conservative estimates. Thus, if the EBM method is to be used instead of a single-panel FE model, the length of beam should be multiplied by a factor between 0.7 and 0.9. For conservative estimates, a factor of 0.9 or close to it may be used as a first approximation.

5.3 Pre-Tensioned Concrete Double-T Beam Floors

Table 5.3 below compares the results obtained by the analytical methods with the experimental results for the five floors of this type. Typical calculations for the Swindon floor are given in Appendix B.3.

Table 5.3: Comparison of Results for Double-T Beam Floors

Site	Fundamental Frequency (Hz)				
	Field	EBM	FEM (Single-Panel)	SDM	
				SDOF Formula (EBM Deflections)	Modified SDOF Formula (FEM Deflections)
Swindon	4.9	4.61	4.58	4.10	4.57
Reading	5.6	5.27	5.23	4.68	5.22
Sutton	5.5	5.02	4.98	4.46	4.97
Basildon	4.6	4.38	4.35	3.89	4.34
Tunbridge Wells	5.8	5.27	5.23	4.68	5.22

5.3.1 Discussion

Based on the results for the five tests given in Table 5.3 above, the estimation of fundamental frequency for this type of floor can be summarise as follows:

EBM: This method always under-estimates the fundamental frequency. The use of an equivalent span length is not applicable to this floor type because the double-T beams are simply supported and, therefore, their full length takes part in any vibration response.

FEM: Same conclusions as in section 5.1.1.

SDM: This method provides two estimates of the fundamental frequency using the SDOF and modified SDOF formulae. Both the formulae always

under-estimates the fundamental frequency but the modified SDOF formula results are better of the two.

5.4 Composite Steel-Concrete Slab Floors

The results obtained from the analytical methods are compared with the experimental results for the ten floors of this type in Table 5.4 below. Typical calculations for the Millwall floor are given in Appendix B.4.

5.4.1 Discussion

Based on the results for the eight tests given in Table 5.4 above, the estimation of fundamental frequency for this type of floor can be summarise as follows:

EBM: This method offers better estimates of the fundamental frequency for the case of beam supporting slab only. The use of an equivalent span length is not applicable to this floor type because the steel beams are simply supported at girders (as shown in FE modelling) and, therefore, their full length takes part in any vibration response.

Dunkerly: This method does not produce consistent estimates of the fundamental frequency.

SDM: The three different approaches of this method do not produce consistent estimates for the fundamental frequency. The Wyatt and Allen-Murray estimates are reasonably close. However, the frequency estimation using FE deflections are the closest of the three methods.

FEM: Same conclusions as in section 5.1.1. The uniform slab thickness model is simple as compared to the actual slab profile model and requires considerably less CPU time for analysis.

Table 5.4: Comparison of Results for Composite Floors

Site	Fundamental Frequency (Hz)											
	Field	EBM			SDM						FEM	
		Beam	Girder	Combined (Dunkerly)	Wyatt		Allen-Murray			FE	Uniform Slab Thickness Model	Actual Slab Profile Model
					Mode-1	Mode-2	Beam Panel	Girder Panel	Combined (Dunkerly)			
London-1	12.6	11.7	14.4	9.1	11.7	11.3	12.2	15.2	9.5	12.3	11.0	10.5
Worcester	8.1	6.2	10.1	5.3	6.3	7.4	6.3	10.6	5.6	7.1	7.9	N - A
Maidenhead	8.8	12.0	14.0	9.1	12.7	11.7	12.1	14.9	9.4	9.3	9.9	8.6
Heathrow	9.1	13.5	12.9	9.3	10.6	N / A	14.0	13.5	9.7	10.0	10.4	8.8
Windsor	10.6	10.0	14.0	8.1	9.9	9.9	10.4	14.6	9.0	9.4	9.9	8.3
London-2	14.0	16.8	17.4	12.1	16.3	12.9	22.4	22.8	16.7	14.3	15.0	12.2
Cardington	6.4	6.4	10.6	5.5	6.4	7.7	6.6	11.2	5.8	6.7	7.2	6.4
Guildford	8.6	4.9	N / A	N / A	5.0	N / A	5.0	N / A	N / A	8.2	7.3	6.8

N / A = Not Applicable

N - A = Not Analysed (Due to the absence of a girder, two panels were required to be modelled. This would involve too large a number of elements and too much CPU time/computer memory)

Note: The SDM frequencies for FE are based on modified SDOF formula using the deflections of uniform slab thickness model, see Table 5.1 and Table 4.13

Chapter 6 CONCLUSIONS

The main objective of the research was to study the various analytical techniques for the estimation of fundamental frequency of floors. This Chapter presents a summary of the findings of the research on frequency estimation based on the comparisons made in Chapter 5. A brief discussion is included on damping estimation and conclusions of a parametric study of the FE models. Recommendations are suggested and some suggestions are made for future research.

6.1 Conclusions

6.1.1 Frequency Estimation Methods

The various analytical techniques for the estimation of the fundamental frequency of floors were reviewed in Chapter 1. The fundamental frequency for all the floors tested was calculated by these methods and compared with the experimental results in Chapter 5. Each method was found to have a different application and suitability for different floor types. The following is a summary of the use of each method for the floors tested.

Equivalent Beam Method (EBM)

The EBM depends on a reasonable estimate of an equivalent beam span and an effective slab width supported by the beam, which is recommended in the BS 8110 (1985), for beam and slab, and flat slab floors. The choice of equivalent beam span depends on the boundary conditions and may range between 0.825 and 0.925 for the beam and slab type floors and between 0.7 and 0.9 for the flat slab type floors, respectively. A conservative equivalent beam span and a higher effective slab width may result in closer frequency estimates. In general, the EBM gives good estimates of fundamental frequency and may be used if a conservative estimates of equivalent beam span and effective slab width are used.

The beam formula for simple supports is directly applicable to double-T floors because the double-T beam units are simply supported; this is an assumption in the derivation of the formula. Therefore, for all practical purposes, the beam formula can be used to predict the fundamental frequency of double-T floors. For composite floors, the results for both the cases of beam supporting the slab and girder supporting the beams are not consistent and depends on the layout and section dimensions. For simplicity, therefore, the case of beam supporting the slab may be used for initial estimates of the fundamental frequency.

Plate Method (PM)

The PM is not directly applicable to all the floors because the boundary conditions of the panels tested are not either simply supported or corner supported. Also, the columns supporting these slabs are monolithic with the slab resulting in a very rigid connection around their perimeter. Therefore, they cannot be assumed as point supports and should be modelled as fixed supports around their perimeter. The inconsistency in the results is also due to the summation of stiffnesses in both the directions. The presence of beams in one direction, in the case of beam and slab floors, for example, result in a higher relative stiffness. The PM is not applicable to double-T and composite floors. In the absence of any exact formula for all the practical cases, the PM in its present form (equation 1.3, section 1.2.2) is not recommended for fundamental frequency estimation.

Concrete Society Method (CSM)

The CSM is similar to EBM. It offers two estimates for the fundamental frequency in which the number of panels in each direction plays a very important role. The CSM does not identify whether all the panels in each direction should be considered or only those with similar dimensions and support conditions. Obviously, this selection leads to inaccurate results because reducing the number of panels increases the frequencies and vice-versa. The CSM is not applicable to double-T and composite floors. Since this method is not based on any experimental evidence and its application does not lead to any reliable conclusions, it is not recommended for use.

Finite Element Method (FEM)

The FEM offers the closest possible frequency estimates but depends to a large extent on the material properties and boundary conditions of the floors. Since a single constant value of the concrete strength and thus the modulus of elasticity of concrete was assumed for all the floors except where notified (in the case of double-T beam floors), some of the frequency estimation is not very close. Since the single-panel model developed shows good correlation in most cases, it may be reasonably assumed that if the actual strengths were known for all the floors, accurate estimates of the fundamental frequency would have resulted. The FE model, however, allows the analyst to vary the different parameters in order to achieve higher frequencies and/or lower static deflections. The FEM can be easily employed on any available FE package and is strongly recommended for both fundamental frequency and static deflection estimates.

Static Deflection Method (SDM)

The SDM leads to inaccurate estimates of the fundamental frequency except in the case of static deflections obtained from FE analysis. The SDM, however, can be used reliably only after necessary modification of the SDOF system frequency formula. The SDM requires estimates of the maximum static deflection of the floors which can either be selected before design or calculated from FEM for a single-panel or beam models. The modified SDOF formula, therefore, offers flexibility in either controlling frequency or deflections of the floors at the design stage.

For composite floors, both Wyatt's and Allen-Murray's approaches lead to reasonable estimates of fundamental frequency and may be used in the absence of a FE package.

Dunkerly's Formula

The application of Dunkerly's formula to both the EBM and SDM approaches always lead to an under-estimation of fundamental frequency. Since the frequency estimation of the system by this formula depends on the two estimates of frequency for the beam and girder elements, the results are not always consistent. This is because most floors are inherently continuous and cannot be separated into individual components, this was noted

in the case of beam and slab type floors (section 4.1.1). This formula is, therefore, not recommended for any frequency estimation at all.

6.1.2 Minimum Fundamental Frequency

In order to control vibration problems, it is vitally important to ensure a high fundamental frequency for the floors at the design stage. Table 6.1 below gives the estimated range, average and the recommended minimum fundamental frequencies for the floors tested. It may be noted, however, that the recommended minimum fundamental frequencies are for general purpose buildings and are based on CSA (1990) and Wyatt (1989) with due consideration to the economy of construction.

Table 6.1: Fundamental Frequency Estimates

Floor Type	Fundamental Frequency (Hz)		
	Estimated Range	Average	Recommended Minimum
Beam and Slab	5.8-11.2	8.6	6.0
Flat Slab	5.9-12.7	9.4	6.0
Double-T Beam	4.6-5.8	5.3	4.5
Composite	6.4-14.0	9.8	7.0

From Table 6.1, it is clear that both the maximum estimated and average fundamental frequencies are for composite floors. The above minimum fundamental frequencies are recommended to avoid any objectionable vibrations due to walking at or near a frequency of 2 Hz. This is because floor frequencies above the second harmonic of walking frequency or not an exact multiple of that has been found to be difficult to excite by normal daily life activities.

6.1.3 Damping Estimation

The inherent floor damping depends mainly on the material properties, suspended ceilings, partition or support walls, false floors, and other floor attachments apart from the loading on the floor including furniture etc. Damping estimates also depends on the location of measurement because exciting a floor near a support wall would not result in an accurate estimate of true damping as compared to excitation at the midspan, for example. The estimation of damping using the Half-Power method requires accurate estimation of half-power frequencies and the floor natural frequency (see Figure 2.10). This, in turn, depends on the frequency resolution. Since it was not possible to measure data for a high frequency resolution in some cases, the estimation of damping in these cases is not accurate. Other reasons for such inaccuracies include closely spaced modes, noise and other ambient vibrations in the data.

Another method of estimating damping accurately would be to excite the floor at its fundamental frequency and allowing the vibration to decay. The log-decrement method can then be used for estimating damping. However, this requires the prior knowledge of the floor fundamental frequency which was the unknown in the present research.

Table 6.2 below gives the estimated range and average values of damping for the floors tested.

Table 6.2: Damping Estimates

Floor Type	Damping Ratio (% Critical)	
	Estimated Range	Average
Beam and Slab	1.9-3.7	2.6
Flat Slab	1.0-7.1	2.6
Double-T Beam	1.0-3.4	1.7
Composite	1.0-11.4	4.3

From Table 6.2, it is clear that both the maximum estimated and average damping values are for composite floors. Therefore, although it is difficult to predict damping at the design stage, a minimum damping ratio of 5% of critical is recommended for all floors to ensure that all objectionable vibrations die out in a reasonable amount of time.

6.1.4 Span / Depth Ratios and Static Deflections

In the parametric studies in Chapter 4, only the thickness of the floor slab was varied in the case of beam and slab, flat slab and composite floors whereas the length of beam was varied in the case of double-T beam floors. The following conclusions are based on these studies.

Beam and Slab Floors

Based on the results of the four floors of this type, a lower span/depth ratio of the slab was obtained for a floor with a wide beam of large cross-section area and a higher span/depth ratio was obtained for a floor with a narrow beam of small cross-section area. It may be mentioned here that the effect of the span/depth ratio of beams on fundamental frequency was not studied in this research. Table 6.3 below shows the estimated and recommended maximum span/depth ratios.

Table 6.3: Maximum Span/Depth Ratios for Beam and Slab Floors

Span Direction	Maximum Span/Depth Ratios	
	Estimated	Recommended
Short	42	40
Long	78	70

The Concrete Society (1994) recommends a maximum span/depth ratio of 45 for these slabs for spans less than 13 m and more than 6 m. This limit, however, is only for the slab's long span direction whereas the limits given in Table 6.3 restricts both the spans to avoid frequencies below 6 Hz.

Similarly, a static deflection limit of 10.0 mm was obtained for these floors. However, these conclusions may not be generalised due to the limited amount of tests on this floor type. Moreover, these conclusion are based on a minimum fundamental frequency of 6 Hz and will be different for other choices of minimum frequency.

Flat Slab Floors

Table 6.4 below shows the estimated and recommended maximum span/depth ratios based on the results of the twelve floors of this type.

Table 6.4: Maximum Span/Depth Ratios for Flat Slab Floors

Span Direction	Maximum Span/Depth Ratios	
	Estimated	Recommended
Short	33.5	30
Long	47.8	45

The Concrete Society (1994) recommends a maximum span/depth ratio of 44 for flat slabs with drop panels for spans less than 13 m and more than 6 m. This limit, however, is only for the slab's long span direction whereas the limits given in Table 6.4 restricts both the spans to avoid frequencies below 6 Hz.

Similarly, a static deflection limit of 9.0 mm was obtained for these floors. However, these conclusions are based on a minimum fundamental frequency of 6 Hz and will be different for other choices of minimum frequency.

Double-T Beam Floors

The dynamic behaviour of these floors depend on the span length of the beams and their cross-sections. Based on the results of the five floors of this type, limits for their span lengths have been suggested in section 4.3.2.1. Similarly, a static deflection limit of 8.5 mm was obtained for these floors. However, these conclusions are based on a minimum fundamental frequency of 4.5 Hz and will be different for other choices of minimum frequency.

Composite Floors

The dynamic behaviour of these floors depend on the slab thickness and the beam or girder sections. A static deflection limit of 5.5 mm was obtained for these floors, based on a minimum fundamental frequency of 7 Hz. Based on the results of the eight floors of this type, their dynamic behaviour may be improved by increasing the beam or girder section irrespective of the slab thickness or a minimum fundamental frequency (see section 4.4.2.1).

6.1.5 Modified SDOF Formula

It has been shown in Chapter 4 that the fundamental frequency of the floors tested can be closely approximated by the following modified form of the SDOF system frequency formula using static deflections:

$$f = \frac{K}{\sqrt{\Delta_s}} \tag{6.1}$$

where K is a constant dependent on the type of floor. The average value of this constant, as estimated from the frequency versus deflection relationship for the floors tested (see Chapter 4), and its recommended minimum values are given in Table 6.5 below. In addition, the estimated and recommended maximum static deflection limits for these floors are also given in Table 6.5.

Table 6.5: Maximum Static Deflections and Constant K for Modified SDOF Formula

Floor Type	Maximum Static Deflections (mm)		K	
	Estimated	Recommended	Estimated Average	Recommended Minimum
Beam and Slab	10.0	9.0	17.0	15.8
Flat Slab	9.0	8.0	18.7	18.0
Double-T Beam	8.5	8.0	17.7	17.5
Composite	5.5	5.0	18.6	15.8

6.2 Recommendations

Following recommendations are suggested which are based on the author's experience of vibration testing of floors and the comparisons given in Chapter 5:

Testing

1. The testing should always be carried out in a very quiet environment.
2. A minimum number of 512 samples should be used for acquiring vibration data. This will result in smooth plots and, therefore, easy identification of peaks in the transfer function.
3. A high sensitivity value should be used for the accelerometer when collecting vibration data. This will ensure that only the floor response is being measured and, therefore, will result in a clean data.
4. The vibration data should be analysed a number of times for an average estimation of the dynamic characteristics.
5. When analysing the vibration data, the corresponding phase variation should be closely studied to check the pattern and detect any closely spaced modes, if any.
6. A backup data storage system should always be carried to the site to allow for extra set of data points to be measured. This is because sometimes there may be different floor types or panels available for testing on the site.
7. The layout dimensions should always be measured on site to check if the original design has not been altered.
8. Every effort should be made to obtain the actual material properties used in the design of the site being tested.

Frequency Estimation

1. The single-panel FE model developed in this thesis may be used at the design stage for the estimation of the fundamental frequencies. The model allows the variation of the different parameters in ensuring high floor frequencies and/or lower static deflections.

2. The span/depth ratio limits obtained for beam and slab, and flat slab type floors may be used as a guide at the design stage to avoid low fundamental frequencies.
3. The span length limits obtained for double-T beam type floors may be used as a guide at the design stage to avoid low fundamental frequencies.
4. Equation 6.1 may be used for the estimation of the fundamental frequency of floors. Alternatively, the static deflections may be limited based on a minimum fundamental frequency.

6.3 Future Research

Acceptable floor vibrations mainly depend on the floor fundamental frequency and associated damping. It has been established that a single-panel FE model can be used to predict the fundamental frequency of a floor, whereas a more detailed model of the whole floor may be needed to estimate the higher floor frequencies. However, the estimation of floor damping need to be investigated in detail and methods for ensuring and enhancing the floor damping should be developed.

The span/depth ratios for beam and slab, flat slab and composite floors and span length limits for double-T beam type floors should be further studied to include the effect of floor accelerations due to various human activities. Therefore, acceleration limits should be studied and developed for different floors in addition to the existing deflection and span/depth ratio limitations.

Floors which have been designed for high fundamental frequency and damping performance and low deflection and acceleration limits could have their dynamic behaviour significantly improved.

REFERENCES AND BIBLIOGRAPHY

[1] ACI 318-89R-92. (1994). "**Building Code Requirements for Reinforced Concrete**". ACI Manual of Concrete Practice Part 3: Use of Concrete in Buildings - Design, Specifications and Related Topics, Detroit, Michigan, USA.

[2] ACI 363R-92. (1994). "**State-of-the-art Report on High Strength Concrete**". ACI Manual of Concrete Practice Part 1: Materials and General Properties of Concrete, Detroit, Michigan, USA.

[3] ANSI S3.29-1983 (1983). "**Guide to the Evaluation of Human Exposure to Vibrations in Buildings**". American National Standards Institute, New York, USA.

[4] Allen, D.E.; Murray, T.M. (1993). "**Vibration of Composite Floors**". Proceedings of the Symposium on Structural Engineering in Natural Hazards Mitigation, Irvine, CA, pages 1491-1496.

[5] Allen, D.E.; Murray, T.M. (1993). "**Design Criterion for Vibrations Due to Walking**". AISC Engineering Journal, 4th Quarter, pages 117-129.

[6] Allen, D.E. (1990). "**Building Vibrations From Human Activities**". Concrete International, Volume 12, Number 6, pages 66-73.

[7] Allen, D.E. (1990). "**Floor Vibrations From Aerobics**". Canadian Journal of Civil Engineering, Volume 17, Number 5, pages 771-779.

[8] Allen, D.E.; Rainer, J.H.; Pernica, G. (1985). "**Vibration Criteria For Assembly Occupancies**". Canadian Journal of Civil Engineering, Volume 12, Number 3, pages 617-623.

[9] Allen, D.E.; Rainer, J.H.; Pernica, G. (1979). "**Vibration Criteria For Long-Span Concrete Floors**". Proceedings of the ACI Symposium on Vibrations of Concrete Structures, New Orleans, USA, pages 67-78.

[10] Allen, D.E.; Rainer, J.H. (1976). "**Vibration Criteria For Long-Span Floors**". Canadian Journal of Civil Engineering, Volume 3, Number 2, pages 165-173.

[11] ASCE (1986). "**Structural Serviceability: A Critical Appraisal and Research Needs**". Ad Hoc Committee on Serviceability Research, Committee on Research

of the Structural Division, ASCE Journal of the Structural Engineering, Volume 112, Number 12, pages 2646-2664.

[12] Bachmann, H. (1992). "**Practical Cases Of Structures With Man-Induced Vibrations**". Proceedings of the Symposium/Workshop on Serviceability of Buildings, 16-18 May 1988, Ottawa, Ontario, Canada, Volume I, pages 419-434.

[13] Bachmann, H. (1992). "**Case Studies Of Structures With Man-Induced Vibrations**". ASCE Journal of the Structural Engineering, Volume 118, Number 3, pages 631-647.

[14] Bachmann, H. (1992). "**Vibration Upgrading of Gymnasia, Dance Halls and Footbridges**". Structural Engineering International, Volume 2, Number 2, pages 118-124.

[15] Bachmann, H. (1984). "**Vibration of Building Structures Caused by Human Activities, Case Study Of a Gymnasium**". National Research Council of Canada (NRCC), NRC/CNR TT-2077.

[16] Bachmann, H. and Ammann, W. (1987). "**Vibrations in Structures Induced by Man and Machines**". IABSE, Structural Engineering Document, Zurich, Switzerland.

[17] Blevins, R.D. (1995). "**Formulas for Natural Frequency and Mode Shape**". Krieger Publishing Company, Malabar, Florida, USA.

[18] Bolton, A. (1978). "**Natural Frequencies of Structures for Designers**". The Structural Engineer, Volume 56A, Number 9, pages 245-253.

[19] BS 6472, (1984). "**British Standard Guide To Evaluation Of Human Exposure To Vibration In Buildings (1 Hz To 80 Hz)**". British Standards Institution, London, U.K.

[20] BS 8110 (1985). "**Structural Use of Concrete: Part 1 - Code of Practice for Design and Construction and Part 2 - Code of Practice for Special Circumstances**". British Standards Institution, London, U.K.

[21] CSA Standard CAN3-S16.1-M89 (1989). "**Steel Structures For Buildings (Limit States Design) - Appendix G: Guide For Floor Vibrations**". Canadian Standards Association (CSA), NRCC, Rexdale, Ontario, Canada, pages 127-134.

[22] CSA Standard (1990). "**Serviceability Criteria For Deflections And Vibrations**". The Supplement to the National Building Code of Canada (NBCC), Commentary A to part 4, NRCC, pages 146-152.

[23] Chen, Y; Aswad, A. (1994). "**Vibration Characteristics of Double Tee Building Floors**". PCI Journal, Volume 39, Number 1, pages 84-95.

[24] Chui, Y.H. and Smith, I. (1988). "**A Serviceability Criterion to Avoid Human Discomfort for Light-Weight Wooden Floors**". Proceedings of the Symposium/Workshop on Serviceability of Buildings, 16-18 May 1988, Ottawa, Ontario, Canada, Volume I, pages 512-525.

[25] Clough, R.W. and Penzien, J. (1993). "**Dynamics of Structures**". McGraw-Hill International Inc., New York, USA.

[26] Concrete Society (1994). "**Post-Tensioned Concrete Floors: Design Handbook**". CS Technical Report Number 43.

[27] DIN 4150 (1975). "**Vibrations in Civil Engineering. Part-2: Effects on People in Buildings (In German)**". German Institute for Standardisation, Berlin, Germany.

[28] Ebrahimpour, A.; and Sack, R.L. (1988). "**Crowd-Induced Dynamic Loads**". Proceedings of the Symposium/Workshop on Serviceability of Buildings, 16-18 May 1988, Ottawa, Ontario, Canada, Volume I, pages 451-464.

[29] Ebrahimpour, A.; and Sack, R.L. (1992). "**Design Live Loads for Coherent Crowd Harmonic Movements**". ASCE Journal of the Structural Engineering, Volume 118, Number 4, pages 1121-1136.

[30] Ellingwood, B; Tallin, A. (1984). "**Structural Serviceability: Floor Vibrations**". ASCE Journal of Structural Engineering, Volume 110, Number 2, pages 401-418.

[31] Ellis, B.R. (1994). "**Dynamic Testing**". Proceedings of the First Cardington Conference, Cardington, UK.

[32] Ellis, B.R.; and Ji, T. (1994). "**Floor Vibration Induced by Dance-Type Loads: Verification**". The Structural Engineer, Volume 72, Number 3, pages 45-50.

[33] Elnimeiri, M. and Iyengar, H. (1989). "**Composite Floor Vibrations: Predicted and Measured**". ASCE Structures Congress, May 1989, New York, USA, pages 487-493.

[34] Eriksson, P.E. (1994). "**Vibration of Low-Frequency Floors - Dynamic Forces and Response Prediction**". PhD Thesis, Chalmers University of Technology, Department of Structural Engineering, Goteborg, Sweden.

[35] Ewins, D.J. (1995) "**Modal Testing: Theory And Practice**". Research Studies Press Ltd., Taunton, England, and John Wiley and Sons Inc., Chichester, England.

[36] Foschi, R.O.; and Gupta, A. (1987). "**Reliability of Floors Under Impact Vibration**". Canadian Journal of Civil Engineering, Volume 14, pages 683-689.

[37] Galambos, T.V. (1988). "**Vibration of Steel Joist-Concrete Slab Floors**". Technical Digest Number 5, Steel Joist Institute, South Carolina, USA.

[38] Halvorsen, W.G.; Brown, D.L. (1977). "**Impulse Technique For Structural Frequency Response Testing**". Sound and Vibration, pages 8-21.

[39] Inman, D.J. (1994). "**Engineering Vibration**". Prentice-Hall International, Inc., New Jersey, USA.

[40] Irwin, A.W. (1978). "**Human Response to Dynamic Motion of Structures**". The Structural Engineer, Volume 56A, Number 9, pages 237-244.

[41] ISO 2631-2 (1989). "**Evaluation of Human Exposure to Whole-Body Vibration-Part 2: Human Exposure to Continuous and Shock-Induced Vibrations in Buildings (1-80 Hz)**". International Organisation for Standardisation, Geneva, Switzerland.

[42] ISO 10137 (1992). "**Bases for Design of Structures - Serviceability of Buildings Against Vibration**". International Organisation for Standardisation, Geneva, Switzerland.

[43] Ji, T.; and Ellis, B.R. (1994). "**Floor Vibration Induced by Dance-Type Loads: Theory**". The Structural Engineer, Volume 72, Number 3, pages 37-44.

[44] Lenzen, K.H. (1966). "**Vibration Of Steel Joist Concrete Slab Floors**". AISC Engineering Journal, Volume 3, pages 133-136.

[45] Leon, M.R. and Alsamsam, A.M.I. (1993). "**Performance and Serviceability of Composite Floors**". ASCE Symposium on Structural Engineering in Natural Hazards Mitigation, New York, USA, pages 1479-1484.

[46] Maguire, J.R.; Severn, R.T. (1987). "**Assessing The Dynamic Properties Of Prototype Structures By Hammer Testing**". Proceedings of The Institution of Civil Engineers, Part 2, Volume 83, pages 769-784.

[47] Matthew, P.W.; and Bennett, D.F.H. (1990). "**Economic Long-Span Concrete Floors**". British Cement Association, Publication 97.311.

[48] Matthews, C.M. and Montgomery, C.J. (1988). "**Dynamic Study of a Stub Girder Floor System**". Proceedings of the Symposium/Workshop on Serviceability of Buildings, 16-18 May 1988, Ottawa, Ontario, Canada, Volume I, pages 465-476.

[49] Matthews, C.M. and Montgomery, C.J. (1988). "**A Dance Floor with Unsatisfactory Dynamic Response**". Proceedings of the Symposium/Workshop on Serviceability of Buildings, 16-18 May 1988, Ottawa, Ontario, Canada, Volume I, pages 533-546.

[50] MODENT (1993). "**Modal Analysis Program by ICATS - Reference Manual**". Imperial College of Science, Technology and Medicine, London, UK.

[51] Mouring, S.E.; and Ellingwood, B.R. (1994). "**Guidelines to Minimise Floor Vibrations from Building Occupants**". ASCE Journal of the Structural Engineering, Volume 120, Number 2, pages 507-526.

[52] Mouring, S.E.; and Ellingwood, B.R. (1993). "**Minimising Floor Vibration Caused by Building Occupants**". Proceedings of the International Colloquium on Structural Serviceability of Buildings, Goteborg, Sweden, IABSE Reports, Volume 69, pages 125-132.

[53] Murray, T.M.; and Allen, D.E. (1993). "**Floor Vibrations: A New Design Approach**". Proceedings of the International Colloquium on Structural Serviceability of Buildings, Goteborg, Sweden, IABSE Reports, Volume 69, pages 119-124.

[54] Murray, T.M.; and Allen, D.E. (1993). "**Floor Vibrations: A New Design Approach**". Proceedings of International Colloquium on Structural Serviceability of Buildings, Sweden, IABSE Reports, Volume 69, pages 119-124.

[55] Murray, T.M. (1991). "**Building Floor Vibrations**". AISC Engineering Journal, Volume 28, Number 3, pages 102-109.

[56] Murray, T.M. (1988). "**Practical Aspects of Floor Serviceability Design**". Proceedings of the Symposium/Workshop on Serviceability of Buildings, 16-18 May 1988, Ottawa, Ontario, Canada, Volume I, pages 495-511.

[57] Murray, T.M. (1981). "**Acceptability Criterion for Occupant-Induced Floor Vibrations**". AISC Engineering Journal, Volume 18, Number 2, pages 62-70.

[58] Murray, T.M. (1975). "**Design To Prevent Floor Vibrations**". AISC Engineering Journal, Volume 12, Number 3, pages 82-87.

[59] NBCC (1990). "**National Building Code of Canada**", Ontario, Canada.

[60] Neville, A.M. (1995). "**Properties of Concrete**". Longman Group Ltd., Harlow, England, UK.

[61] Ohlsson, S.V. (1988). "**Ten Years of Floor Vibration Research - A Review of Aspects and Some Results**". Proceedings of the Symposium/Workshop on Serviceability of Buildings, 16-18 May 1988, Ottawa, Ontario, Canada, Volume I, pages 435-449.

[62] Onysko, D.M. (1988). "**Performance and Acceptability of Wood Floors - Forintek Studies**". Proceedings of the Symposium/Workshop on Serviceability of Buildings, 16-18 May 1988, Ottawa, Ontario, Canada, Volume I, pages 477-493.

[63] Osborne, K.P.; Ellis, B.R. (1990). "**Vibration Design And Testing Of A Long-Span Light-Weight Floor**". The Structural Engineer, Volume 68, Number 10, pages 181-186.

[64] Parmalee, R.A.; and Ramirez, M.R. (1987). "**Dynamic Criteria for Human Response to Floor Vibrations**". Proceedings of the Structures Congress '87, Orlando, Florida, USA, pages 448-454.

[65] Pernica, G.; Allen, D.E. (1982). "**Floor Vibration Measurements In A Shopping Centre**". Canadian Journal of Civil Engineering, Volume 9, Number 2, pages 149-155.

[66] PMF (1994). "**ComFlor 51 and 70**". Brochures on Composite Floor Decking Systems, Precision Metal Forming Limited, UK.

[67] Rainer, J.H.; Allen, D.E.; and Pernica, G. (1988). "**Dynamic Response of Floors Due to People in Motion**". Proceedings of the Symposium/Workshop on Serviceability of Buildings, 16-18 May 1988, Ottawa, Ontario, Canada, Volume I, pages 566-572.

[68] Rosenthal, I and Itskovitch, M. (1988). "**Vibration Response of a Ribbed Slab Floor to Dancing**". Proceedings of the Symposium/Workshop on Serviceability

of Buildings, 16-18 May 1988, Ottawa, Ontario, Canada, Volume I, pages 526-531.

[69] Smith, I.; and Chui, Y.H. (1988). **"Design of Light-Weight Wooden Floors to Avoid Human Discomfort"**. Canadian Journal of Civil Engineering, Volume 15, pages 254-262.

[70] Tolaymat, R.A. (1988). **"A New Approach to Floor Vibration Analysis"**. AISC Engineering Journal, pages 137-143.

[71] Tolaymat, R.A. (1988). **"An Automated Approach to Floor Vibration Analysis"**. Proceedings of the Symposium/Workshop on Serviceability of Buildings, 16-18 May 1988, Ottawa, Ontario, Canada, Volume I, pages 558-565.

[72] Wiss, J.F.; and Parmalee, R.A. (1974). **"Human Perception of Transient Vibrations"**. ASCE Journal of the Structural Engineering, Volume 100, Number ST4, pages 773-787.

[73] WSSL (1995). **"Advertisement - Westok Structural Services Limited"**. The Structural Engineer, Vol. 74, No. 5/7, page A2.

[74] Wyatt, T.A. (1989). **"Design Guide On The Vibration Of Floors"**. The Steel Construction Institute, U.K., SCI Publication 076.

[75] Wyatt, T.A. (1985). **"Floor Excitation by Rhythmic Vertical Jumping"**. Engineering Structures, pages 208-210.

[76] Zienkiewicz, O.C. (1981). **"The Finite Element Method"**. McGraw-Hill International Inc., New York, USA.

Appendix A

Floor Types

This appendix presents typical isometric sketches for each of the four floor types tested. Typical plan layout and cross-sections have already been given in Chapter 3. For the composite floors, only the profiles used in the floors tested are given along with their corresponding dimensions. For full structural details and dimensions, see Chapter 3.

A.1 Post-Tensioned Concrete 1-Way Spanning Solid Floor Slabs with Beams

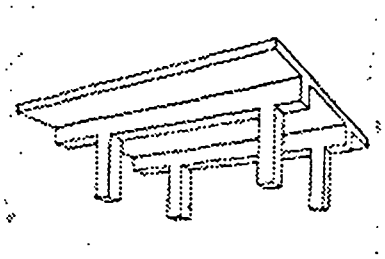

Beam and Slab Floor

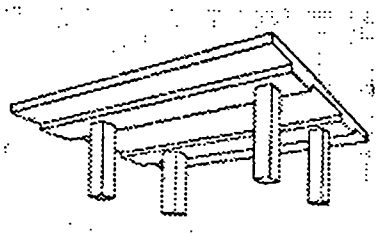

Banded Flat slab Floor

A.2 Post-Tensioned Concrete Solid Flat Slab Floors

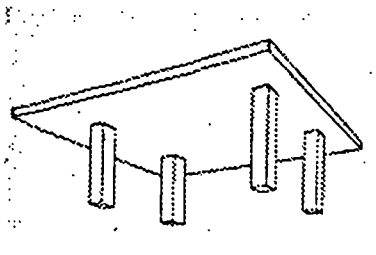

Solid Flat Slab Floor

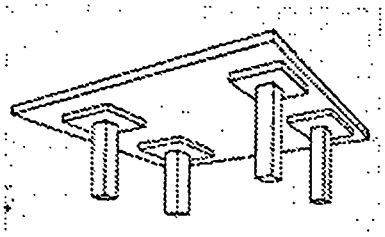

Solid Flat Slab Floor with Drop Panels

A.3 Pre-Tensioned Concrete Double-T Beam Floors

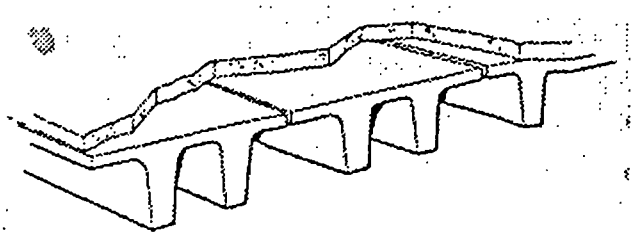

Precast Double-T Beam Floor

A.4 Composite Steel-Concrete Slab Floors

COMFLOR 51

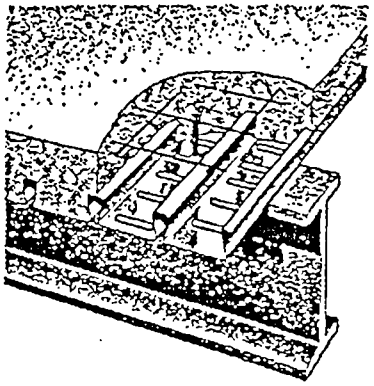

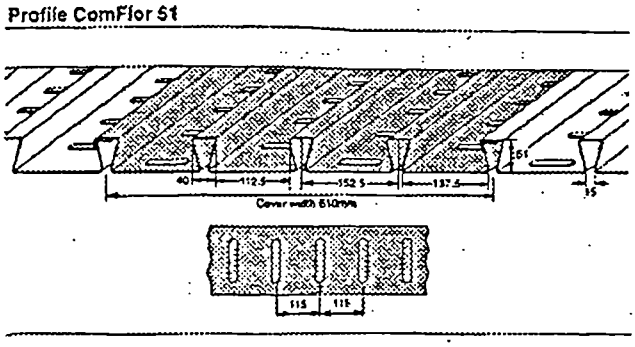

CF 51 Profile with Dimensions

COMFLOR 70

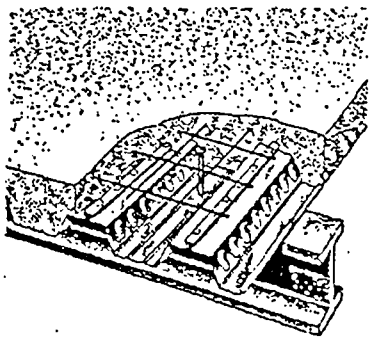

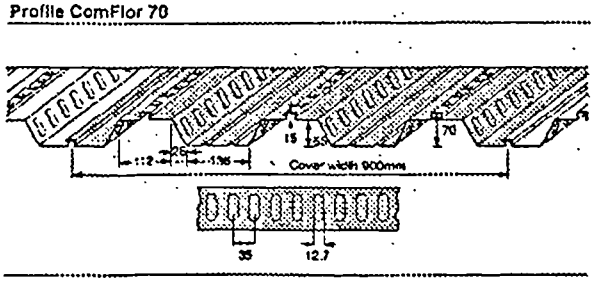

CF 70 Profile with Dimensions

Appendix B

Typical Calculations

This appendix presents the typical calculations for frequency estimation by the various methods given in Chapter 1 for each of the four floor types tested. However, results for finite element method are not given here (see Chapter 4). Calculations for only one representative floor in each category are presented. The results for all the floors are given and discussed in Chapter 5.

B.1 Post-Tensioned Concrete 1-Way Spanning Solid Floor Slabs with Beams

Typical calculations for the High Wycombe floor are given here. Results for other floors of this type follow the same procedure. Material properties for this floor type are as follows:

Density of concrete (ρ) = 2400 kg/m^3

Modulus of elasticity of concrete (E) = 34.79 kN/mm^2 (GPa)

Equivalent Beam Method (EBM)

Effective beam length (L) = c/c distance = 12.05 m

Width of beam web (w_b) = 0.665 m

Effective T-beam width = $w_b + 0.75 \times \frac{L}{5} = 2.4725$ m

Centroid of T-beam = 0.2221 m

Moment of inertia of T-beam (I) = 0.0264 m^4

Area of cross-section (A) = 0.8118 m^2

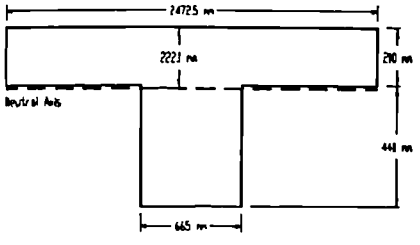

Fundamental natural frequency $= \frac{\pi}{2}\sqrt{\frac{EI}{\rho AL^4}} = 7.43$ Hz (simple supports)

Fundamental natural frequency $= \frac{(4.73)^2}{2\pi}\sqrt{\frac{EI}{\rho AL^4}} = 16.84$ Hz (fixed supports)

Plate Method (PM)

Poisson ratio of concrete (ν) = 0.2

Slab thickness (h) = 0.21 m

Long span (L_x) = 12.05 m

Short span (L_y) = 7.305 m

$\frac{L_x}{L_y} \cong 1.65$

For simply supported plate, $\lambda^2 = \pi^2\left[1+\frac{L_x^2}{L_y^2}\right] = 36.73$

Fundamental natural frequency $= \frac{\lambda^2}{2\pi L_x^2}\sqrt{\frac{Eh^2}{12\rho(1-\nu^2)}} = 9.48$ Hz

For corner supported plate,

$\lambda^2 = 1.5467x(1.65)^3 - 9.82x(1.65)^2 + 20.803x(1.65) - 5.41 \cong 9.13$

Fundamental natural frequency $= \frac{\lambda^2}{2\pi L_x^2}\sqrt{\frac{Eh^2}{12\rho(1-\nu^2)}} = 2.36$ Hz

Concrete Society Method (CSM)

Moment of inertia of slab ($I_x = I_y = \frac{1x0.21^3}{12}$) = 0.00077175 m^4/m

Number of spans along short span (n_x) = 3

Number of spans along long span (n_y) = 1

$\lambda_x = \frac{n_x L_x}{L_y} = 1.8187$ $\quad K_x = 1 + \frac{1}{\lambda_x^2} = 1.3023$

$$\lambda_y = \frac{n_y L_y}{L_x} = 1.6496 \qquad K_y = 1 + \frac{1}{\lambda_y^2} = 1.3675$$

For slabs with perimeter beams,

$$f_x = k_x \frac{\pi}{2}\sqrt{\frac{EI_y}{\rho A L_y^4}} = 3.25 \text{ Hz} \qquad f_y = k_y \frac{\pi}{2}\sqrt{\frac{EI_x}{\rho A L_x^4}} = 9.29 \text{ Hz}$$

Static Deflection Method (SDM)

Using the EBM values of area, length and moment of inertia with acceleration due to gravity (g) = 9.80665 m/sec^2:

Static deflection of equivalent beam (Δ_s) = $\frac{5\rho A g L^4}{384EI}$ = 5.71 mm (simple supports)

Fundamental natural frequency = $\frac{1}{2\pi}\sqrt{\frac{g}{\Delta_s}}$ = 6.59 Hz

Static deflection of equivalent beam (Δ_s) = $\frac{\rho A g L^4}{384EI}$ = 1.14 mm (fixed supports)

Fundamental natural frequency = $\frac{1}{2\pi}\sqrt{\frac{g}{\Delta_s}}$ = 14.75 Hz

FE maximum static deflection (Δ_s) = 3.78 mm

Fundamental natural frequency = $\frac{17}{\sqrt{\Delta_s}}$ = 8.74 Hz

B.2 Post-Tensioned Concrete Solid Flat Slab Floors

Typical calculations for the Hammersmith floor are given here. Results for other floors of this type follow the same procedure. Material properties for this floor type are the same as for 1-Way Spanning Solid Post-Tensioned Concrete Slabs with Beams, given in Appendix B.1.

Equivalent Beam Method (EBM)

Effective beam length (L) = c/c distance (long span) = 8.4 m

Width of beam = 1.0 m

Area of beam (A) = 1 x 0.225 = 0.225 m^2

Moment of inertia (I) $= \frac{1x0.225^3}{12} = 0.00095\ m^4$

Fundamental natural frequency $= \frac{\pi}{2}\sqrt{\frac{EI}{\rho AL^4}} = 5.51$ Hz (simple supports)

Fundamental natural frequency $= \frac{(4.73)^2}{2\pi}\sqrt{\frac{EI}{\rho AL^4}} = 12.48$ Hz (fixed supports)

Plate Method (PM)

Poisson ratio of concrete (ν) = 0.2

Slab thickness (h) = 0.225 m

Long span (L_x) = 8.4 m

Short span (L_y) = 7.2 m

$\frac{L_x}{L_y} \cong 1.17$

For simply supported plate, $\lambda^2 = \pi^2\left[1+\frac{L_x^2}{L_y^2}\right] = 23.30$

Fundamental natural frequency $= \frac{\lambda^2}{2\pi L_x^2}\sqrt{\frac{Eh^2}{12\rho(1-\nu^2)}} = 13.27$ Hz

For corner supported plate,

$$\lambda^2 = 1.5467x(1.17)^3 - 9.82x(1.17)^2 + 20.803x(1.17) - 5.41 \cong 7.95$$

Fundamental natural frequency $= \frac{\lambda^2}{2\pi L_x^2}\sqrt{\frac{Eh^2}{12\rho(1-\nu^2)}} = 4.53$ Hz

Concrete Society Method (CSM)

Moment of inertia of slab ($I_x = I_y = \frac{1x0.225^3}{12}$) = 0.00095 m^4/m

Number of spans along short span (n_x) = 5

Number of spans along long span (n_y) = 5

$\lambda_x = \frac{n_x L_x}{L_y} = 4.28$ $\quad K_x = 1 + \frac{1}{\lambda_x^2} = 1.0544$

$\lambda_y = \frac{n_y L_y}{L_x} = 5.83$ $\quad K_y = 1 + \frac{1}{\lambda_y^2} = 1.0294$

For slabs without perimeter beams,

$$f_x' = k_x \frac{\pi}{2}\sqrt{\frac{EI_y}{\rho A L_y^4}} = 5.80 \text{ Hz}$$

$$f_y' = k_y \frac{\pi}{2}\sqrt{\frac{EI_x}{\rho A L_x^4}} = 7.71 \text{ Hz}$$

$$f_b = \frac{\frac{\pi}{2}\sqrt{\frac{EI_x}{\rho A L_x^4}}}{\sqrt{1 + \frac{I_x}{I_y}\frac{L_y^4}{L_x^4}}} = 4.44 \text{ Hz}$$

$$f_x = f_x' - (f_x' - f_b)\left(\frac{\frac{1}{n_x} + \frac{1}{n_y}}{2}\right) = 5.50 \text{ Hz}$$

$$f_y = f_y' - (f_y' - f_b)\left(\frac{\frac{1}{n_x} + \frac{1}{n_y}}{2}\right) = 6.98 \text{ Hz}$$

Static Deflection Method (SDM)

Using the equivalent beam method values of area, length and moment of inertia with acceleration due to gravity (g) = 9.80665 m/sec^2:

Static deflection of equivalent beam (Δ_s) = $\frac{5\rho AgL^4}{384EI}$ = 4.89 mm (simple supports)

Fundamental natural frequency = $\frac{1}{2\pi}\sqrt{\frac{g}{\Delta_s}}$ = 7.13 Hz

Static deflection of equivalent beam (Δ_s) = $\frac{\rho AgL^4}{384EI}$ = 2.08 mm (fixed supports)

Fundamental natural frequency = $\frac{1}{2\pi}\sqrt{\frac{g}{\Delta_s}}$ = 10.93 Hz

FE maximum static deflections (Δ_s) = 4.89 mm

Fundamental natural frequency = $\frac{18.7}{\sqrt{\Delta_s}}$ = 8.46 Hz

B.3 Pre-Tensioned Concrete Double-T Beam Floors

Typical calculations for the Swindon floor are given here. Results for other floors of this type follow the same procedure. The Plate and Concrete Society Methods donot apply to this floor type. Material properties for this floor type are as follows:

Site	ρ (kg/m^3)	E (kN/mm^2)
Swindon, Sutton	2500	38.89
Reading, Basildon, Tunbridge wells	2350	39.85

Equivalent Beam Method (EBM)

Effective beam length (L) = c/c distance = 16.045 m

Area of beam (A) = 0.4242 m^2

Moment of inertia (I) = 0.01559 m^4

Fundamental natural frequency $= \frac{\pi}{2}\sqrt{\frac{EI}{\rho AL^4}} = 4.61$ Hz

Static Deflection Method (SDM)

Using the equivalent beam method values of area, length and moment of inertia with acceleration due to gravity (g) = 9.80665 m/sec^2:

Static deflection of T-beam (Δ_s) $= \frac{5\rho AgL^4}{384EI} = 14.8$ mm

Fundamental natural frequency $= \frac{1}{2\pi}\sqrt{\frac{g}{\Delta_s}} = 4.10$ Hz

FE maximum static deflections (Δ_s) = 15.0 mm

Fundamental natural frequency $= \frac{17.7}{\sqrt{\Delta_s}} = 4.57$ Hz

B.4 Composite Steel-Concrete Slab Floors

Typical calculations for the Millwall Stadium, London floor are given here. Results for other floors of this type follow the same procedure. The Plate and Concrete Society Methods donot apply to this floor type. Material properties for this floor type are as follows:

Density of Concrete (ρ_c)	=	1900 kg/m^3
Modulus of Elasticity of Concrete (E_c)	=	22 kN/mm^2
Density of Steel (ρ_s)	=	7820 kg/m^3
Modulus of Elasticity of Steel (E_s)	=	206.8 kN/mm^2
Modular Ratio (n) = $\frac{E_s}{E_c}$	=	9.4

Equivalent Beam Method (EBM)

a) Beam (UB356x127x33) Supporting CF70 Profile Slab

Slab thickness (t) = least of t_1 or t_2 = 105 mm (see PMF (1994)):

Profile based thickness: $t_1 = 130 - \frac{112+164}{2} x \frac{55}{300} = 105$ mm

Weight based thickness: $t_2 = \frac{2.07x1000}{9.80665x1900} x1000 = 110$ mm

Beam length (L_b) = 6.75 m

Area of beam = 4180 mm^2

Moment of inertia of beam = 8200,0000 mm^4

Beam spacing (S_b) = 2.665 m

Effective slab width (ESW) = least of $\frac{L_b}{4}$ or S_b

= 1.6875 m

Transformed width = $\frac{ESW}{n}$ = 180 mm

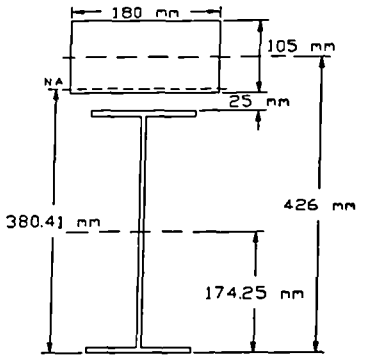

Centroid = 380.41 mm from base

Transformed moment of inertia (I_{Tb}) = 316305176.3 mm^4

Beam mass/length (m_B) = 33 kg/m

Supported mass (m_b) = S_b x t x ρ_c + m_B

= 2.665 x 0.105 x 1900 + 33 = 564.6675 kg/m

Fundamental natural frequency of beam (f_b) = $\frac{\pi}{2}\sqrt{\frac{E_s I_{Tb}}{m_b L_b^4}}$ = 11.73 Hz

b) Girder (UB610x229x101) Supporting Two Beams

Girder length (L_g) = 8.3 m

Area of girder = 12920 mm^2

Moment of inertia of girder = 75720,0000 mm^4

Girder spacing (S_g) = 6.75 m

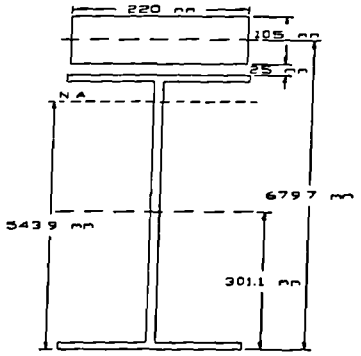

Effective slab width = least of $\frac{L_g}{4}$ or S_g = 2.075 m

Transformed width = $\frac{ESW}{n}$ = 220 mm

Centroid = 543.90 mm from base

Transformed moment of inertia (I_{Tg}) = 1966082782 mm^4

Girder mass/m (m_G) = 101 kg/m

Supported mass (m_g) = 2 x m_b x $\frac{L_b}{L_g}$ + m_G

= 2 x 564.6675 x $\frac{6.75}{8.3}$ + 101 = 1019.4351 kg/m

Fundamental natural frequency of girder (f_g) = $\frac{\pi}{2}\sqrt{\frac{E_s I_{Tg}}{m_g L_g^4}}$ = 14.40 Hz

Dunkerly's Formula

$$f = \frac{1}{\sqrt{\frac{1}{f_b^2} + \frac{1}{f_g^2}}} = 9.10 \text{ Hz}$$

Static Deflection Method (SDM)

a) Wyatt's Approach

For 1.2 mm thick CF70 profile deck (see PMF (1994)):

Neutral Axis (N.A.) of profile = 30.32 mm from bottom

Area of profile = 1585 mm^2/m

Moment of inertia of profile = 760000 mm^4/m

$$\text{Slab N.A.} = \frac{\frac{1000}{9.4}x105x\frac{105}{2} + 1585x(130-30.32)}{\frac{1000}{9.4}x105+1585} = 58.36 \text{ mm from top}$$

Moment of inertia of slab (I_s):

$$I_s = \frac{1000}{9.4}x\frac{105^3}{12} + \frac{1000}{9.4}x105x(58.36-\frac{105}{2})^2 + 760000 + 1585x(130-30.32-58.36)^2$$

I_s = 14112351.23 mm^4/m

Mode-1: Slab - Fixed between beams

Slab width = 1 m

Slab length (L_s) = 2.665 m

Slab mass (m_s) = 0.105 x 1900 = 199.5 kg/m^2

Assuming acceleration due to gravity (g) = 9.80665 m/sec^2,

Static deflection of slab (Δ_s) = $\frac{m_s g L_s^4}{384 E_s I_s}$ = 0.0880585 mm

Beam - Simply supported between girders

Static deflection of beam (Δ_b) = $\frac{5 m_b g L_b^4}{384 E_s I_{Tb}}$ = 2.2882871 mm

Total deflection (Δ_T) = Δ_s + Δ_b = 2.37634556 mm

Fundamental natural frequency = $\frac{18}{\sqrt{\Delta_T}}$ = 11.68 Hz

Mode-2: Slab - Fixed between beams

Static deflection of slab (Δ_s) = 0.0880585 mm

Beam - Fixed between girders

Static deflection of beam (Δ_b) = $\frac{m_b g L_b^4}{384 E_s I_{Tb}}$ = 0.45765741 mm

Girder - Simply supported between columns

Static deflection of girder (Δ_g) = $\left(\frac{23}{648} m_b \frac{L_b}{L_g} + \frac{5}{384} m_G\right) \frac{g L_g^4}{E_s I_{Tg}}$

= 2.01628 mm

Total deflection (Δ_T) = $\Delta_s + \Delta_b + \Delta_g$ = 2.56199591 mm

Fundamental natural frequency = $\frac{18}{\sqrt{\Delta_T}}$ = 11.25 Hz

b) Allen-Murray Approach

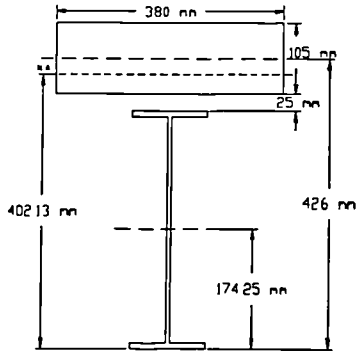

Modular Ratio (n) = $\frac{E_s}{1.35 E_c}$ = 6.96

Beam Panel Mode:

Deck weight = 2.07 kN/m^2

= $\frac{2070}{9.80665}$ = 211.08 kg/m^2

Effective slab width = least of 0.4 L_b or S_b = 2.665 m

Transformed width = $\frac{ESW}{n}$ = 380 mm

Centroid = 402.13 mm from base

Transformed moment of inertia (I_{Tba}) = 358456673.5 mm^4

Supported mass (m_{ba}) = deck weight x $\frac{ESW}{n}$ + m_B

= 211.08 x 2.665 + 33 = 595.5315 kg/m

Beam deflection (Δ_{ba}) = $\frac{5 m_{ba} g L_b^4}{384 E_s I_{Tba}}$ = 2.13 mm

Fundamental natural frequency = 0.18 $\sqrt{\frac{g}{\Delta_{ba}}}$ = 12.21 Hz

Girder Panel Mode:

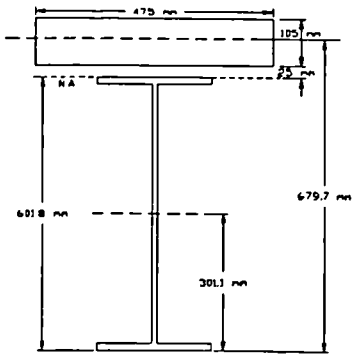

Effective slab width = least of 0.4 L_g or S_g

= 3.32 m

Transformed width = $\frac{ESW}{n}$ = 475 mm

Centroid = 601.8 mm from base

Transformed moment of inertia (I_{Tga}) = 2273917335 mm^4

Supported mass (m_{ga}) = 2 x m_b x $\frac{L_b}{L_g}$ + m_G = 1069.6 kg/m

Girder deflection (Δ_g) = $\frac{5m_{ga}gL_g^4}{384E_sI_{Tga}}$ = 1.38 mm

Fundamental natural frequency = 0.18 $\sqrt{\frac{g}{\Delta_b}}$ = 15.18 Hz

Combined Mode:

Slab rigidity (D_s) = $\frac{I_s}{n}$ = 19051674.16 mm^4/m

Beam rigidity (D_b) = $\frac{I_b}{spacing}$ = 134505318.4 mm^4/m

Beam panel effective width = 2 $\left(\frac{D_s}{D_b}\right)^{1/4} L_b$ = 7.68 m < $\frac{2}{3}L_{total}$

Since L_g = 8.3 m > 7.68 m

Fundamental natural frequency = 0.18 $\sqrt{\frac{g}{\Delta_b + \Delta_g}}$ = 9.52 Hz

c) Finite Element Method

For the constant slab thickness FE model:

FE maximum static deflections (Δ_s) = 2.28 mm

Fundamental natural frequency = $\frac{18.6}{\sqrt{\Delta_s}}$ = 12.32 Hz

Appendix C

Typical FE Model Input File

This appendix presents a typical ANSYS input file for the dynamic analysis of a single-panel FE model, as discussed in Chapter 4. The modelling has been described by including comments using the "!" sign. For further details on FE modelling using I-DEAS and ANSYS, see respective manuals.

```
/file,Model1
/title, Hammersmith Cark Park (mesh size = 6x6)
/units,si                              ! N, m, kg
! Build model
/prep7
! Element type
et,1,shell63                           ! First element type
! Material properties
mp,ex,1,3.479e10                       ! E for first element type
mp,dens,1,2400                         ! Density for first element type
! Real constants
r,1,0.225                              ! Thickness for first element type
! Node generation
n,2,0.15                               ! Generate node 2
! Generate set of nodes, node increment, from node, to node, node increment, x, y
ngen,7,1,2,2,0,1.15,0                  ! Horizontal nodes (2 - 8)
n,10,0,0.15                            ! Generate node 10
ngen,2,9,2,8,1,0,0.15                  ! Vertical nodes (2 - 17)
n,18,7.2,0.15                          ! Generate node 18
ngen,7,9,10,18,1,0,1.35                ! Vertical nodes (10 - 72)
ngen,2,9,65,71,1,0,0.15                ! Vertical nodes (65 - 80)
! Element generation
en,2,2,3,12,11                         ! Generate element 2
! Generate element increment, set of elements, node increment, from element,
! to element, element increment
engen,1,6,1,2,2,0                      ! Horizontal elements (2 - 7)
engen,8,8,9,2,7,1                      ! Vertical elements (2 - 63)
en,9,10,11,20,19                       ! Generate element 9
engen,8,6,9,9,9,0                      ! Vertical elements (9 - 49)
engen,7,2,7,9,49,8                     ! Horizontal elements (9, 16, 17, 24, 25, 32, 33,
!                                      40, 41, 48, 49, 56, 58, 63)
```

```
! Boundary conditions
d,2,all                          ! Fix nodes 2, 8, 10, 11, 17, 18, 64, 65, 71, 72,
!                                74, 80
d,8,all
d,10,all
d,11,all
d,17,all
d,18,all
d,64,all
d,65,all
d,71,all
d,72,all
d,74,all
d,80,all
Finish
! Start solution
/solu
antype,modal                     ! Analysis type
! Options      (method, number of modes, from frequency , to frequency,
!              reduced modes, normalise)
modopt,subsp,10,0,20,,off
mxpand,5,0,20,no
solve
Finish
! Start post-processing
/post1
```

Note: Nodes 1, 9, 73, and 81 have not been modelled because they represent the column centres at the four corners of the model and, therefore, would be fixed in the same manner as the perimeter of these columns (nodes 2, 10, 11; 8, 17, 18; 64, 65, 74; and 71, 72, 80).

The above input file is for the Hammersmith floor. Figure 4.11 shows this model.

THE
END